Appendices

Appendix A	OU1 Cap Design Summary Document
Appendix B	OU1 GMS White Paper
Appendix C	OU1 SWAC White Paper
Appendix D	Numerical Model Assessment of Bed Shear Stress for Wind-Waves and Flows on LLBdM (OU1), Fox River (Baird 2007)
Appendix E	Effects of Ice on Sediments in LLBdM, Lower Fox River above Appleton, Wisconsin (Ashton 2006)
Appendix F	Lower Fox River Feasibility Study Cost Analysis (*Appendix H*)

OU1 Cap Design Summary Document

1. Introduction

A summary of the OU1 engineered cap design is presented here, and further details and discussion are presented in the OU1 Cap Design Document, Revision 2 (Foth, 2007).

The OU1 Optimized Remedy includes an engineered cap to be placed over 112 acres of sediment area in OU1. The plan involves placing a 13-inch engineered cap over undredged sediments with an average PCB concentration between 2 and 10 ppm in the top 8-inch interval. The 13-inch cap thickness is considered to be comprised of 6-inches of sand and 7-inches of armor, with each media layer including a 3-inch overplacement allowance. The minimum design thickness of 7 inches is considered to be comprised of 3 inches of sand and 4 inches of armor.

Cap design was influenced by cap design criteria and guidance and OU1 specific cap design considerations. OU1 specific cap design considerations have been drafted with careful consideration of OU1 sediment characteristics, review of cap design addressed for the Lower Fox River OU2-5 project (Shaw and Anchor, 2006), and other attributes of the OU1 Design Supplement, such as dredging and sand cover. In addition, cap design has been influenced by a series of cap design workgroup meetings and correspondence with the Agencies and Oversight Team (A/OT).

This summary addresses the cap design with the following organization. Section 2 addresses the cap design approach, guidance and OU1 specific design criteria. Section 3 addresses key elements of the cap design, particularly,

- a summary of targeted and minimum cap layer thicknesses
- operational thickness, concept of target thickness and minimum design thickness
- properties and expected interactions of cap media with the sediment to be capped, including considerations of consolidation and settlement, geotechnical stability, and mixing layer characteristics
- chemical isolation considerations, including a summary of chemical isolation modeling and monitoring considerations
- media gradation considerations for the armor and sand layers
- bioturbation layer considerations
- erosion layer considerations, including resistance to various forces, including propeller wash, extreme flow events, extreme wind-wave events, and ice scour

Section 4 presents a summary of placement, monitoring, and quality assurance considerations.

2. Cap Design Approach and Criteria

Engineered capping of contaminated sediments requires long-term physical, biological, and chemical isolation of contaminated sediments. The design of engineered caps must be appropriately conservative, such that there is a reasonable level of assurance that the cap is designed, installed, monitored, and maintained for long-term performance. Caps need to resist natural and human-induced erosive forces that are expected to act on the cap. These erosive forces include 100-yr. flood event flows, high wind-wave conditions, propeller action from boating (prop wash), and ice scour.

The proposed cap design, monitoring, and maintenance plan are developed so that there is a high probability of achieving long-term physical stability and physical/chemical isolation of the cap. Guidance for cap design, specifically, cap thickness and media selection in order to achieve chemical and physical isolation were followed for OU1. (Palermo, *et al.* 1998b, Palermo, *et al.* 2002).

The overall protectiveness of the cap design depends not only on the susceptibility to damage and the potential impacts, but on whether that damage can be detected and appropriately corrected as part of planned monitoring and maintenance operations. The general preference of the proposed cap design, however, was to provide a high level of protectiveness against activities or processes that would impair the function of the cap. In addition, the proposed cap design does not rely on significant institutional controls in order to reach the intended overall protectiveness.

OU1 specific cap design considerations generally controlled the extent of the proposed cap areas. These are summarized below.

2.1 OU1 specific cap design considerations

The OU1 cap design efficiently addresses the spatial distribution of PCB contamination for areas in which capping is allowed. Water depth is also a critical design parameter for two major reasons. First, the post-cap water depth must be at least 3 feet for navigability (OU1 ROD), and armoring is required for cap areas with shallow water depths due to the potential erosive forces from boat propellers (prop wash). Erosion characteristics of extreme wind-wave and flow events also affect cap design.

Selection of potential cap areas is highly associated with the spatial distribution of the sediment contamination and available water depths, as interpreted form the 3D model (GMS-SED) and spatial database (ArcGIS). The horizontal resolution of the spatial database was greater than 30 ft. Further details are presented in the OU1 Cap Design Document, Revision 2 (Foth 2007).

Cap design criteria for OU1 also include several exclusion conditions. Restrictions to capping will be presented first, followed by attributes of PCB concentrations and factors influencing the erosive stability of the cap. Further discussion is also given to the coordination of the proposed capping plan with other elements of the OU1 Plan.

2.1.1 Restricted capping areas for OU1 Plan

Capping contemplated in the contingent remedy will not be permitted in certain areas of OU1:

- No capping in areas of navigation channels (with appropriate buffer zone).
- No capping in areas of infrastructure such as pipelines, utility easements, bridge piers, etc (with appropriate buffer zone).
- No capping in areas with PCB concentrations exceeding Toxic Substances Control Act (TSCA) levels.
- No capping in shallow water areas (bottom elevations which would result in a cap surface at elevation greater than -3ft chart datum for OU1 without prior dredging to allow for cap placement.

Of the infrastructure identified to date in OU1, only the Highway 441 bridge and the submerged pipeline immediately south of the bridge are located near proposed cap areas. Exact infrastructure locations will be more precisely identified during future design and remedial action phases of the project.

2.1.2 Sediment characteristics of proposed OU1 cap areas

Values for the surficial PCB concentration (the average concentration in the top 8 inches of soft sediment) are less than 10 ppm in all of the proposed cap areas, and less than 5 ppm in 97% of the areas. The maximum PCB concentrations in the 1.0 ppm prism range from 1.2 ppm to 49.1 ppm. Roughly 90% of the proposed cap areas have maximum PCB concentrations below 25 ppm and 72% of the areas have maximum PCB concentrations below 10 ppm.

The total proposed cap area is estimated as 112 acres. The 1 ppm isopach (sediment depth expected at the deepest extent of sediments with a concentration of 1 ppm or greater) ranges from 0.1 ft. to 2.8 ft. for the proposed cap areas. If dredged to the 1 ppm isopach, the cap area would represent 265,830 cubic yards with an average cut of roughly 1.5 ft. The sediments within the isopach are generally soft, with approximately 80% of the areas having an average percent solids ranging from 15-20% solids. Approximately 94% of the proposed cap areas fall within the OU1 Sub-areas E1, E2, and E3-South (E3S). These areas are primarily deep and depositional.

2.1.3 Water depths and bed shear characteristics of proposed OU1 cap areas

Final water depths reported here are based on consideration of the low-water datum, the proposed cap thickness (13 inches), and without consideration of expected consolidation of the underlying sediment or cap media. Consolidation is addressed separately. Final water depths in the proposed cap areas are expected to range from 6.0 ft to over 20 ft. Roughly 75% of the proposed cap areas have post-cap water depths greater than 7.6 ft. and 50% of the areas have post-cap water depths greater than 8.4 ft.

The proposed OU1 cap areas are primarily depositional because the fluid shear stresses acting on the sediment bed (bed shear stresses) are low. Areas with higher sediment PCB concentrations at depth tend to be more depositional in nature. The upper sediment bed is

composed of soft, organic silts with moderate plasticity. Under high bed stresses, these sediments would erode. However, more than 90% of the proposed cap areas have soft sediment thicknesses of 3 feet or more, and 50 % of the areas have thicknesses of 7 feet or more.

The placement of armored caps is expected to greatly increase the erosional resistance of the sediment bed. However, erosion resistance for the proposed cap areas is evaluated on the basis of the resistance to extreme events, primarily 100-year flow conditions, 100-year combined wind-wave and current events, and prop wash events.

Resistance to prop wash is considered with a prop wash model. Prop wash considerations, including selection of design vessels and expected usage characteristics, are handled stochastically, with a Monte Carlo modeling approach. Model outcomes for stable particles at a given probability level are provided for a given water depth. Outcomes of the prop wash model were a major factor in limiting capping areas to areas in which the final water depth would be 6.0 ft. or greater. Further details of the prop wash model are addressed below (Section 3).

Cap erosion stability for the less turbulent wind-wave and 100-year flow event forces are evaluated from model-estimated bed shears at all proposed cap locations. Bed shear stresses were calculated using hydrodynamic and wind-wave models (Baird 2006 and Baird 2007). Wind-wave bed shear stresses for a 100-year return period were estimated from combining waves generated from hourly winds with a 50-year return period and daily flows with a 2-year return period. Maximum bed shear stresses in the proposed cap areas range from less than 10 dynes/cm^2 (1.0 Pa) to less than 40 dynes/cm^2. More than 99% of the proposed cap areas had maximum bed shear stresses less than 30 dynes/cm^2 and 90% of the areas had maximum bed shear stresses less than 22 dynes/cm^2. In comparison, all proposed cap areas had bed shear stresses less than 10 dynes/cm^2 for simulation of a 100-yr flow event.

Particle stability of the proposed cap media is discussed below (Section 3), in terms of resistance to expected bed shear stresses from extreme events of prop wash, wind-wave, and 100-year flow.

2.2 Coordination of capping activities with other OU1 Plan elements

GW Partners does not anticipate that dredging will occur simultaneously with capping operations in OU1. In fact, in order to meet capping restraints and operational efficiencies, some areas previously considered as potential cap areas were dredged in 2007. Accordingly, a detailed analysis of the required isolation distance between dredging and capping operations is unnecessary. The proposed placement of sand cover, however, may be implemented in close coordination with the capping plan.

The representations of OU1 Optimized Remedy action areas for dredging, capping, sand cover, and natural recovery are currently based on an efficient ArcGIS representation. Although the footprint of the proposed capping areas is generally contiguous, the current

representation of the proposed cap areas may appear rough, with jagged edges and some internal gaps. For the purposes of the OU1 Plan, the efficiency of the selection of potential cap areas (and the rapid computation of the effects of the proposed remedies) outweighs the objective to provide a cap design with smooth edges. Prior to implementation of the cap design, the proposed boundaries of the cap will be formed along smooth model contours of PCB concentrations and water depth (meeting the same criteria) and the apparent roughness of the cap design will be greatly reduced. Further details regarding geometric refinement are presented in the OU1 Cap Design Document, Revision 2 (Foth 2007).

2.3 Verification and monitoring

A series of sampling, quality assurance and control measures will be taken to meet cap design criteria as well as applicable rules and regulation. Cap placement quality assurance measures will consist of testing placement accuracy and precision on dry land, physical measurements to verify the proper placement thickness of each layer, and statistically valid measurements to assure a minimum placement thickness of each layer in at least 90% of the capped areas. Measures will be taken to address any capped portions that are found to have cap layers less than the minimum protective thickness.

Further details regarding recommended verification and monitoring procedures are presented in the OU1 Cap Design Document, Revision 2 (Foth 2007).

3. Proposed Cap Design Layers and Cap Media Selection

The proposed cap design is based on the characteristics of the proposed OU1 cap areas (Section 2), cap design guidance, a multi-barrier approach for selecting cap layer thicknesses, and selection of cap media that provide effective formation of cap (mixing layer), effective layering (filter criteria), and erosive stability (armor layer). The potential for ice scour and hydrodynamic modification should be considered. In addition, geotechnical considerations regarding consolidation, slope stability, and foundation strength should be addressed.

3.1 Multi-barrier approach and conceptual cap design layers

An engineered cap is designed to provide long-term, in situ containment of contaminated sediments and long-term stability against physical attack in the LLBdM environment. Engineered cap design is based on a conservative, multi-barrier approach (Palermo, *et al.* 1998b, Palermo, *et al.* 2002). The functions of the conceptual layers of the cap are:

- An operational thickness to address sand-sediment mixing (formation of a filter layer) needed to establish the cap over soft sediment (T_m)
- A chemical isolation layer to contain contaminants in the underlying sediment (T_i)
- A bioturbation layer to provide physical isolation of burrowing benthic organisms (T_b)
- A consolidation layer to correct for any consolidation of the cap media (T_c)
- An erosion layer to provide sufficient thickness and an appropriate gradation of media on the top of the cap that is resistant to erosion (T_e)

Operational considerations, including the mixing layer (T_m), filtering and geotechnical foundation for armored erosion layers, media placement accuracy, and other processes, may also require additional media thickness (T_o).

The multi-barrier approach is generally additive, although some of the conceptual layers can be combined under certain conditions. For the settings of OU1 (Palermo, *et al.* 2002), the bioturbation and erosion layers (excluding any additional armoring requirements) can be combined into one bioturbation/erosion layer ($T_{b/e}$). For low contaminant concentrations, where very thin layers for chemical isolation are suitable, the chemical isolation layer can be combined with the underlying mixing layer (T_m). If capping were to be proposed for areas with higher PCB concentrations, a layer of uncompromised sand may be needed for additional chemical isolation.

For granular cap media with a low fines content, no consolidation of the cap media is expected ($T_c = 0$). However, the consolidation of underlying soft sediment may be significant and the sediment pore water expressed from that consolidation is considered as part of the chemical isolation design.

A summary of proposed OU1 cap media selection and thicknesses for different sediment and erosion conditions is presented in Table A-1. For all cap conditions, a segment of the operational thickness of 3.0 inches is assigned to deal with sand-sediment mixing. For low PCB concentrations (e.g., average PCB concentration in the top 8 inches is less than 10 ppm), the mixing layer is expected to provide adequate chemical isolation and the combined thickness of the cap is as follows:

$$T = T_{b/e} + T_o$$

As mentioned above, chemical isolation is incorporated into a mixing layer (part of the operational thickness). Since the minimum thickness of the bioturbation layer is generally considered 4 inches and the minimum operational (mixing) layer is generally considered 3 inches, the minimum design thickness of the applied cap could be considered as 7 inches. The cap thickness is 13 inches with overplacement (3 inches overplacement for each media type).

Further details regarding the main layers of the cap design are addressed below.

3.1.1 Mixing layer

For all cap conditions, a segment of the operational thickness of 3.0 inches is assigned to deal with sand-sediment mixing. The mixing layer is the equivalent amount of applied sand needed to establish a clean sand layer. Although sand may penetrate the sediment to sediment depths greater than 3 inches, the mass fraction of sand is expected to fall off relatively quickly from the sand-sediment interface and the amount of applied sand is expected to be less than 3 inches for the proposed OU1 cap areas. The selection of the mixing layer was considered appropriately conservative as evaluations from the 2007 Cap Placement Test in OU1 confirmed very thin mixing layers (i.e, approximately one-inch thick mixing layer). In addition, a three-inch mixing layer was selected for similar sediments addressed by the proposed cap for the OU2-5 design (Shaw and Anchor, 2006). Further details and results are presented in the OU1 Cap Design Document, Revision 2 (Foth 2007).

Table A-1
Cap Layer and Total Thickness for Proposed OU1 Cap Areas

Layer	Category for Thickness	Cap Media	Design Thickness (in.)	Design Thickness with Operational Overplacement (in.)
Bioturbation / Erosion Layer	Operational, overplacement	armor stone	0	3
	Bioturbation / Erosion		4	4
Chemical Isolation Layer	Operational, overplacement		0	3
	Chemical Isolation / Operational Mixing Layer	sand	3	3
Total Thickness			7	13

Note: Final operations overplacement allowance will be specified in the work scope and agreements with the selected contractors(s).

3.1.2 Chemical isolation layer

A chemical isolation model has been used to verify that 1 inch of sand is protective to chemically isolate sediment PCBs from benthic organisms ($T_i \leq 1.0$ inch). The chemical isolation layer is considered to be biologically inactive, providing a physical, diffusion barrier from the bioturbation-erosion layer. This model is based on conservative assumptions regarding surface PCB concentrations, total organic contents in the underlying sediment and in the benthic layer, and allowances for limited advection through the cap. Chemical isolation model calculations were run for the peak surface PCB concentration of 10 ppm, as well as with consideration of higher PCB concentrations at depth. Although upward flow from the sediments to the cap is not expected, a conservative analysis of regional groundwater gradients and cross-section hydrogeologic modeling was used to develop an upper-bound estimate for upward groundwater advection (specific discharge of 16.3 cm/yr). Chemical isolation calculations were then used to verify that a 1-inch chemical isolation layer was protective in terms of limiting PCB mass fluxes from the underlying sediment and for maintaining low PCB concentrations in the benthic layer, in perpetuity.

The pore water expected to be expressed through the cap due to the consolidation of the underlying sediments was also considered in the evaluation of the chemical isolation layer. Given the very low concentrations of PCBs expected in the pore water and some sorption from the cap media itself, a very thin layer of sand (on the order of 1 mm) was found to provide adequate isolation from the consolidation pore water. Therefore, no additional thickness for the chemical isolation layer was required to address the consolidation concern. Consolidation of the cap media itself was also considered negligible.

Details on chemical isolation modeling and groundwater advection analysis are presented in OU1 Cap Design Document, Revision 2 (Foth 2007).

3.1.3 Operational overplacement for chemical isolation / mixing layer

Cap guidance documents (Palermo, et al. 1998a and Palermo, et al. 1998b) address the consideration of overplacement as a portion of the operational thickness. This portion of the cap guidance effectively increases the operational thickness of caps in order to assure a minimum placement.

A chemical isolation layer of 1 inch or less, considered to be combined within the 3-inch operational mixing layer, poses some difficultly with respect to monitoring and verification of chemical isolation. However, potential overplacement of sand, forming an observational layer of unmixed sand over the mixing layer, can be documented by field measurements.

The targeted sand overplacement allowance of 3 inches is provided primarily as assurance to meet the minimum design thickness of applied sand. A final operations overplacement allowance will be specified in the work scope and agreements with the selected contractors(s). Results from the 2007 Cap Placement Test will be used to help determine that 3 inches is a suitable overplacement amount for applied sand.

3.1.4 Bioturbation-Erosion layer

The bioturbation-erosion layer thickness is set by a conservative selection for the bioturbation thickness, or 4 inches. This thickness is supported by a significant body of evidence developed for soft sediments. The thickness is also consistent with the selection from the OU2-5 cap design (Shaw and Anchor, 2006). An upper layer of the sediment cap is expected to become biologically active, but only after years of nutrient enrichment and organic matter flow into the (interstitial) pores of coarse cap media.

Aspects of the granular media and the availability of uncapped soft sediment at nearby locations are expected to limit bioturbation within cap areas. A more likely scenario would be that organic, soft sediments continue to deposit on top of the armor, and the biological active zone would be established within this freshly deposited layer, with limited biological penetration into the armor.

The erosion portion of the bioturbation-erosion layer is not limiting, because the thickness required for erosion protectiveness is generally considered to be at least 2 times the stable median particle diameter (D_{50}) meeting erosional resistance criteria, and at least 1.5 times the maximum stone diameter (D_{100}) (Palermo, et al. 1998a, Appendix A). The D_{50} of the armor is expected to be less than 0.75 inch and the D_{100} is expected to be less than 1.3 inch, so the thickness required for erosion protectiveness is less than 2 inches.

The design thickness for the bioturbation-erosion layer is 4 inches, with the intended application of at least 4 inches of armor media that provides suitable erosional resistance. However, for purposes of verification, the cap criteria for the bioturbation-erosion layer may be satisfied for a cap area that is shown to have a bioturbation-erosion layer

thickness of at least 4 inches, suitable armor media on top, and a suitable thickness of armor media. For example, if the minimum armor thickness required is 1.5 inches (with armor media $D_{100} \leq 1.0$ inch and $D_{50} \leq 0.75$ inch), the cap criteria would allow a 4-inch bioturbation-erosion layer to consist of 2.5 inches of sand (lower portion) and 1.5 inches of armor (upper portion).

3.1.5 Operational overplacement for bioturbation-erosion layer

An overplacement allowance of 3 inches is targeted primarily as assurance to meet the minimum design thickness of applied armor media. A final operations overplacement allowance will be specified in the work scope and agreements with the selected contractors(s). Results from the 2007 Cap Placement Test will be used, in part, to demonstrate the suitable overplacement amount for armor media.

3.1.6 Summary and discussion of minimum cap thickness

The intended minimum cap thickness is 7 inches, with 3 inches of applied sand and 4 inches of armor media. An overplacement allowance of 3 inches is expected for each media layer. A final operations overplacement allowance will be specified in the work scope and agreements with the selected contractors(s).

For the purposes of verification of the minimum cap protective thickness, it is important to note that the criteria of the cap design is expected to be met if the total applied thickness of the cap is at least 7 inches, there is an adequate thickness of sand available to assure chemical isolation, 4 inches of cap media are available above the chemical isolation layer for a bioturbation-erosion layer, the armor layer is suitably thick and the armor layer media provides suitable erosional resistance.

For the proposed OU1 cap design, it is expected that overplacement will be a natural outcome of the cap design, project specifications, and cap placement contractor agreement. The average and maximum overplacement will be dependent on the placement method and project specifications. Average expected overplacement is included in the cost estimate, and is used to estimate post-cap water depths. Measures will be taken to address any capped portions that are found to have cap layers less than the minimum protective thickness.

3.2 Selection of cap media

The proposed cap design includes two separate media, sand used to form the combined mixing layer and chemical isolation layer, and armor (stone) used to form the bioturbation-erosion layer. In addition to meeting media requirements for the individual layers, the sand and armor media must also pass media gradation filter criteria so that the media do not mix appreciably during or after placement. In order to reduce turbidity during placement of the cap media, the cap media should be clean and relatively free of fines.

The selected media are based on demonstrated usage within the 2007 Cap Placement Test. Further details regarding media selection, evaluations of the performance of media selected for the 2007 Cap Placement Test and further specifications for cap media are addressed in the OU1 Cap Design Document, Revision 2 (Foth 2007).

3.2.1 Sand gradation specifications

The sand selected as the lower cap media is expected to be consistent of ASTM C33 fine aggregate (concrete sand), which is the poorly graded sand used that was used for the 2007 Cap Placement Test Demonstration Project. The D_{85} of the sand is roughly 1.55 mm, the D_{50} is roughly 0.49 mm, and the D_{15} is roughly 0.28 mm. The coefficient of uniformity (Cu) is 2.3 and the coefficient of curvature (Cc) is roughly 1.0 to 1.1. The fines content is less than 1%. The sand could be described as a medium-coarse, poorly graded sand with a low fines content.

The sand media has been demonstrated to be compatible with the fine, soft sediments in areas of the 2007 Cap Placement Test. The mixing layer was observed to be less than 3 inches and a clean sand layer was present above the mixing layer. Filter criteria (discussed section 3.2.3) would not be applicable to this mixing layer.

3.2.2 Armor stone gradation specifications

The armor media selected as the upper cap media is expected to be consistent with the armor stone (ASTM #467) used for the 2007 Cap Placement Test. The D_{85} of the stone is roughly 30 mm (1.2 in.), the D_{50} is roughly 17 mm (0.67 in.), and the D_{15} is roughly 7 mm. The maximum particle size is 32 mm (1.25 in.). The coefficient of uniformity (Cu) is 3.2 and the coefficient of curvature (Cc) is roughly 1.5. The armor stone (a well graded gravel by USCS description), similar to the sand, has a low fines content.

3.2.3 Filter criteria

Filter criteria are used to select compatible sand and armor stone media. Filter criteria are used to reduce the potential for internal erosion of the sand into the armor layer, due to temporary currents (from waves and other sources) within the armor stone layer. Poorly selected media, failing the filter criteria, may result in mixing of the gravel and the sand. This may result in a deterioration in the erosional resistance of the armor layer.

One of filter criteria states that the D_{15} armor stone size should be no greater than 5 times the D_{85} sand size. Since the measured D_{85} of the sand is 1.55 mm, the D_{15} of the armor stone should be no greater than 7.75 mm (0.31 in.). The D_{15} of the armor media is 7 mm. so this filter criterion is met. Other applicable filter criteria are also met and these are addressed in the in the OU1 Cap Design Document, Revision 2 (Foth 2007).

3.2.4 Stability criteria for armor stone

The selected armor stone for the purposes of the cap design has been shown to meet stability criteria identified from analysis of prop wash, the 100-year flow event, and the combined 100-year wind-wave and flow events. The prop wash model considers a dynamic stability model of the armor stone, while particle stability for the wind-wave and

100-year flow event analyses is based on the Shield's curve (US Army Corps of Engineers, 1995).

3.2.4.1 Stability criteria for armor stone – prop wash model results

The Lower Fox River OU2-5 Design Team worked extensively over the past 2 years with the A/OT in the selection and evaluation of an appropriate Prop Wash Model for the Lower Fox River. It is our understanding the A/OT has accepted the JETWASH model, with certain modifications, as documented in the Coast Harbor & Engineering Technical Memorandums, dated August 17, 2007.

Given the extensive prop wash work completed by the OU2-5 Design Team and the A/OT, GW Partners has decided to accept the basis of this work for application at OU-1.

Separate boat surveys were completed for OU1 and OU2-5. As a brief summary, the OU2-5 boat survey (which included Lake Winnebago and the Lower Fox River to the Bay of Green Bay) showed that the OU2-5 survey consisted of more vessels in the larger size range than the OU1 boat survey. In order to be consistent and protective over time, the OU2-5 boat survey will conservatively be used for the OU1 Prop Wash Cap Design work.

Prop wash results for use at OU1, using the OU2-5 Boat Survey, and the agreed to JETWASH model inputs, as shown on Figure A-1. These results show stable grain size (as D_{50} diameters), for the armor component of the cap, at various water depths and at various Monte Carlo confidence outputs.

The 13-inch engineered cap at OU1, with an over-placement allowance, will consist of 6-inches of sand and 7- inches of armor (minimum design thickness of 3-inches of sand and 4-inches of armor). The selected grain size of the armor layer, at a given depth, varies depending on which modeled output from the Monte Carlo analysis is applied for the Lower Fox River.

For the design basis at OU-1, the model results show that the following armor stone sizes would be required to achieve the associated prop wash Monte Carlo output:

Water Depth (ft.)	Acres	Armor Stone (D50)	Monte Carlo Output
6.0-6.5	5.1	0.6"	90%
6.5-7.0	8.2	0.5"	95%
7.0 +	99.0	0.25"	95+%

The 6.0-6.5 post-cap water depth, where GW Partners is proposing a 90% Monte Carlo output, represents a small area (5.1 acres), in a central portion of LLBdM, of the total proposed 112 capping acres. All told, 107 acres of the 112 acres (95% of the area) will be capped with armor stone at or exceeding the 95% model output criteria. In essence, 95% of the area will exceed 95% of the Prop Wash model output. However, these values assume no consolidation of the soft sediments under the placed material. Considering

consolidation, we believe nearly 100% of the proposed cap areas will meet the 95% model output criteria.

Cap construction based on the design will include media selection that will need to be reviewed and approved by the Agencies on a case-by-case/area-by-area basis. When costs associated with media placement (media costs plus placement-related costs) for armor media with a larger D_{50} are virtually the same as the media with a minimum D_{50} required for erosional resistance, the larger stone will be selected preferentially.

3.2.4.2 Stability criteria for armor stone – wind-wave and flow model results

As discussed in Section 2.1.3, the maximum, wind-wave bed shear in the proposed OU1 cap areas was less than 40 dynes/cm^2 (4.0 Pa), and less than 22 dynes/cm^2 in more than 90% of the areas. A particle diameter of 5 mm is expected to be stable under 40 dynes/cm^2 and a particle diameter of 3.1 mm is expected to be stable under 22 dynes/cm^2.

For OU1, wind-wave effects generally lead to higher bed shear than the 100-year flow event. Hydrodynamic modeling of the OU1 cap regions showed that 100-year flow events produce bed shear stresses less than 10 dynes/cm^2. Under these bed shear conditions, a coarse sand with a particle diameter of roughly 2 mm would be stable.

3.2.4.3 Stability criteria for armor stone – summary

For the limiting post-cap water depth of 6.0 ft., stable stone diameters from the prop wash analysis (20 mm at the 95th percentile, 15 mm or 0.6 in. at the 90th percentile) were most critical. At depths of 7.6 ft. or greater (75% of proposed cap areas), stable particle diameters from the prop wash analysis were less than 4 mm. At intermediate depths (7.6 ft) and deeper, wind-wave forces may be most critical (stable diameter less than 5 mm for all areas). Bed shear conditions for the 100-year flow event were not critical.

The OU1 Design Supplement is currently based on the selection of armor stone with a D_{50} of 15 mm (0.6 in.). With some consideration of consolidation, this D_{50} is expected to meet prop wash conditions at the 95th percentile for all areas. Without consideration of consolidation, this D_{50} is expected to meet prop wash conditions at the 90th percentile for all areas and at the 95th percentile for 95% of the proposed cap areas. For 75% of the proposed cap areas with water depths greater than 7.6 ft., the stable particle diameter of 5 mm is considered to be appropriately conservative.

3.3 Consideration of ice scour

During the winter months, LLBdM will be partially covered with ice. Special considerations need to be given to various ice related processes in the cap design as they will affect the long term stability of the cap. Depending on the characteristics of a particular lake system shallow sediments or sediment caps may be susceptible to the erosive forces of ice flows during ice breakup. As the main ice mass covering a lake thaws and fractures during periods of warm weather, wind and other hydrodynamic forces have the potential to move thick sheets of ice to shallow near shore areas causing erosion of bank and sediments. Ice jams in river systems also have the potential to alter normal flow velocities and cause increased erosion of sediments or sediment caps.

Finally, frazil and anchor ice has the potential to form when fast flowing water is super cooled. These latter ice formations have the potential to dislodge and erode sediment and sediment caps.

GW Partners contracted with an expert to evaluate effects of ice on cap design proposed for OU1. GW Partners' technical consultant, George Ashton, evaluated ice jamming at the old railroad trestle and the 441 bridge, and concluded that ice jamming associated with ice breakup does not occur in LLBdM. Ice jamming at the old railroad trestle is highly unlikely. The maximum likely velocity there for a very high winter flow of 11,100 cfs is only about 0.82 fps. It is generally understood that the threshold velocity at which ice pieces are swept under an ice cover and begin forming a jam is about 2 fps. Thus ice pieces may lodge against the trestle but will remain at the surface and no jam would form. At the 441 bridge the velocities are even lower and estimated at less than 0.5 fps for the same conditions. Again, large floating ice sheets may lodge against the piers but would not submerge to form a jam.

There is a slight possibility of limited frazil ice to be generated during cold periods, immediately down stream of the dams, at the southern reaches of OU1. Considering the average water flow velocities expected during the winter months is relatively low, significant accumulation or downstream migration of frazil ice in the vicinity of the capped areas is highly unlikely. The proposed cap areas are over 5,200 feet from the areas where frazil ice potentially could be generated. Other ice processes that could potentially pose a hazard to capped areas were examined including the physical blockage of the flow cross section by ice cover thickness anticipated during winter months. These types of blockages increase the shear stress on the river bed, relative to the same discharge during open water periods. The shear stress on the river bed caused by these blockages is much less than the bottom shear stress at high discharges associated with a 100-year return flow. The overall conclusion of the ice scour evaluation is that ice conditions do not change the selection of capping materials in the capping areas (Ashton 2006).

Further details regarding ice conditions and the potential for ice scour in OU1 are addressed in the OU1 Cap Design Document, Revision 2 (Foth 2007).

3.4 Consideration of water depth and hydrodynamic modification

The flow of the Fox River through OU1 is controlled by upstream and downstream dams and generally well understood (Retec 2002). In general, hydrodynamic modifications from dredging, sand covering, and capping in OU1 are expected to be minor, even for 100-year flow events. The geometric changes made to LLBdM cross-section from dredging and capping activities are relatively minor. Modeling of hydrodynamic and wind-wave conditions was performed with expected final (after implementation of OU1 Plan). Dredged areas in southern and south-central portions of OU1 have resulted in a slight local increase in the carrying capacity and proposed cap areas result in a slight local decrease in carrying capacity. Areas that have higher river velocity and higher bed stresses generally have low PCB concentrations, due to past erosion and limited fine sediment deposition. So, as a natural consequence of the contamination loading history,

past flow events, and sediment-contamination characteristics, a large portion of OU1 action areas are isolated from the more critical flow areas of OU1. As a result, hydrodynamic effects from the expected changes in water depth in OU1 are expected to be minor.

The net change in water depth from conditions prior to 2004 to conditions upon completion of the Optimized Remedy are estimated to be 0.8% more water volume in OU1 over the 499 acre entire 1 ppm RAL region. Considering the entire 1363 acre OU1, the effect will be significantly less than 0.8%. The final water depth above capped areas will be at least 6 feet deep.

Further details regarding estimated area distributions for water depths in OU1 are addressed in the OU1 Cap Design Document, Revision 2 (Foth 2007).

3.5 Consideration of consolidation of underlying sediment

A large portion of the proposed OU1 cap areas have thick deposits of soft sediments (soft sediment thicknesses of 4 feet or more with percent solids contents generally less than 20%). Consolidation of the sediment underlying the proposed cap areas is expected to be significant. The increase in effective stress from the applied 13-inch cap is expected to be roughly 60 psf, leading to 12 inches or more of consolidation for many of the proposed cap areas. Areas with soft sediment thickness less than 6 ft. are expected to have less consolidation, and consolidation for areas with sediment thickness greater than 6 ft. may be overestimated due to the lack of consolidation data at greater depths. Further details with respect to measured consolidation of capped areas is addressed from analysis of the 2007 OU1 Cap Placement Test , and further details and discussion of consolidation is presented in the OU1 Cap Design Document, Revision 2 (Foth 2007).

3.6 Consideration of shear strength of capped OU1 sediment

An evaluation of sediment shear strength, slope stability, and the potential for bearing (punch-through) was made for proposed OU1 cap areas. In addition, the stability of the soft sediment base materials was inspected as part of the 2007 OU1 Cap Placement Test. While the shear strength of the soft surface sediments is particularly low, the sediment shear strength is expected to be adequate to prevent slope failure in the proposed OU1 cap areas. Capping will be limited to slopes less than 5:1 (horizontal to vertical distance). No slide or sub-grade failures were observed as part of the 2007 OU1 Cap Placement Test and several observations were made indicating acceptable resistance to a punch-through failure.

In general, the shear strength of the sediment underlying the proposed cap areas is expected to increase as it consolidates. During a brief period after loading, the undrained shear strength is expected to be low, and possibly unsuitable. However, as the pore pressures in the underlying sediment are significantly dissipated over a period of days to weeks, the sediment is expected to strengthen significantly. During capping, monitoring is planned to investigate potential movement of underlying sediment. Evidence of any slope or foundation failures will be cause for delaying cap placement operations. Further

details regarding geotechnical stability considerations are presented in the OU1 Cap Design Document, Revision 2 (Foth 2007).

3.7 Consideration of Liquefaction

The issue of liquefaction falls within the general topic of erosive and physical integrity of the cap. A review of the potential for wave-induced liquefaction was addressed as part of the wind-wave report (Baird, 2007, Section 4.2), and further discussion will be provided in the forthcoming document, OU1 Cap Design Revision No. 2 (Foth, 2007).

Baird (2007) had noted that the potential for a liquefaction failure is limited, but mentioned that the "possible interaction between wave-induced pore-water flows and the native material under the cap may be another issue to consider, however, this is more a question of appropriate filtering design between the layers." The discussion of filter criteria and the assessment of a sand-sediment mixing layer will be provided in the forthcoming Cap Design Revision No. 2.

Liquefaction would be expected occur only if the effective shear strength of the sediment falls below a critical limit value, due to a build-up of pore pressures within the sediment. While pore pressures increase with wave height, so does the confining pressure. So, the hydrostatic pressure wave does not induce a change in effective stress within the sediment. A body force, such as prop wash or wave-generated bed shear or seismic event, is needed to suddenly increase pore pressures within the sediment. It is the resulting body shear force, not the hydrostatic pressure itself, that leads to the buildup of pore pressures from waves. Because of erosion protection issues, the proposed OU1 cap is at final water depths greater than 6 ft. and in areas with low bed shear.

Dynamic, differential pressures from waves (peak to valley) can also lead to an oscillatory bed shear, although seepage within the more permeable (upper) regions of the cap is expected to dampen bed pressure oscillations. Because studies have shown that the allowable wave height increases with consolidation time (De Wit and Kranenburg 1997, as cited by Baird 2007), the most vulnerable periods for the cap would seem to be during placement and, possibly, during storms shortly after cap placement. The dynamic, differential pressures and other stresses brought on during cap placement are likely most relevant to OU1. Therefore, the initial post-placement monitoring (occurs in an area shortly after cap placement) will be able to capture whether a liquefaction failure has occurred. In addition, because of the timing of placement and storms that may induce failures, failures are likely to be localized and might be corrected by additional capping.

Given that there is a lack of guidance regarding engineering cap design and liquefaction, and that there is little evidence that liquefaction failures have been a problem at other capping sites in the US, a more thorough geotechnical evaluation of the potential for liquefaction failures in OU1 was not conducted. This judgment was shaped in part from the project team's experience to date in OU1 with capping and sand cover over very soft sediments.

In summary, while liquefaction failures are not expected, such failures, if they do occur, are likely to be observed during and soon after cap placement. However, the vulnerability of the capped areas to liquefaction is expected to decrease with time after placement. If liquefaction failures are detected, the contingency plan will address corrective actions, which may include additional capping or adjustments to the cap design.

4. Cap Placement, Monitoring and Quality Assurance Plan

4.1 Method of Cap Placement

A hydraulic transport and mechanical broadcast-type spreading system for sand placement was tested during the 2004 RA. The sand placement system was designed to minimize mixing the sand capping material into the sediment. For placing the sand portion of the OU1 Optimized Remedy caps, a transport/placement process similar to the 2004 operation is anticipated. A process similar to that used for sand placement is envisioned for transporting and placing the gravel/stone portion of the engineered armored caps. In addition, methods for cap placement are currently also being evaluated on the basis of a 2007 Cap Placement Test carried out in three areas in Sub-area E2 (Foth, 2007c). The 2007 Cap Placement Test involves a detailed process plan for material specifications, stockpile management, slurry delivery to the placement barge, effective broadcast methods of the capping equipment, accurate positioning and position controls, and site logistics to maintain performance criteria of the project. Details and objectives for the capping demonstration are discussed in the 2007 Cap Placement Test Plan (Foth 2007c).

A variety of controls are in place to assure effective capping and to reduce environmental impacts from the capping. These include metering controls, Dredgepack and Wonderware software, navigational control, media testing to assure clean media is placed, turbidity monitoring of the water column near the capping areas, and a variety of other quality control and monitoring strategies. Best management practices will be used for cap placement operations, such as working in a upstream to downstream manner, using high-grade mufflers to limit engine noise, and clear chain-of-command procedures for emergencies and project communications.

General quality control steps (measures before and during placement to meet design goals) are summarized above and quality assurance steps (measures during and after placement to verify that minimum design criteria were met) are presented in section 4.2. Further details regarding both will be presented in the Cap Design Revision No. 2.

4.2 Production Rates and Quality Assurance (CQAP)

The current production rate estimated for placement of both the sand and armor stone portions of the cap is approximately 50 cy/hr. Experience gained from the 2007 cap placement test will be used in the final design of the cap. The armoring gravel will be placed in a separate operation following the sand placement, but within the same season as the sand placement. Sand and armor stone are planned to be placed in separate, single lifts.

Cap placement quality assurance measures will consist of the following:

- Testing placement accuracy and precision on dry land
- Physical measurements to verify the proper placement thickness of each layer
- Statistically valid measurements to assure a minimum placement thickness of each layer in at least 90% of the capped area

An evaluation of the performance of the 2007 Cap Placement Test is ongoing. Further details regarding quality assurance measures and reporting of the 2007 Cap Placement Test will be reported in the Cap Design Revision No. 2 (Foth 2007).

4.3 Monitoring, Maintenance and Contingency Response Plan

A long-term monitoring, maintenance and contingency response plan, including repair (as necessary) of damaged capped areas, is part of the Optimized Remedy and will be prepared to ensure the integrity and reliability of the *in-situ* cap. The objectives of the cap monitoring program will be to detect and evaluate any physical changes in the cap that would potentially reduce protectiveness over time. The long-term cap monitoring program will include the following components:

- **Bathymetric Surveys** – Bathymetric surveys will be completed to evaluate the physical integrity and thickness of the capped areas. These surveys will be conducted initially post-construction and then at specific time intervals (along the same transects) to identify potential areas of significant erosion, deposition, or consolidation.
- **Coring and Surface Grab Sampling** – Coring will be conducted to visually inspect the cap and cap thickness. Coring will also be conducted to supplement any elevation data discrepancies obtained from the bathymetric surveys that may indicate significant elevation loss. Follow-up sediment cores will be collected to determine whether the elevation loss is a result of erosion or settlement based on visual evaluation of the cores, considering core compaction.

The cap monitoring and maintenance plan will identify the specific details regarding frequency, location and type of sampling. A contingency response plan will be prepared in conjunction with the Long-Term Monitoring and Maintenance Plan that will identify specific criteria to be monitored and possible outcomes of the monitoring. Evaluation criteria will be identified and a range of responses/actions will be included depending on the results of the evaluation. The Agencies will also evaluate cap performance and the need for and scope of continued cap monitoring and maintenance as part of the five-year CERCLA review process.

References:

Baird & Associates, 2006. *Numerical Model Assessment of Bed Shear Stress for the 100-year Return Flow, Little Lake Butte des Morts, Fox River*. Prepared for Foth & Van Dyke and Associates, Project No. 11172.000, November, 2006.

Baird & Associates, 2007. *Numerical Model Assessment of Bed Shear Stress for Wind-Waves and Flows on Little Lake Butte des Morts (OU1), Fox River*. Prepared for Foth Infrastructure & Environment, LLC., Project No. 11172.010, June 29, 2007.

Coast & Harbor Engineering. "Prop Wash Technical Memorandums, Nos. 1-6". August, 17, 2007.

Foth Infrastructure and Environment, 2007. "OU1 Cap Design Document, Revision 2", in preparation, expected submittal December 2007.

Palermo, M., Maynord, S., Miller, J., and Reible, D., 1998a. "Guidance for In-situ Subaqueous Capping of Contaminated Sediments," EPA 905-B96-004, Great Lakes National Program Office, Chicago, IL.

Palermo, M.R., Clausner, J.E., Rollings, M.P., Williams, G.L., Myers, T.E., Fredette, T.J., and Randall, R.E., 1998b. "Guidance for Subaqueous Dredged Material Capping," Technical Report DOER-1, U.S. Army Corps of Engineers, Waterways Experiment Station, Vicksburg, MS.

Retec Group, Inc., 2002. *Final Feasibility Study, Lower Fox River and Green Bay, Wisconsin. Remedial Investigation and Feasibility Study*. Prepared for the Wisconsin Department of Natural Resources. December 2002.

Shaw and Anchor, 2006. *Final Basis of Design Report. Lower Fox River and Green Bay Site. Brown, Outagamie, and Winnebago Counties, Wisconsin.* Prepared for Fort James Operating Company, Inc. and NCR Corporation by Shaw Environmental and Infrastructure, Inc. and Anchor Environmental, LLC. June 16, 2006.

U.S. Army Corps of Engineers, 1995. "Sedimentation Investigation of Rivers and Reservoirs," Engineering Manual, EM 1110-2-4000, Change 1, October 31, 1995.

White Paper

Development of Sediment Prisms in Lower Fox River OU1

This Document has been
Prepared by:

Gerald R. Eykholt, Ph.D., P.E.
Steve G. Lehrke
Denis M. Roznowski, P.E.

Foth & Van Dyke
Green Bay, Wisconsin

March 2004
Revised June 2004

Abstract

This white paper describes the rationale and approach for use of a sediment modeling tool, GMS (Environmental Modeling Systems, Inc.), to delineate the lateral and vertical extent of PCB contaminated sediment deposits in Little Lake Butte des Morts (LLBdM), Lower Fox River, Wisconsin. LLBdM is commonly referred to as Operable Unit 1 (OU1) when described in the context of the Lower Fox River and Green Bay Record of Decision (ROD). Delineation of sediment deposits is an important component of the Remedial Design work in LLBdM.

GMS was used to organize sediment sampling data, to estimate the spatial distribution and volume of contiguous deposits with total PCB concentrations greater than the Remedial Action Limit (RAL), and to provide a platform for visualization and data export to CADD and other computer application environments. This white paper emphasizes the use of the GMS inverse distance weighted (IDW) approach in 3D (Shepard's method). The white paper also discusses the rationale for selection of GMS and the interpolation method, the general approach for use of GMS for 3D sediment modeling, and refinement measures used to assess and improve the quality of modeling results.

Ultimately, the primary goal for sediment deposit modeling is to accurately delineate regions of PCB contamination – so that remedial actions are successful in achieving remedial action objectives. Remedial designs need to address regions with total PCB concentrations above the RAL.

The economy and effectiveness of remedial designs depend on accurate delineation of the contaminated regions. The physical extent of the soft sediment deposits is used to establish an overall modeling boundary. PCB sample results are then used to interpolate contamination concentrations to a dense, 3D model mesh. The 3D mesh represents the PCB characterization of the deposit with high resolution. The specific modeling process with GMS for OU1 deposits is described in the white paper.

Typically, contaminated regions in OU1 are shallow, as data show contamination in only the top 12 inches (30 cm) over large areas. The stratified nature of sediment deposits can be incorporated within the IDW method, using a z-scale anisotropy factor. The IDW method considers nearest neighbor sampling points to the mesh, and weights the influence of each point inversely with distance. The z-scale anisotropy factor effectively stretches the distance in the vertical direction, so that points that are at the same depth at some horizontal spacing are given more influence. This weighting technique allows stratified deposits to be effectively modeled in 3D by considering possible correlations in the vertical dimension. This white paper discusses the rationale and implications regarding the selection of the z-scale anisotropy factor and the number of nearest neighbor points to consider for modeling work in OU1.

This white paper documents the current state of practice for sediment modeling in support of the remedial design for OU1.

White Paper
Development of Sediment Prisms in Lower Fox River OU1

Contents

Page

1. Introduction 1
   1.1 Purpose and Scope 1
   1.2 Background 1
      1.2.1 RI/FS Methodology 1
      1.2.2 Record of Decision Requirements 2
      1.2.3 Use of Model for Remedial Design 2
   1.3 Rationale for Selection of GMS and IDW Methods for Sediment Modeling 3
      1.3.1 Need for Model to Match Characteristics of Sediment Deposits 3
      1.3.2 Need for 3D Interpolation of Sediment Deposits 3
      1.3.3 Selection of GMS as 3D Interpolation Tool 4
      1.3.4 Selection of GMS Interpolation Algorithms 5
      1.3.5 Current State of Review of GMS 6
2. GMS Approach for OU1 7
   2.1 Entering Sediment Sampling Data 7
      2.1.1 Interpolation Set Data Exclusion and Addition Criteria 8
   2.2 Developing Surfaces for Upper and Lower Extent of Sediment Deposit 9
      2.2.1 Setting Horizontal Extent of TINs 9
      2.2.2 Setting the Horizontal Resolution of the TINs 10
      2.2.3 Developing the Top TIN 11
      2.2.4 Developing the Bottom TIN 12
   2.3 Developing the 3D Mesh for Sediment Sub-area Calculations 12
   2.4 3D Interpolation to the Mesh 13
   2.5 Isosurface Volume Calculation 14
   2.6 Visualization 15
   2.7 Export and Ease of Review 16
3. Quality Assurance and Model Refinement 17
   3.1 Testing “Capture” of Scatter Point Sets 17
   3.2 Model Refinements to Improve Model Outcomes 17
      3.2.1 Inaccuracy of Isosurface Volume 17
      3.2.2 Discarding Data Outliers 17
      3.2.3 Truncation 18
   3.3 Testing Quality Improvement from Dataset Exclusion or Inclusion 18
   3.4 Use of Percent Solids as a Covariate Evaluation 18
4. Summary 19
5. References 20

Tables

Table 2.1 General Format for Sediment Sampling Data to be Loaded Into GMS
Table 2.2 Characteristics of Surface TINs Used to Describe OU1 Sub-areas

Figures

Figure 1.1 Idealized Profile of Sediments Where 2D Interpolation May Fail to Accurately Delineate the Deposit
Figure 2.1 Preliminary Surface TIN for Sub-area C
Figure 2.2 Idealized Depth Profile Used to Distinguish Removal Prism (Isopach) From Isosurfaces at a Set RAL
Figure 2.3 Cardhouse Representation of PCB Concentrations in a Sediment Deposit.

1. Introduction

This white paper has been prepared in response to a request by the Wisconsin Department of Natural Resources (WDNR) to present the methodology used to identify boundaries of polychlorinated biphenyl (PCB) contaminated sediments in Lower Fox River Operable Unit 1 (OU1).

1.1 Purpose and Scope

The purpose of this white paper is expressed in three parts:

1) address the rationale for development of PCB contaminated sediment prisms in OU1 using three-dimensional modeling software;

2) describe the three-dimensional (3D) modeling approach and associated software (GMS[1]), and;

3) discuss refinements applied to GMS for the application of modeling contaminated sediment deposits in OU1.

Following this introductory section, Section 2 describes the general modeling approach and Section 3 presents the measures that have been taken to refine the GMS model for use in OU1. Although GMS is intended for a wide range of geo-environmental applications (GMS, 2002), the scope of this white paper is limited to application of GMS for modeling PCB contaminated sediment deposits in OU1.

1.2 Background

The specific goals and strategies employed to date for site characterization and sediment modeling in OU1 have varied for the Fox River Mass Balance Study, the Remedial Investigation (RI), the Feasibility Study (FS), and the Record of Decision (ROD). This white paper addresses how 3D sediment modeling meets the needs of the remedial design/remedial action phase of the project. Additional background on the RI/FS methods and ROD requirements are also provided.

1.2.1 RI/FS Methodology

The goals of deposit modeling methods used for the RI/FS were to provide estimates of PCB mass distribution and the potential impacts of contaminated sediments, as well to provide estimates of sediment volume and sediment properties needed to evaluate remedial options.

Historically, WDNR has employed a two-dimensional (2D) interpolation modeling strategy in OU1 to estimate sediment volumes, sediment thicknesses, and PCB mass associated with particular deposits. WDNR's model evaluated PCB contamination in sediments using independent, multiple layers of sediment sorted by increasing depths – and incorporated a 2D interpolation method with the following attributes:

- Inverse distance weighting (IDW) with a power parameter of 5.

[1] GMS is a computer application licensed by Environmental Modeling Systems, Inc., South Jordan, Utah.

- Interpolation radius of 400m (1230 ft.), with data segregation in 10 m square grids, and depth intervals of 0-10 cm, 10-30 cm, 30-50 cm, 50-100 cm, 100-150 cm, 150-200 cm, 200-250 cm, 250-300 cm and >300 cm.

A more detailed description of the interpolation method used by WNDR is presented in the Final Model Documentation Report (WDNR, 2002a).

1.2.2 Record of Decision Requirements

The ROD for OU1 and OU2 was issued by WDNR and U.S. EPA in December 2002 (WDNR, 2002b). For OU1, the ROD requires that pre-design sampling and characterization work define the horizontal and vertical extent ("footprint") of the sediment with a total PCB concentration above the Remedial Action Limit (RAL) of 1 ppm. A portion of this footprint will be dredged while other portions could be amenable to capping as the contingent remedy.

The ROD did not specify a method or model that should be used to estimate the RAL footprint.

1.2.3 Use of Model for Remedial Design

In August 2003, a pre-design sediment characterization report for Deposit A presented an approach for delineating the RAL footprint (Foth & Van Dyke, 2003). The model in the characterization report uses a three-dimensional (3D), inverse-distance weighted (IDW) interpolation method and the computer application GMS version 4.0.

GMS has since been used for more detailed modeling work in OU1 to support engineering evaluations, project planning, and the remedial design. While the WDNR 2D model was suitable for the RI/FS, the GMS-based, 3D model is considered to be more applicable and useful to the design process where 3D grading plans for setting of dredge grades and more precise volume determinations are required. Since the model varies from the WDNR model, this white paper was generated to more fully discuss the rationale and methods for the 3D modeling process.

For deposits that are to be dredged or capped, the economy and effectiveness of remedial designs depend largely on accurate delineation of the contaminated regions. Doing this well is a technical challenge with high stakes, and two major tradeoffs. The first tradeoff is one of sampling density. Accurate delineation of contaminated regions generally increases with greater sampling density, but sampling and analysis costs also rise accordingly. Effective sample designs often use modeling tools, adaptive sampling techniques and staged approaches to optimize the sampling plans. The second tradeoff deals with the level of conservatism used to address uncertainty in the remedial design. If there is a relatively uncertain delineation of the contaminated region, the certainty of removal of contaminated regions generally increases as more sediment is removed. However, remediation costs are directly related to the amount of sediment to be removed and processed. Poor delineation and excessive removal of cleaner sediment can have large cost consequences.

Deposit modeling for accurate delineation of contaminated regions provides a critical link between sampling and remedial actions. The extent of the soft sediment deposits is used to establish a modeling boundary, and sample results are used to interpolate contamination

concentrations to a dense, 3D model mesh. The 3D mesh then represents the characterization of the whole deposit with high resolution.

1.3 Rationale for Selection of GMS and IDW Methods for Sediment Modeling

The rationale and criteria for the selection of GMS and the IDW method for sediment modeling in OU1 are discussed below

1.3.1 Need for Model to Match Characteristics of Sediment Deposits

There are several general aspects of Lower Fox River OU1 sediment deposits that are important in the selection of a modeling tool:

- Soft sediment in the river is composed of silts and silty clays, and most of the PCB contamination is found in the soft sediments.
- Soft sediment thickness generally ranges from 0 – 6.5 ft. Soft sediment deposits may be bounded laterally by shoreline or by fine sand and gravel deposits. Near these boundaries, soft sediment thickness may be negligible. With depth, soft sediment is most often bounded by a clayey, glacial till.
- Soft sediment thickness may vary by 0.5 ft. or more in distances of 100 ft. or less.

A large portion of the PCB mass found in OU1 soft sediment deposits has been found in the upper 1 foot (30 cm) of sediment. For example, WDNR estimated that Sub-areas A, E, and POG contain about 91% of the PCB mass present in OU1. For these sub-areas, about 53% of the PCB mass is present in the upper 1 foot (30 cm) of sediment (WDNR, 2002c.).

Sub-area A data indicate a relatively shallow zone of PCB contamination over an area of roughly 40 acres. While WDNR estimates 53% of the PCB mass of certain deposits is located in the top 1 ft., it is also relevant to the design aspects of the project that 88% of the samples reporting above the RAL were found in the top 1 ft (WDNR 2002c).

Modeling to support delineation of PCB contaminated sediments in OU1 should, therefore, be scrutinized with respect to accuracy with depth. Suitable models should “capture” contaminated samples at depth without establishing dredge prism elevations that would result in excessive removal of sediments with PDB levels less than the RAL.

1.3.2 Need for 3D Interpolation of Sediment Deposits

Contaminated sediment deposits tend to be stratified vertically. Previous attempts to estimate contaminated sediment deposit volumes have been based on a 2D interpolation method (WDNR, 2002a). This method effectively treats the deposit as if there was no correlation of PCB concentration occurring in different sediment layers. 2D interpolation is also made more difficult if the sampling interval with depth is irregular, if datasets from different sampling periods are combined, and if the deposit includes channels, eddy features, or sand ridges.

A 3D interpolation strategy can offer a more refined characterization of the sediment deposit concentration trends and the deposit volume. An idealized profile of a soft sediment deposit is

shown in Figure 1.1. By considering the potential correlation of sediments at various sediment depths, 3D interpolation offers a more accurate representation of the sediment deposit. In addition, the ease of use is increased because less preprocessing of data is needed to assign a given sample to a model layer.

Since the correlation of PCB concentrations with depth is generally much less than with lateral distance, 3D interpolation methods that account for vertical heterogeneity are more appealing. For instance, in certain shallow deposits, contaminant concentrations at different positions may be completely uncorrelated at vertical distances of 2 ft., as compared to lateral distances of 300 ft. However, at greater depths, the degree of horizontal correlation in PCB concentrations may be much less. 3D interpolation offers flexibility in selecting modeling parameters to provide an acceptable match to the data horizontal and vertical distribution. There is a balance that can be reached between the accuracy of concentrations predicted at the surface versus effective delineation of the contamination at depth. As normally applied, 2D interpolation lacks this general flexibility offered by 3D interpolation models.

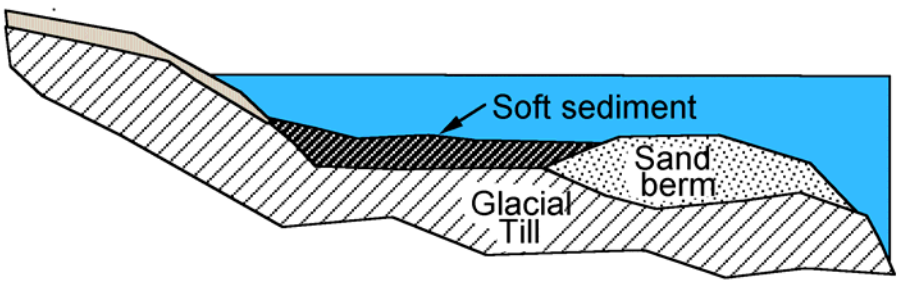

Figure 1.1 Idealized Profile of Soft Sediment Deposit Where 2D Interpolation May Fail to Accurately Delineate the Deposit.

1.3.3 Selection of GMS as 3D Interpolation Tool

GMS (v. 4.0, Environmental Modeling Systems) is one of several available platforms to perform 3D interpolation. GMS provides powerful tools for digital terrain modeling. In fact, GMS is organized around a set of terrain modeling tools that were first developed for cut-and-fill imaging and volume calculations used in civil and geotechnical engineering (Jones 1990, Jones and Wright, 1993). Research and development of the terrain modeling tools at the University of Texas at Austin was supported by the US Army Corps of Engineers. Further development of GMS (Department of Defense Groundwater Modeling System) was led by Prof. Norm Jones and Jim Nelson of Brigham Young University, with funding from the U.S. Department of Defense, the Department of Energy, the Environmental Protection Agency, and the Environmental Modeling Research Laboratory at Brigham Young University.

GMS offers the use of several 3D interpolation methods, including kriging, natural neighbor, and various IDW methods. Other factors that led to the selection of GMS for estimating contaminated sediment deposit volumes were:

1. Accuracy. Prior to commencing dredging activities the stakeholders should be confident that, by following the dredge plan, effective removal to the RAL will occur. The interpolation options and basic methods within GMS have been tested and verified

for accuracy as described in Section 2 of this white paper. In addition, the flexibility of modeling options allows for ongoing refinement to improve the quality of the estimates.

2. Capture of sample points with total PCB concentrations above the RAL. GMS can be used with other graphics and analysis packages to verify that all sample points with concentrations above the RAL are included in the RAL isopach. While it is possible that the interpolation methods employed may not capture isolated samples with concentrations above the RAL, supplemental data processing strategies are used to identify outliers. Once identified, outliers can be incorporated into the overall dredge scheme if appropriate.
3. Use of GMS as a sampling design tool. GMS may be used to identify regions of sparse sampling near the PCB isopach boundary. As such, GMS is useful as a sampling design tool for future sampling efforts (if needed) to refine the isopach delineation.
4. Validation. Ability to test statistical properties of interpolated results, jackknife interpolation, and other geostatistical methods.
5. Compatibility with CADD. Mapping data can be imported into GMS from CADD (or equivalent program), and results of surface models and interpolated PCB isopachs at the RAL from GMS can be exported to CADD (or equivalent program). GMS also offers compatibility with spreadsheet and plotting applications.
6. Ease of use, ability of others to review results. A demonstration version of GMS is available for the public, offering reviewers an opportunity to review datasets and methods used in GMS. GMS is widely distributed at the U.S. Army Corps of Engineers, and is available to US EPA and other federal agencies.
7. Visualization. GMS offers outstanding visualization features, including color contours, shaded surfaces, cross-sections, and animation. Graphics can be exported to image files for display and presentation.

Although GMS has a wide range of features, other applications with overlapping features may be used. In particular, CADD (or equivalent program) is used to provide higher-resolution maps, to prepare engineering drawings such as dredge grading plans and cross-sections, as well as output files for use by dredging contractors (e.g., DXF or DGN files for Dredgepack® software[2]).

1.3.4 Selection of GMS Interpolation Algorithms

Several interpolation algorithms are available within GMS. GMS work to date on OU1 has been based, almost exclusively, on the use of a modified inverse distance weighted (IDW) method. This method is also called Shepard's method because the power (p) of the weighting function is 2 (Shepard, 1968). GMS implementation of the Shepard's IDW method uses a normalized weighting function (Franke & Nelson, 1980) that differs somewhat from the classical IDW weighting function.

Factors which have led to a preference for the use of Shepard's IDW method in 3D over other alternatives (kriging, other IDW methods, natural neighbor, and others) include:

[2] Dredgepack® is a registered computer application from Coastal Oceanographics, Inc., Middlefield, CT.

1. WDNR used a 2D IDW method in order to develop sediment volume and PCB mass estimates for the Lower Fox River RI/FS studies.

2. Suitable agreement to sampling data were found with Shepard's method. The kriging algorithm in GMS, even after multiple trials, was not found to produce results in 3D that were representative of the sampling data.

3. A particular advantage of Shepard's method is its ability to address vertical heterogeneity. In addition, Shepard's method works relatively well in subregions of low sample density as well as high sample density.

Limited evaluations of natural neighbor and other IDW algorithms within GMS have been considered unsuccessful, because of poor overall model performance (inaccurate predictions, slow processing time, and memory-related application errors). These limitations have generally not been found when using Shepard's method.

While Shepard's method will likely continue to be the preferred interpolation algorithm for OU1 deposits, other algorithms could prove to be more representative for some deposits given deposit-specific sampling schemes, data sets, and geometry.

1.3.5 Current State of Review of GMS

GMS has been applied and discussed within a previous Sub-area A sediment characterization report (Foth & Van Dyke, 2003). Since then, GMS has been used to refine estimates in other OU1 sediment sub-areas. To date, GMS has been used for Lower Fox River deposits to:

- organize and display sediment core sampling data,
- model the geometry of certain deposits (shoreline boundary, top of sediment, soft sediment thickness),
- estimate the volume of sediment and sediment properties above a threshold or limit concentration, and to
- visualize spatial trends in contaminant concentration.

This white paper addresses the current state of GMS as applied to OU1.

2. GMS Approach for OU1

This section summarizes the general approach for the use of GMS to model contaminated sediment deposits in OU1. This section addresses the main steps used to:

- enter sediment sampling data into GMS
- form the sediment deposit mesh
- perform the interpolation
- calculate the isosurface volumes
- export the results to CADD (or equivalent program)
- visualize the results

2.1 Entering Sediment Sampling Data

For Sub-area A, the general strategy for composing the active dataset for GMS is to initially include all the validated 2003 Pre-design sampling data and data from the WDNR Fox River Database (FRDB), then to edit points according to an explicit process and usage criteria. These criteria are discussed below. The active data sets for other sub-areas are initially constructed with 2003 Pre-Design sampling data alone, and may be enhanced with Phase 2 sampling data and/or historical data from the FRDB if data gaps are evident.

Sediment sampling data can be loaded into GMS from simple, delimited text files. The text import routine supports a variety of formats and data type targets. In this case, sample data are loaded as 3D scatter point sets. A sample data file format is shown in Table 2.1. The elevation coordinate (Z) is loaded in units of feet, as the elevation relative to the top-of-sediment (e.g., if the sample was at a depth of 1.3 ft., the value of Z would be listed as –1.3). [3]

Core sample data are reported for a sampling interval, but GMS treats each sample as a point value. As a representative value for PCB interpolation, the elevation at the middle of the sample interval has been used. .

Table 2.1 General Format for Sediment Sampling Data to be Loaded Into GMS.

Sample I.D.	X (ft.)	Y (ft.)	Z (ft.)	PCB (ppm)	Percent Solids	TOC (ppm)
C-01-A	2369210.02	806441.23	-0.33	6.0	16	-999
C-01-A-C	2369210.02	806441.23	-0.66	2.3	24	-999
C-01-D	2369210.02	806441.23	-0.98	0.089	27	-999
C-01-E	2369210.02	806441.23	-1.31	0.064	27	-999
C-02-A	2369325.41	807046.64	-0.33	0.049	53	-999

[3] WDNR's preferred vertical datum for the Lower Fox River sediment remediation projects, as of July 2003, is NAVD 88, and the horizontal datum, WTM 83. Final Design outputs for dredge elevations and post dredge verification work will conform to these datums.

Total PCB concentrations are loaded in units of mg/kg (ppm). If the reported PCB concentration is less than one-half of the reported detection limit (RDL) for that sample, the PCB concentration is assigned the value of one-half the RDL. Percent solids (%),TOC (mg/kg), and other data may also be entered. Missing values are assigned a missing value flag (commonly –999).

2.1.1 Interpolation Set Data Exclusion and Addition Criteria

In general, the exclusion of real samples and inclusion/modification of data values at specified locations is avoided – so that geostatistical properties of the dataset are properly reported as input to the model. In addition, a record for all OU1 sampling data is kept in a multiple worksheet spreadsheet file (MS Excel or other spreadsheet application), listing the data considered, the data used for GMS, added data points, and the data excluded. Sample data used for each sub-area model are also clearly described.

There are limited cases for which sample data are excluded and other values are added to the active GMS dataset. The criteria and rationale for editing data values in the active GMS set are listed below.

Criterion #1: Exclude duplicates.

Rationale: Since GMS cannot load multiple 3D scatter point data at the same point in space, duplicates are removed prior to loading the set into GMS.

It is important to note that duplicates are clearly marked prior to analysis and that duplicates were obtained for analytical QA/QC purposes only. Exclusion of duplicates was based on sample identification prior to delivery to the laboratory, not the lab-determined concentrations of the primary or duplicate samples.

Criterion #2: Exclude sample data from full-length composite core samples, unless the sampling depth is shallow, there are no other sampling locations nearby, or if the PCB concentration is below the RAL. The criterion applies to historical (pre-2003) data only.

Rationale: In certain datasets for Sub-area A, some samples were collected from composite samples incorporating the entire core length, with a resulting thick sampling interval from the surface to depths of 3 ft. or greater. However, nearly all recent samples (2002 and newer) are more consistently collected and analyzed with relatively thin sample intervals (e.g., 0 – 10 cm or 0 – 0.33 ft.). Since the majority of PCB contamination is present in the upper 1 foot of OU1 Fox River sediments, it is likely that the process of including data from a full-length composite core sample would lead to an inaccurate assessment of PCB contamination at depth. For example, where a core with many samples may show high PCB concentrations to a depth of 1.0 ft. (but low PCB concentrations from depths of 1-3 ft.), a 3-foot composite core sample collected at the same location could be misinterpreted as a sample with high PCB concentration to it's mid-point depth. Alternatively, if a historic composite core sample reports a PCB concentration below the RAL, it is appropriate to include the sample since the sample is expected to have a PCB concentration near or below the RAL over the whole depth.

Criterion #3: Represent sample stations with "no soft sediment" as a surface sample.

Rationale: WDNR allows special consideration of sampling stations if no sample could be obtained due to the physical absence of soft sediment. In such cases, we have assumed the PCB concentration at the sampling location to be 0.025 ppm, the average PCB concentration determined from 7 samples taken below soft sediment at the top of the native clay layer in Sub-area A during the Foth & Van Dyke 2002 sampling event (Foth & Van Dyke, 2003). The sample ID is designated by the name of the sampling station and the suffix "–NS". For example, no soft sediment was found at Sub-area A sampling station A13, so the sample point is named "A-13-NS" and assigned a depth interval of 0.00 – 0.10 ft. For all of OU1, there were 116 stations at which –NS designations were assigned and added to the active GMS sample dataset which totals approximately 5100 samples.

Criterion #4: Exclude older samples at locations for which more recent confirmation sampling is applied at the same, or adjacent location.

Rationale: Confirmation sampling is a tool to determine whether or not a former sample was correctly quantified, or whether or not conditions have changed at a particular sample location. For the cases in which additional, more recent sampling is specifically targeted to address uncertainty at the same location as a prior sample, the more recent sample is retained and the prior sample is excluded. A comment is added to the excluded sample record, indicating that it was replaced by a confirmation sample. For the active GMS dataset for OU1, samples taken in 2000 at station LLBM-A-80 were excluded (FR1279 and FR1280, PCB concentrations 2.06 ppm and 0.08 ppm, respectively). Confirmation samples (with the same sample intervals) collected at station A-28 in 2003 (A-28-A, A-28-A-C) revealed lower PCB levels (0.41 ppm, 0.04 ppm respectively) at this location at the same depth intervals.

2.2 Developing Surfaces for Upper and Lower Extent of Sediment Deposit

Modeling of the sediment deposit as a continuous 3D solid requires generating surfaces to describe the top and bottom of the sediment, and using GMS tools to build 3D meshes, 3D grid models, or other solid object representations. Surfaces are described by triangulated irregular networks (or TINs). TIN nodes can be imported as 2D scatter point files, or created within GMS. The TIN nodes are points with 3D position coordinates (XYZ). GMS uses automatic triangulation algorithms to connect the nodes into a network of triangles. Upon triangulation, the TIN nodes become the common vertices of the triangles.

2.2.1 Setting Horizontal Extent of TINs

TINs are confined by the shoreline, and, if desired, any predetermined sub-area boundaries. In general, the TIN should extend beyond all sampling locations in the deposit – or, at least, all sampling points in the deposit with PCB concentrations near the RAL. It is important to note that sample subsets from adjacent sub-areas may be included in the interpolation, even though these points lie outside the modeled sub-area boundary.

Boundaries should be imported to GMS from CADD (or equivalent program) to define the shorelines and sub-area boundaries. It is important that CADD and GMS boundaries and other mapping objects be accurately positioned and consistent.

2.2.2 Setting the Horizontal Resolution of the TINs

Setting the horizontal resolution, or the TIN density, is a decision made by the modeler based on site-specific conditions. In general, TIN density should be considerably higher than the sampling density, be set to allow effective delineation of the shoreline and other boundaries, and be limited to a manageable total number of TIN vertices.

For Sub-area A and other OU1 sub-areas with a more uniform sample grid spacing (e.g. 230' or 350' triangular), the TIN density is established using a uniform 30 ft. triangular grid with the inclusion of actual sample locations as additional TIN nodes. The characteristics of surface TINs for Sub-areas A and C are summarized in Table 2.2. A preliminary image of the top TIN surface for Sub-area C is shown on Figure 2.1.

Table 2.2 Characteristics of Surface TINs Used to Describe OU1 Sub-areas

Sub-area	TIN vertices	TIN triangles	TIN area (Ac)	Average number of TIN nodes per acre	Average number of triangles per acre	Average number of sampling stations per acre
A	4231	8189	71.4	59	115	2.0
C	1158	2128	18.6	62	115	1.0

Figure 2.1 Preliminary Surface TIN for Sub-area C. Positions of sampling stations (•) and grid lines spaced at 500 ft. (---) are also shown.

2.2.3 Developing the Top TIN

The upper surface, or top TIN, may be flat or contoured to portray the top of sediment. Experience to date with GMS has shown that the flat TIN top surface works best, for two reasons. The first reason is that the interpolation results were found to be more representative with a flat model. Although efforts have been made with OU1 data to use an elevation-based top TIN, the resulting volume estimates have been larger than physically possible (given the deposit area and average soft sediment thickness). The errors that occur are likely due to an implied correlation of PCB concentrations with elevation (rather than depth). Performing the same operations with a flat top TIN produces a more reasonable volume estimate. The second reason is

that most of the WDNR archival sampling data are reported in terms of sample interval depths (not elevations). Building an elevation-based top TIN would require the estimation of the elevations for these sets. Converting the depth-based isopachs to elevation-based maps for design plans is easily accomplished using elevation-based surface data collected during the 2002 and 2003 OU1 sampling events.

2.2.4 Developing the Bottom TIN

The lower extent of the interpolation region, or bottom TIN, is designed to be contoured to match depths to a confining layer. Since the bottom TIN will define the lowest extent of the 3D mesh, the design of the bottom TIN can be a crucial step towards the goal of accurate delineation of contamination in a sediment deposit. The following guidance is offered:

- Evaluate core logs and sediment probing data to determine the thickness of the soft sediment in the sub-area.

- Evaluate the sample data to determine the lowest extent of PCB contamination above a threshold value. The depth of the bottom TIN should extend to a depth greater than the lowest sample with a PCB concentration over a threshold value (i.e., a RAL).

Once the mesh is formed and PCB sampling data are interpolated to the mesh, there may be additional modeling steps to accurately delineate the lower extent of contamination. These steps should include:

- Comparison of isopach depth versus mesh extent. If there is evidence of deeper contamination in soft sediment beneath the bottom TIN, the bottom TIN would need to be extended to greater depth.

- Evaluation of samples below the bottom TIN. If a given sample has a PCB concentration above the RAL, and is beneath the bottom TIN, the bottom TIN would be extended to provide “capture” of the sample point.

2.3 Developing the 3D Mesh for Sediment Sub-area Calculations

A 3D mesh is used as the primary 3D solid model of the sediment deposits. A 3D mesh is a connected network of multiple, triangulated layers. 3D scatter point data, such as PCB concentrations can be interpolated to the nodes of the 3D mesh. Data values produced from interpolation, such as PCB concentrations or percent solids values, are stored at each mesh node. Imaging and volume calculation tools can then be used to explore and reveal properties of the sub-area.

Once the top and bottom TINs are formed, 2D and 3D meshes can be generated. The 2D mesh can be formed directly from the top TIN. For this process to work smoothly, the 2D mesh, top TIN, and bottom TIN need to be aligned with the same XY coordinates and have the same number of nodes. The 3D mesh requires the existence of a 2D mesh, and is formed by selecting the top and bottom TINs, then “filling” between the TINs with a number of uniformly spaced layers. The maximum vertical spacing can be set to the smallest depth interval for sampling (such as a 4 in. or 10 cm spacing).

2.4 3D Interpolation to the Mesh

For OU1 sediment sub-areas the GMS implementation of Shepard's method has been used almost exclusively for interpolation of PCB sample concentrations to the 3D mesh. The interpolation routine requires the selection of two main parameters, the number of points used in calculating interpolation weights (N_p) and the z-scale anisotropy factor (α_z). If $N_p = 10$, the interpolation algorithm considers the 10 nearest points to a mesh node, calculates the interpolation weights based on distances, and uses these interpolation weights along with the concentrations at the nearest 10 sample points to determine the PCB concentration at the mesh node. The interpolation weights are larger for smaller distances between the sample point and the mesh node.

The z-scale factor, α_z, is a model parameter to compensate for the anisotropy in the vertical direction. If the distances between scatter points along the vertical traces are significantly smaller than the differences between scatter points along the horizontal plane, the effects of clustering along vertical traces can be minimized using the z-scale factor. For instance, if a z-scale factor of 100 is applied, a vertical distance of 1 ft. would be treated with the same weight as a horizontal distance of 100 ft. This can result in improved accuracy, especially for cases in which the degree of horizontal correlation is significantly greater than the vertical correlation, as is the case with OU1 sediments.

One strategy for setting IDW parameters is to select a z-scale factor from the ratio of horizontal and vertical sample spacings. For many sub-areas in OU1, the horizontal spacing is roughly 250 ft. and is based on an even triangular grid. The common vertical spacing is 4 in. (0.333 ft.). A z-scale factor set to the ratio of horizontal to vertical sample spacings, therefore, would be 750.

Initial selection of α_z and N_p can also be based on jack-knife interpolation results. One data point is temporarily excluded, and the rest of the set is used to interpolate a data value at that isolated location. This is done for the whole set, and errors between the interpolated values and the actual dataset are summarized. Once selected, the interpolated parameters should be optimized, if necessary, to maximize capture of sample locations with PCB concentrations exceeding the RAL, and to minimize excessive dredging at locations known to contain PCB concentrations below the RAL, as described below.

The main objectives are to maximize capture of all locations with PCB concentrations above the RAL and to minimize excessive dredging at locations known to have PCB concentrations below the RAL. The evaluation of jack-knife errors, therefore, will be most effective when there is particular focus on the quality of PCB concentration estimates for sample points that are expected to be located near the RAL isopach. Evaluation of jack-knife errors without this focus can be misleading, since the errors at a few points, particularly at sample points with the highest concentrations, can overwhelm the errors that may be more useful for delineating PCB concentrations near the RAL.

For most sub-areas in OU1, we have found excellent capture with a range of z-factors when the interpolation neighborhood is relatively small ($N_p = 4$ or $N_p = 8$). However, in order to also minimize excessive dredge cuts (with depth or horizontal extent) into regions with sample concentrations below the RAL, the z-factor is adjusted.

Once these two interpolation parameters are set and the 3D PCB scatter point dataset is selected, the user applies the command to interpolate that set to the 3D mesh. The 3D interpolation assigns PCB concentrations to all nodes of the mesh. Relatively dense meshes may have 50,000 node points or more. Mesh post-processing options within GMS include volume calculations, visualization and statistical tools to evaluate the data distributions.

2.5 Isosurface Volume Calculation

An isosurface is the 3D equivalent of the contour line. Each isosurface represents a certain concentration level. GMS uses interpolation between 3D mesh nodes to estimate the location of the isosurfaces. As the volume representing the subregion with a total PCB concentration above the RAL is of the most interest, the discussion below will focus on the RAL isosurface.

Since subregions with total PCB concentrations above the RAL may be clustered and discontinuous, the RAL isosurface may actually be a set of isosurfaces. There are a few aspects of isosurfaces that are particularly relevant to the estimation of sediment volumes. These aspects are:

- A higher mesh density generally provides for more precisely located isosurfaces. Since linear interpolation is used to estimate the location of an isosurface (between mesh nodes), the user may be assured that the selected interpolation method is responsible for the location of an isosurface when there is a higher density mesh. In addition, the curvature of an isosurface is better estimated with a higher mesh density.

- The generated isosurface may have an irregular shape and may extend the full depth of the mesh. A depth profile of an isosurface, such as is shown on Figure 2.2, may show isolated clusters of cleaner sediment, with PCB concentrations below the RAL, embedded within the RAL isosurface region. The region to remove (dredge) should extend from the top of sediment to the deepest extent of the isosurface – and this removal region could be described as a TIN or an isopach

- The isosurface may not capture all sample scatter points with PCB concentrations above the RAL. This is possible when an isolated sample point is slightly above the RAL, and other concentrations in the same area are well below the RAL. If the interpolated concentration at the nearest mesh nodes is below the RAL, a RAL isosurface will not be developed near the isolated sample point. This effect can be reduced if the mesh nodes are aligned to the sample points.

- The RAL isosurface may extend into subregions in which no sample has a PCB concentration above the RAL. This is possible when a subregion of highly contaminated material is adjacent to a relatively clean area. The influence of the samples with higher concentration may be greater than the influence of samples with lower concentrations that happen to be closer to the mesh nodes.

- The RAL isosurface may extend into subregions in which no samples are present. For this reason, it may be necessary to provide additional sample points to further delineate the RAL isosurface (Phase 2 sampling). With depth, it may be important to consider whether the RAL isosurface has extended into a confining glacial till or rock unit.

Alternatively, the deepest extent of the mesh could be confined to the regions of soft sediment (see sections 2.2.4 and 3.2.1 for further discussion).

Isosurface volumes can be verified by CADD (or equivalent program) and by other external calculation methods. Exported data for the RAL isosurface is used to develop a RAL isopach surface for CADD (or equivalent program). One simple check to evaluate the validity of the magnitude of the interpolated isosurface volume is to estimate the mean depth of the isosurface, then to multiply that estimate by the surface area of the isosurface.

Once the PCB-contaminated sediment delineation at the RAL has been interpolated using GMS, and the isosurfaces exported to CADD (or equivalent program), the sediment removal plans (dredge grading plans) will be engineered taking into account dredging accuracy, allowable overcut, and appropriate side slopes. Therefore, the implementation dredge prism volumes will likely exceed the GMS interpolated volumes at the RAL in each sub-area.

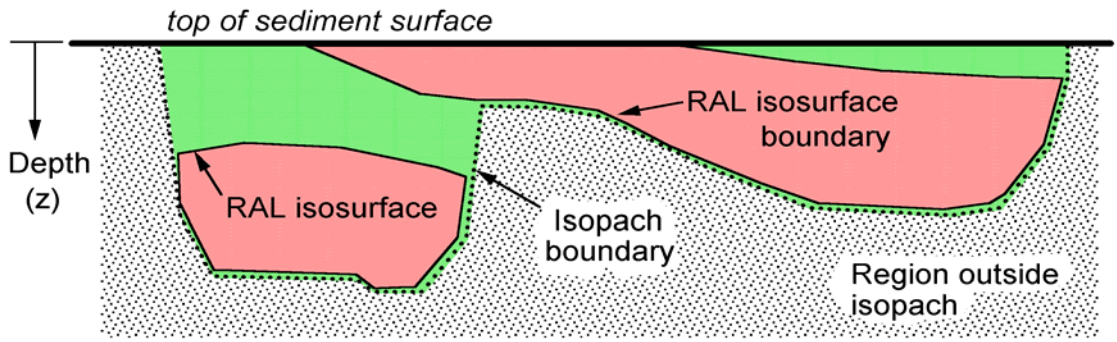

Figure 2.2 Idealized Depth Profile Used to Distinguish Removal Prism (Isopach) From Isosurfaces at a Set RAL. Isosurfaces are the result of interpolation and delineate regions with PCB concentrations above the RAL (shaded light red). Removal prism (isopach) extends from the top-of-sediment surface to depth to include all RAL isosurfaces and some cleaner regions (shaded green).

2.6 Visualization

GMS can be used to generate color images, sections, and video streams to better visualize sediment deposit characteristics. Once the 3D mesh is generated and data values are interpolated to the mesh, there are a wide variety of visualization features available to the user. These include:

- plan view, profile views, oblique (isometric) views from any compound angle,
- contour plots,
- shaded surface plots,
- sections and
- animation (.avi file generation)

Interpolation results can be compared visually to color-coded sample scatter points. Cut away sections can be used to isolate specific exposures of the sediment deposit. An example cardhouse section image for a sediment deposit is shown in Figure 2.3.

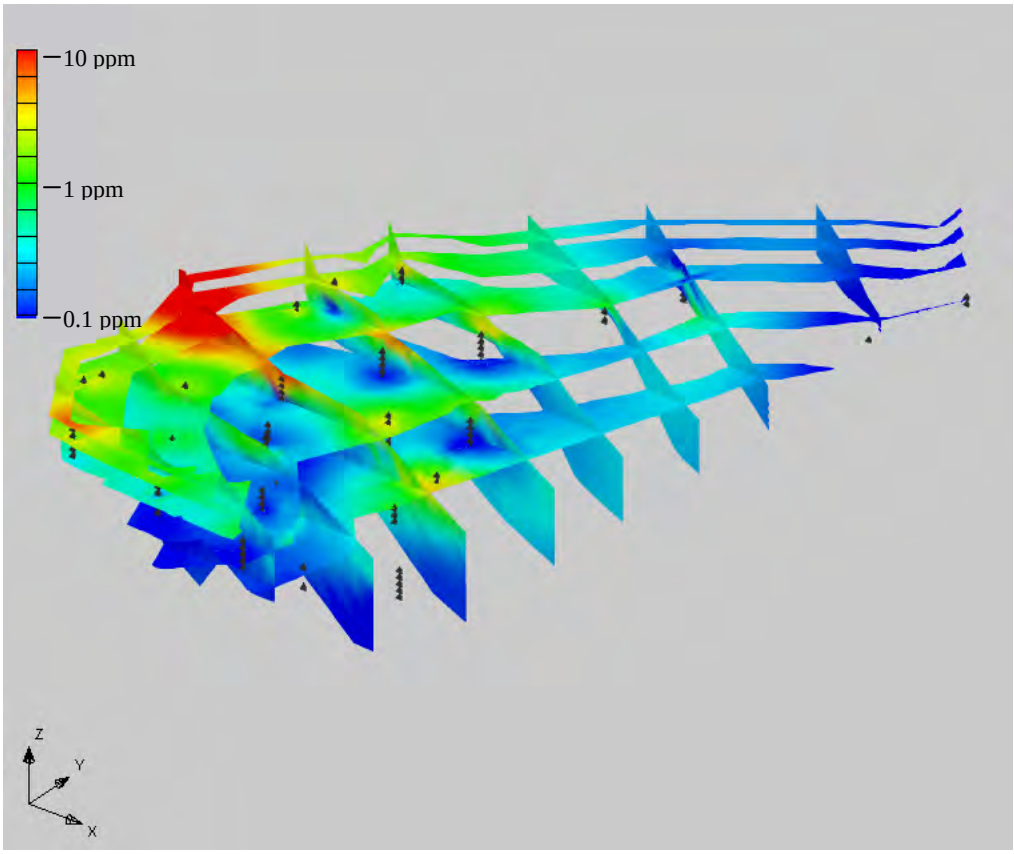

Figure 2.3 Cardhouse Representation of PCB Concentrations in a Sediment Deposit. Vertical scale is exaggerated 100 times.

2.7 Export and Ease of Review

GMS supports several common file formats for data export. GMS offers coordinate conversion and other tools to coordinate mapping and image data. In addition, a full function demo version of GMS (saving, export features, and printing disabled) is available for reviewers (see http://www.ems-i.com/gms for more details).

Supported export formats for GMS include:

- text file export of 3D mesh data (node id, X, Y, Z, data values)
- text file export of TIN data
- text file and .dxf export of map data
- image file export (.tiff)
- other formats

Data are easily copied-and-pasted into spreadsheet applications. Import and export of scatter-point and DXF image data between GMS and CADD are straight-forward.

3. Quality Assurance and Model Refinement

This section addresses several quality assurance and model refinements methods used to aid the characterization and analysis of sediment deposits.

3.1 Testing "Capture" of Scatter Point Sets

Since there are often many sampling data points with a range of PCB concentrations, it is sometimes difficult to review the sampling scatter points graphically in GMS. As such, other graphics applications can be applied in which a data filter strategy is utilized. Plan view plots of the sub-areas are viewed with the following criteria for the scatter points:

- Show only sample points above a threshold PCB concentration (at RAL)
- Show only sample points below a given depth (0, 1, 2 ft.)
- Color the plot symbol relative to PCB concentration

Using this plotting strategy, one can quickly identify the general distribution of samples at various depths that exceed the RAL and compare these observations with GMS views of the interpolated isosurface, or superimposed plots of the 3D mesh.

3.2 Model Refinements to Improve Model Outcomes

There are several refinements that may be used within GMS to improve model outcomes. These include ways of identifying and correcting inaccurate isosurface volumes, discarding sample data outliers, and using data truncation as an interpolation option.

3.2.1 Inaccuracy of Isosurface Volume

As a check, GMS provides the results of the calculation of mesh volume with the reporting of the isosurface volume. If the error is appreciable, isosurface volume estimates are scrutinized. Efforts to reduce the errors may include applying slightly different interpolation options, expanding or refining the mesh, or checking the volumes of isosurfaces that may correspond to different concentration levels.

As described in Section 2.5, isosurface volumes are checked by CADD (or equivalent program) and other external calculation methods. A large relative error may indicate a problem with the interpolation routine.

3.2.2 Discarding Data Outliers

As an example, for work in Sub-area A, an evaluation of the historic data from the FRDB resulted in a decision to exclude some of the older data from the GMS interpolations. The samples that were excluded were from full-length composite cores collected over sample intervals as large as 70 cm. Since the middle depth of the sample interval is input as the sample depth (z) in our GMS interpolations, a large inconsistency is found when comparing these samples with more recent, nearby samples with thin sample intervals.

For samples that were from the composite cores, the PCB concentrations were more reflective of

the more recent samples collected near the surface. Nearby samples with intermediate depth intervals below 1 ft. were typically found to have low or nondetect PCB concentrations. Therefore, there was strong justification for excluding the few samples from composite cores from the interpolation dataset.

3.2.3 Truncation

An option within the interpolation methods is truncation. Interpolation data can be truncated to fit within the range of existing data (controls extrapolation). Truncation of interpolated results does not affect the interpolation algorithm, but acts as a data filter to control the interpolated result to a specified bound. This may be necessary for estimation of quantities such as percent solids, where concentrations should fit within the range of 5-90%. Another approach is to set the truncation limits to values that are a set percentage of the range above the maximum and below the minimum value in the dataset. A histogram of the dataset can be generated in GMS, and this may be used to provide basis for an allowable range for the interpolation. Truncation of interpolated PCB concentrations to (min, max) values within the extremes of the data range should be avoided, and has not been used in OU1 modeling work.

3.3 Testing Quality Improvement from Dataset Exclusion or Inclusion

Efforts can be directed to scrutinize and rules for the inclusion of archival datasets. In general, newer datasets should outweigh older datasets. One test of improvement should show reduced variability of the determined isosurface volume as the number of data is increased.

Jackknife interpolation can also be used to test the general improvement or deterioration of the interpolation result when a particular dataset is included or excluded. However, the tests should be on the basis of whether regions with PCB concentrations near the RAL are adequately detected, rather than the objective of minimizing raw error at sample locations with higher concentrations.

3.4 Use of Percent Solids as a Covariate Evaluation

Percent solids data and PCBs can be interpolated to the same mesh. In general, percent solids data are correlated with PCB data (low percent solids associated with higher PCB concentrations) and, furthermore, the percent solids data are less spatially variable. Contours of percent solids and TOC can be useful for selecting PCB interpolation methods or designing the mesh, on the basis of correlations. For example, PCB interpolation methods that project the RAL isosurface into sandy regions (high percent solids) should be scrutinized to assess the validity of the model input parameters as, historically, high percent solids values in the Fox River sediments have correlated with low PCB values.

Once the RAL isopach is developed, a new mesh can be generated to better estimate PCB mass and percent solids within the isopach. This may be very useful for the design of dredge and dewatering strategies, and for estimating the benefit in risk-reduction from removal of the PCB mass.

4. Summary

The main objectives of sediment deposit modeling are to accurately delineate regions of PCB contamination and to support remedial design and engineering tasks. The support tasks include dredge prism development, solids estimates, dredge plan guidance, and contingent remedy (capping) appropriateness. 3D modeling of OU1 sediment sub-areas is essential for developing more accurate representations of PCB contaminated sediments at a given RAL by considering the potential correlation of sediment contamination at various depths.

This white paper addresses the rationale, general approach, and refinements used for the selection and application of GMS for sediment modeling in OU1. The two primary modeling tasks having the most significant effect on the results are forming the 3D mesh for the interpolation and selecting the model parameters for accurate delineation of contaminated sediments. These parameters are the number of nearest points, (N_p) to consider for mesh interpolation, and the z-scale anisotropy factor (α_z) to correct for clustering and anisotropy in the vertical direction. Using the GMS implementation of Shepard's IDW method, this white paper evaluates these two primary model parameters.

GMS is shown to be an appropriate 3D model for PCB delineation with adequate flexibility to deal with varying conditions present in OU1, such as varying sediment thickness and large swings in PCB concentrations resulting from depositional dynamics. GMS also contains statistical evaluation tools to assess the accuracy and confidence of the model outputs.

5. References

Foth & Van Dyke, 2003. Lower Fox River OU-1: Deposit A Pre-design Sediment Characterization Draft Report. August 2003.

Franke, R. & G. Nielson, 1980, "Smooth interpolation of large sets of scattered data," International Journal for Numerical Methods in Engineering, Vol. 15, pp. 1691-1704.

GMS 2002. Environmental Modeling Systems, Inc., Website: (http://www.ems-i.com/gms).

Jones, N.L., and S.G. Wright, 1993, “Subsurface characterization with solid models,” ASCE Geotechnical Engineering Journal, 119(11):1823-1839.

Jones, N. L. 1990. “Solid Modeling of Earth Masses for Applications in Geotechnical Engineering”, Ph.D. Dissertation, The University of Texas at Austin, 324 p.

Shepard, D., 1968, "A two dimensional interpolation function for irregularly spaced data," Proc. 23rd National Conference of the ACM, pp. 517-523.

WDNR 2002a. Final Model Documentation Report, Lower Fox River and Green Bay, Wisconsin. December 2002.

WDNR, 2002b. Record of Decision, Operable Unit 1 and Operable Unit 2, Lower Fox River and Green Bay, Wisconsin. December 2002.

WDNR 2002c. Final Feasibility Study, Lower Fox River and Green Bay, Wisconsin. December 2002.

Appendix C

OU1 SWAC White Paper

OU1 SWAC Estimation

November 2007

Introduction:

Regulatory decision documents associated with the Fox River PCB Superfund Site require that the surface weighted average concentration (SWAC) of PCBs within each operable unit (OU) achieve certain targets after completion of planned remedial activities. However, without rigorous definition, SWAC calculation methods may vary and cause ambiguity in the final SWAC estimate. As a result of the Boldt Oversight Team June 20, 2007 draft memorandum "SWAC Estimation Procedure", and subsequent OU1 SWAC workgroup discussions, OU1 SWAC calculation methods have been more formally defined.

The purpose of this whitepaper is twofold. First, summarize and provide an example of computational methods which arose from the June 20, 2007 draft memorandum and OU1 SWAC work group discussions. This is referred to as the stratified procedure. Second, review methods of using the sediment bed model (GMS-SED) in calculating SWAC. This method was previously used in the November, 2006 OU1 Final Plan submittal, and is still used for isolated areas without representative sample core data.

Stratified Estimation Procedure:

The June 20, 2007 Boldt Oversight Team draft technical memo "SWAC Estimation Procedure" described a calculation methodology for producing an unbiased SWAC estimate and quantifying the associated estimate uncertainty. This formed the basis of subsequent OU1 SWAC workgroup discussions, which in large maintained the approach.

The SWAC estimation procedure utilizes stratification, where the strata are defined by OU1 remedy techniques. Each stratum is associated with an area (A_h) and an estimated surface concentration ($\bar{x}_h$). The overall OU1 SWAC based on stratified design is calculated as:

$$SWAC_{estimate} = \frac{\sum_h \left(A_h \times \bar{x}_h\right)}{\sum_h A_h}.$$

The uncertainty in the SWAC estimate is quantified by a statistical confidence interval. Because the SWAC is based on sample data, it is only an estimate of the true (population) average surface concentration. While we do not know the true concentration, we can quantitatively describe the expected error associated with the estimate.

Because of the large sample sizes associated with the SWAC estimate, the sampling variation is expected to be approximately normally distributed. A 95% confidence interval of the SWAC estimate is provided by

$$SWAC_{estimate} \pm z_{1-0.05/2} \times \sqrt{\mathrm{var}\left(SWAC_{estimate}\right)}$$

where $z_{1-0.05/2}$ is the upper 97.5th percentile of the standard normal distribution and var($SWAC_{estimate}$) is the variance associated with the SWAC estimate, namely

$$\mathrm{var}\left(SWAC_{estimate}\right) = \frac{1}{A^2}\sum_h A_h^2 \times \mathrm{var}\left(\bar{x}_h\right).$$

The target attainment goal of the OU1 SWAC estimate is 0.25 ppm. If the confidence interval described above for the SWAC estimate contains 0.25, it cannot be stated with statistical certainty that the true average surface concentration differs significantly from 0.25 ppm.

The strata for OU1 are defined as follows:

Table 1
Strata Definitions

Stratum	Name	Description	Area (Ac)
1	Engineered Cap	13-inch cap placement areas	111.9
2	Dredge Only	Areas where only dredging occurred	168.1
3	Interdeposit	Areas of less than 1 ppm in any 8-inch sample	466.6
4	Void	Sampled areas with no soft sediment recovery	225.4
5	Null	No sediment areas (unsampled)	246.8
6	3-Inch Sand Cover Only	Undredged areas with 3-inch sand placement	67.5
7	6-Inch Sand Cover Only	Undredged areas with 6-inch sand placement	46.2
8	Dredge and Sand Cover	Dredged and residual sand cover areas	30.2
9	Artifact/Shoreline	Artifact and shoreline areas modeled (GMS-SED Model) with > 1 ppm, but remedial action not possible	0.7

The boundaries for each stratum were developed in the OU1 Design Supplement utilizing the GMS-SED model and data collected through August 8, 2007. These strata are illustrated in Figure D1.

Data used to estimate the stratum surface concentration, $\bar{x}_h$, and variance, var($\bar{x}_h$), are dependent on the corresponding remedial action. Post-dredge sample core data are used for calculations in stratum 2 (dredge only), and pre-design and re-characterization sample core data are used in stratum 3 (interdeposit). Imputed values are used for stratum 1 and strata 4 through 9 as follows:

- Engineered cap areas (stratum 1) are assumed to have a surface concentration of half the current detection limit, i.e., 0.0065 ppm.

- Void areas are assumed to have a surface concentration of 0.0168 ppm. As given in the 2006 RA Summary Report (page 4-18), this value is the average PCB concentration of 12 native clay samples from different sub-areas within OU1 collected during pre-design sampling in 2003/2004.

- Null areas are assumed to have a surface concentration of 0 ppm.

- 3-Inch and 6-inch sand cover only areas and residual sand cover areas are assumed to have a surface concentration of half the current detection limit, i.e., 0.0065 ppm.

- The artifact/shoreline area differs from the other strata in that it does not have sample core data located within its boundaries, but also is not assumed to have a constant PCB surface concentration. The surface average in this case is obtained from the GMS-SED (pre-dredge) model interpolation.

When calculating $\bar{x}_h$ and var($\bar{x}_h$) from core data (strata 2 and 3), it is necessary to use a weighting scheme to prevent biased estimates of the mean and variance. Specifically, the pre-design sample data were collected at differing sample densities depending on the OU1 Subarea. To account for this, Thiessen polygon weights are used in estimating the sample mean and variance.

The Thiessen polygon weights are calculated as follows:

1) Identify sediment cores within stratum boundaries.
2) Develop a Thiessen polygon shapefile for this data subset.
3) Clip Thiessen polygon shapefile to the stratum boundaries.

An illustration of Thiessen polygon weights is given in Figure D2. The surface average for the stratum is then calculated as:

$$\bar{x}_h = \frac{\sum_i w_i x_{h,i}}{\sum_i w_i}$$

where $x_{h,i}$ are the sediment surface sample results and w_i are the associated Thiessen polygon weights.

The stratum sample variance and variance of the mean are similarly weighted using the Thiessen polygons, and calculated as:

$$s_h^2 = \frac{\sum_{i=1}^{n} w_i \left(x_{h,i} - \bar{x}_h\right)^2}{(n-1)\sum_{i=1}^{n} w_i \Big/ n} \quad ; \qquad \mathrm{var}\left(\bar{x}_h\right) = \frac{s_h^2}{n} \quad .$$

For strata in which imputed values are used for the surface average, $\bar{x}_h$, (strata 1 and 4 through 9) imputed values are also used for var($\bar{x}_h$). In these cases, since it is not possible to estimate the stratum sample standard deviation s_h directly from the data, s_h will instead be estimated by

dividing the expected concentration range by six. This procedure, which among other references is given in *Guidance on Choosing a Sampling Design for Environmental Data Collection* (USEPA, 2002), utilizes the normal distribution for which six standard deviations cover 99.8% of the distribution. The expected concentration range divided by six then provides a rough estimate of the standard deviation.

The concentration range will be taken as a minimum of zero and a maximum of two times the imputed value $\bar{x}_h$. While a sample size *n* is not available, in order to obtain an estimate of var($\bar{x}_h$) we will simply take 1/10th the value of s_h^2. Hence for strata with imputed values,

$$\mathrm{var}(\bar{x}_h) = \frac{\left(\frac{2 \cdot \bar{x}_h}{6}\right)^2}{10}.$$

Note that our choice of *n* is somewhat marginal, since the imputed values for strata 1 and 4 through 8 are either zero or very small. While the imputed concentration value for strata 9 will be larger, the associated area is only 0.7 acres, resulting in very little influence in the overall variance estimate of OU1 SWAC. Hence again the choice of *n* is somewhat marginal.

Surface Sample Thickness:

The surface concentration thickness represents the biologically active layer in the sediment. As discussed in the June 20, 2007 Boldt Oversight Team memo, it is assumed that surface concentrations represent a fixed depth.

Sediment cores collected in OU1 have been sampled at varying interval lengths. Most pre-dredge and post-dredge cores were sampled at either 4-inch or 6-inch intervals. For the purpose of SWAC estimation, the surface depth will be assumed to be six inches. Surface samples collected at 4-inch interval depths will be converted by simple depth weighted averaging as follows:

1) If only a single 4-inch interval exists (total soft sediment thickness is less than six inches) the surface concentration will be the resulting 4-inch sample concentration.

2) If two 4-inch intervals exist, a depth weighted 6-inch average will be calculated as [(4 x Top Interval ppm) + (2 x Second Interval ppm)] / 6.

Stratified SWAC Example:

A summary of the SWAC estimate and 95% confidence interval based on the stratified procedure is given in Table 2. The surface average $\bar{x}_h$, the sample variance s_h^2, variance of the mean $\mathrm{var}(\bar{x}_h)$ and area A_h are given for each stratum, and the overall SWAC estimate and confidence interval are provided at the end of the table.

Both pre-dredge and post-dredge data collected through August 8, 2007 are used in calculation of the Table 2 estimates. Also, to produce example estimates for all strata, areas delineated in the OU1 Design Supplement (illustrated in Figure D1) for sand cover and engineered cap strata are included. Residual sand cover is taken to be areas over 1.7 ppm based on actual post-dredge results.

Table 2
Stratified SWAC Example

Strata	weighted $\bar{x}_h$ (ppm)	weighted s_h^2 (ppm)	$\mathrm{var}(\bar{x}_h)$ (ppm)	A_h (Ac)	Data Source
Engineered Cap	0.0065	0.000005	0.0000005	111.9	Imputed Value
Completed Dredge Areas (Excluding Residual Sand Cover and Void Areas)	0.49	0.16	0.00014	103.4	Post-Dredge Sample Cores
Remaining Dredge Areas	1.01	0.16	0.00014	64.7	Imputed Value
Interdeposit (Excluding Void Areas)	0.391	0.091	0.00028	466.6	Pre-Design Sample Cores plus 2007 Recharacterization Data
Void (Sampled Areas with No Sediment Recovery)	0.0168	0.000031	0.0000031	225.4	Imputed Value Based on 12 Native Clay Samples
Null (No Soft Sediment - Unsampled)	0	0	0	246.8	Imputed Value
3-Inch Sand Cover Only	0.0065	0.000005	0.0000005	67.5	One-Half Current Detection Limit
6-Inch Sand Cover Only	0.0065	0.000005	0.0000005	46.2	One-Half Current Detection Limit
Dredge and Sand Cover	0.0065	0.000005	0.0000005	30.2	One-Half Detection Limit
Artifact/Shoreline (No Action in Unsampled Areas)	6.15	4.20	0.42	0.7	Model Interpolated Surface Average
$SWAC_{estimate}$	0.23				
$\mathrm{var}(SWAC_{estimate})$	0.00003				
$SWAC_{estimate}$ LCL	0.21				
$SWAC_{estimate}$ UCL	0.24				

The SWAC estimate based on these data and strata delineations is 0.23 ppm with a 95% confidence interval of (0.22 ppm, 0.24 ppm). As a note, the SWAC estimate performed with this stratified procedure closely matches the model based estimates generated in the November 2006 Final Plan.

A description of the calculations of the surface average estimate $\bar{x}_h$, sample variance s_h^2, and the variance of the mean $\mathrm{var}(\bar{x}_h)$ for each of the h strata follows.

1. Engineered Cap

This stratum covers 112 acres proposed for capping. The surface average $\bar{x}_h$ for this stratum is assumed to be 0.0065 ppm. The stratum sample variance s_h^2 is assumed to be $\left(\frac{2 \cdot 0.0065}{6}\right)^2$ and the variance of the mean is assumed to be

$$\mathrm{var}(\bar{x}_h) = \frac{\left(\frac{2 \cdot 0.0065}{6}\right)^2}{10}.$$

2. Dredge Only

This stratum covers 168 acres of dredged areas, or areas proposed to be dredged. (It excludes areas designated as residual sand cover areas, and void areas of no soft sediment recovery.)

The surface average $\bar{x}_h$ for completed dredge areas is calculated from 1069 sample locations. In dredged areas, only post-dredge samples are used. Post-dredge composite sample locations are each assigned the resulting concentration of the composite.

The sample collection grids differ in density, and likewise the sample average, sample variance and variance of the mean are weighted with Thiessen polygon areas. The Thiessen polygon weights are calculated as:

1) Identify sediment cores within stratum boundaries. Only post-dredge cores are used within dredged areas.
2) Develop a Thiessen polygon shapefile for this data subset.
3) Clip Thiessen polygon shapefile to the stratum boundaries.

The surface average, sample variance and variance of the mean for this stratum are then calculated as:

$$\bar{x}_h = \frac{\sum_{i=1}^{1069} w_i x_{h,i}}{\sum_{i=1}^{1069} w_i} = 0.49\,ppm$$

and

$$s_h^2 = \frac{\sum_{i=1}^{1069} w_i \left(x_{h,i} - \bar{x}_h\right)^2}{1068 \sum_{i=1}^{1069} w_i \Big/ 1069} = 0.16 \qquad \mathrm{var}\left(\bar{x}_h\right) = \frac{s_h^2}{1069} = 0.00014 .$$

For the "remaining dredge areas" calculation, s_h^2 and $\mathrm{var}\left(\bar{x}_h\right)$ are assumed to be the same as for the dredge completed areas, but including post-dredge results from areas designated as residual sand cover areas, and void areas of no soft sediment recovery . The stratum average, $\bar{x}_h$, is calculated from the dredge completed data as above, but including an additional 198 sample locations in dredged areas exceeding 1.7 ppm designated for residual sand cover, as well as 164 no soft sediment recovery locations found in the dredge completed areas.

3. Interdeposit

This stratum covers approximately 467 acres (excluding void no soft sediment recovery areas). It includes areas of undredged sampled soft sediments with eight inch concentrations less than 1 ppm. The strata boundaries are taken from pre-dredge GMS-SED model.

The surface average $\bar{x}_h$ is calculated from 331 sediment samples analyzed within the top interval of **pre-dredge** sediment cores located within the stratum boundaries. Since the sample collection grids differ in density within the varying subareas, a weighted average is calculated using Thiessen polygon areas as in stratum 2 above. Six inch surface concentrations were calculated from four inch sample intervals by depth weighting as:

6-inch ppm = [(4 x Top Interval ppm) + (2 x Second Interval ppm)] / 6.

The surface average for this stratum is then calculated as:

$$\bar{x}_h = \frac{\sum_{i=1}^{331} w_i x_{h,i}}{\sum_{i=1}^{331} w_i} = 0.391 ppm$$

where $x_{1,i}$ are the sediment surface sample results and w_i are the associated Thiessen polygon weights.

The stratum sample variance and variance of the mean are similarly weighted using the Thiessen polygons, and calculated as:

$$s_h^2 = \frac{\sum_{i=1}^{331} w_i \left(x_{h,i} - \bar{x}_h\right)^2}{330 \sum_{i=1}^{331} w_i \Big/ 331} = 0.091 \qquad \mathrm{var}\left(\bar{x}_h\right) = \frac{s_h^2}{331} = 0.00028 .$$

4. Void (sampled areas with no soft-sediment recovery)

Void areas (no soft-sediment recovery) are areas where sediment sample cores have been attempted but insufficient soft sediment was recovered to analyze. This stratum is defined in both pre-dredge and post-dredge areas, and is bounded by Thiessen polygons surrounding the no soft-sediment recovery core locations. It covers 225 acres. The stratum boundaries are developed as follows:

1) Create a combined spatial dataset of pre-dredge and post-dredge core samples. Use only post-dredge core samples in dredged areas.
2) With the combined spatial dataset, create a Thiessen polygon shapefile.
3) Clip the Thiessen polygon shapefile to OU1 boundaries.
4) Clip all sand cover, cap and null regions from the Thiessen polygon shapefile.
5) Select only Thiessen polygons from the shapefile that correspond to no recovery cores.
6) The resulting shapefile defines the stratum boundaries.

The surface average $\bar{x}_h$ for this stratum is assumed to be 0.0168 ppm. The stratum sample variance s_h^2 is assumed to be $\left(\frac{2 \cdot 0.0168}{6}\right)^2$ and the variance of the mean is assumed to be

$$\mathrm{var}(\bar{x}_h) = \frac{\left(\frac{2 \cdot 0.0168}{6}\right)^2}{10} .$$

5. Unsampled Areas Designated Null

This stratum covers 247 acres designated as null. The surface average $\bar{x}_h$ for this stratum is assumed to be 0 ppm, and the stratum sample variance s_h^2 and variance of the mean $\mathrm{var}\left(\bar{x}_h\right)$ are assumed to be 0.

6. Three Inch Sand Cover Only

Three inch sand cover only areas are undredged areas designated for sand cover. The boundaries are developed by the GMS-SED (pre-dredge) model as areas with one eight inch interval with PCB concentrations between 1 and 1.4 ppm, and all other eight inch intervals less than 1 ppm. This stratum covers 68 acres.

The surface average $\bar{x}_h$ for this stratum is assumed to be 0.0065 ppm, this is half the detection level, based on the non-detect 2007 results obtained from samples collected and analyzed from sand-covered dredged residuals and the sand-chemical isolation layer placed for the 2007 Cap Placement Test. The stratum sample variance s_h^2 is assumed to be $\left(\frac{2 \cdot 0.0065}{6}\right)^2$ and the variance of the mean is assumed to be

$$\mathrm{var}(\bar{x}_h) = \frac{\left(\frac{2 \cdot 0.0065}{6}\right)^2}{10}.$$

7. Six Inch Sand Cover Only

Six inch sand cover only areas are undredged areas designated for sand cover. The boundaries are developed by the GMS-SED (pre-dredge) model as areas with one eight inch interval with PCB concentrations between 1.4 and 2 ppm, and all other eight inch intervals less than 1 ppm. This stratum covers 46 acres. The average, $\bar{x}_h$, sample variance, s_h^2, and variance of the mean, $\mathrm{var}(\bar{x}_h)$, are calculated as in stratum 6 above.

8. Residual Sand Cover Only

This stratum covers 30 acres, which have been dredged and are candidates for sand cover. The average, $\bar{x}_h$, sample variance, s_h^2, and variance of the mean, $\mathrm{var}(\bar{x}_h)$, are calculated as in stratum 6 above.

9. Artifact/Shoreline

This stratum consists of 0.7 acres bounded by the artifact area and 2005 shoreline area which could not be dredged. This stratum differs from the others in that it does not have sample core data located within its boundaries, but also is not assumed to have a constant PCB surface concentration. The PCB surface average, stratum sample variance and variance of the mean in this case are obtained from the GMS-SED (pre-dredge) model, similarly percent solids values, if needed, would have to be obtained from the GMS-SED model.

The GMS-SED model bounded by this stratum contains 146 model nodes (horizontal), each associated with a node surface area and interpolated PCB concentration. The surface average for this stratum is calculated as from the model as:

$$\bar{x}_h = \frac{\sum_{i=1}^{146} w_i y_{h,i}}{\sum_{i=1}^{146} w_i} = 6.15\,ppm$$

where $y_{h,i}$ is the PCB concentration associated with model node *i*, and w_i is the associated model node surface area (Thiessen polygon area). The stratum sample variance s_h^2 is assumed to be $\left(\frac{2 \cdot 6.15}{6}\right)^2$ and the variance of the mean is assumed to be

$$\mathrm{var}(\bar{x}_h) = \frac{\left(\frac{2 \cdot 6.15}{6}\right)^2}{10}.$$

.

GMS-SED Model Based SWAC:

SWAC estimates made using the GMS-SED model were presented in the November, 2006 OU1 Design Supplement. This procedure also is necessary for the artifact/shoreline stratum (stratum 9), since it does not have sample core data located within its boundaries. Although the core-based approach given above will be the preferred SWAC calculation method, the model based procedure is presented here for completeness.

To begin with, a two-dimensional "surface PCB" layout is created from the three-dimensional GMS-SED interpolation. At each two-dimensional XY location, a surface concentration which represents the top four inches is calculated as follows:

1. Determine the nodes (vertically) which represent the top four-inches of sediment. Each node corresponds to the midpoint of a horizontal layer.

2. Find the interpolated PCB concentration and percent solids at each of these nodes.

3. Calculate the associated volume with each of these nodes (or partial volume if a layer does not end precisely at a four-inch depth).

4. Using the PCB, percent solids and volume data, calculate the PCB mass and sediment dry weight associated at each vertical node.

5. Sum the PCB mass and sediment dry weight (vertically) which represents the top four-inches. The estimated surface concentration for the XY location is the PCB mass divided by the sediment dry weight mass.

An example calculation for an XY location from Sub-area A DMU 4 is illustrated here. The XY location selected for the example is highlighted in yellow. This location has an influence area (Thiessen polygon area) of 751 sq.ft.

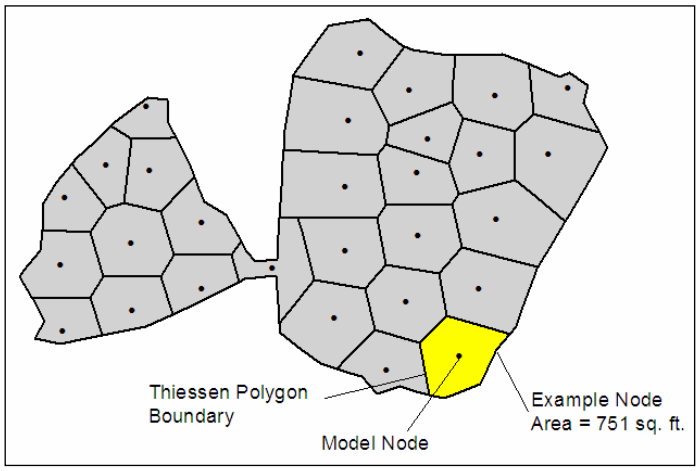

At this XY location, there are 19 corresponding vertical model nodes, each with an associated thickness, interpolated PCB concentration and interpolated percent solids. These results are given in Table 3 for the post-dredge model.

In Table 3 (post-dredge model following second dredge attempt in DMU 4) the total soft sediment thickness at the XY location is 2.52 inches. Therefore all vertical nodes are included in the surface concentration calculation.

The associated volume with each vertical node element is found by multiplying the horizontal influence area (Thiessen polygon area) by the layer thickness. The associated PCB mass is found by multiplying the PCB concentration with the element volume and sediment dry mass. Some of the key mathematical relationships are:

$$PCB\ Mass\,(lb.)_j = \left[PCB_j\ (ppm)\right]\left[\gamma_{d,j}\left(\tfrac{lb.}{ft.^3}\right)\right]\left[V_j\ (ft.^3)\right]\left(\frac{1x10^{-6}}{ppm}\right)$$

$$Sediment\ Dry\ Mass\,(lb.)_j = \left[\gamma_{d,j}\left(\tfrac{lb.}{ft.^3}\right)\right]\left[V_j\ (ft.^3)\right]$$

where

PCB_j is the total (interpolated) PCB concentration (ppm or mg/kg) in layer j at a given XY location,

$\gamma_{d,j}$ is the dry unit weight (or dry density) of the sediment in layer j , at the same XY location, which is estimated (for saturated conditions) from the unit weight of water (γ_w = 62.4 pcf), the percent solids concentration P_j (also interpolated to the 3D mesh) and a selected value for specific gravity of solids, *Gs*, for the sub-area :

$$\gamma_{d,j} = \frac{\gamma_w}{\dfrac{1}{G_s} + \dfrac{1}{P_j} - 1}$$

and V_j is elemental volume of the mesh profile slice j at the same XY location.

The surface average for the XY location is then the sum of the PCB mass divided by the sum of the sediment dry mass for elements which (vertically) represent the top four-inches of soft sediment, i.e.,

$$C = PCB\ Surface\ \ (ppm)\ =\ \frac{\sum_j PCB\,Mass_j}{\sum_j Sediment\ Dry\ Mass_j}\left(\frac{10^6\ ppm}{1}\right)$$

For the example XY location, the post-dredge surface concentration in Table 3 is 2.5 ppm

Table 3
Example of Vertical Model Node Data and Calculation of Top 4-Inch Average PCB Concentration
Post-Dredge Sediment Bed Model

Vertical Layer	Horizontal Footprint Area (sq. ft.)	Layer Thickness[1] (Inches)	Model Node Volume (cy)	Top of Layer Elevation (MSL)	Percent Solids	Dry Sediment Mass[2] (lbs.)	PCB (ppm)	PCB Mass (lbs.)	Total Depth to Layer Bottom (Inches)	Total Dry Sediment Mass in Top 4 Inches[3] (lbs.)	Total PCB Mass in Top 4 Inches[3] (lbs.)	Surface PCB Concentration for XY Location[4] (ppm)
1	751	0.07	0.162	732.00	51.5	203	2.6	0.00053	0.07			
2	751	0.14	0.324	731.99	51.4	406	2.6	0.00105	0.21			
3	751	0.14	0.324	731.98	51.3	405	2.6	0.00104	0.35			
4	751	0.14	0.324	731.97	51.2	404	2.6	0.00103	0.49			
5	751	0.14	0.324	731.96	51.2	403	2.5	0.00102	0.63			
6	751	0.14	0.324	731.94	51.1	402	2.5	0.00101	0.77			
7	751	0.14	0.324	731.93	51.0	401	2.5	0.00100	0.91			
8	751	0.14	0.324	731.92	51.0	401	2.5	0.00099	1.05			
9	751	0.14	0.324	731.91	50.9	400	2.5	0.00098	1.19			
10	751	0.14	0.324	731.90	50.8	399	2.4	0.00098	1.33			
11	751	0.14	0.324	731.89	50.8	399	2.4	0.00097	1.47			
12	751	0.14	0.324	731.87	50.7	398	2.4	0.00096	1.61			
13	751	0.14	0.324	731.86	50.7	398	2.4	0.00096	1.75			
14	751	0.14	0.324	731.85	50.7	398	2.4	0.00096	1.89			
15	751	0.14	0.324	731.84	50.7	398	2.4	0.00095	2.03			
16	751	0.14	0.324	731.83	50.7	398	2.4	0.00095	2.17			
17	751	0.14	0.324	731.82	50.7	398	2.4	0.00096	2.31			
18	751	0.14	0.324	731.80	50.7	398	2.4	0.00096	2.45			
19	751	0.07	0.162	731.79	50.8	199	2.4	0.00048	2.52	7207	0.0178	2.5

[1]In this example, during GMS modeling 19 node layers were created, each node representing a layer midpoint. However, since the top and bottom nodes are placed at the top and bottom of soft sediment, respectively, the representative thickness of the top and bottom nodes is one-half the thickness of the remaining layers.

[2]Sediment dry density calculated as $62.4/(1/G_s + 100/\text{Percent Solids} - 1)$ where $G_s = 2.5$.

[3]Since only 2.52 inches of soft sediment exists, the sum represents less than the top 4 inches.

[4]Calculated as PCB mass / sediment mass * 10^6. The average represents the 2.52 inches of soft sediment.

The SWAC can be calculated for any subset region of Thiessen polygons (such as the artifact/shoreline strata). The SWAC calculation is straightforward:

$$SWAC = \frac{\sum_i (C_i)(A_i)}{\sum_i (A_i)}$$

where the C_i are the surface concentrations and A_i are the Thiessen polygon areas associated with the set of *i* two-dimensional node (XY) locations within the horizontal footprint of interest.

Appendix D

Numerical Model Assessment of Bed Shear Stress for Wind-Waves and Flows on LLBdM (OU1), Fox River (Baird 2007)

Baird

Numerical Model Assessment of Bed Shear Stress for Wind-Waves and Flows on Little Lake Butte des Morts (OU1), Fox River

June 29, 2007
Project No. 11172.010

Numerical Model Assessment of Bed Shear Stress for Wind-Waves and Flows on Little Lake Butte des Morts (OU1), Fox River

Prepared for

FOTH INFRASTRUCTURE & ENVIRONMENT, LLC
2737 South Ridge Road, P.O. Box 19012
Green Bay, WI 54307-9012, USA

Prepared by

Baird

W.F. Baird & Associates Coastal Engineers Ltd.

For further information please contact
Dr. Rob Nairn at (905) 845-5385

Project No. 11172.010

Version	Date	Status	Comments	Reviewed by	Approved by
1	05-09-07	Final		Q. Lu	R. Nairn
2	06-26-07	Revised Final	With revisions from Foth Comments	Q. Lu	R. Nairn

This report was prepared by W.F. Baird & Associates Coastal Engineers Ltd. for Foth Infrastructure & Environment, LLC. The material in it reflects the judgment of Baird & Associates in light of the information available to them at the time of preparation. Any use which a Third Party makes of this report, or any reliance on decisions to be made based on it, are the responsibility of such Third Parties. Baird & Associates accepts no responsibility for damages, if any, suffered by any Third Party as a result of decisions made or actions based on this report.

TABLE OF CONTENTS

1.0 INTRODUCTION 1
2.0 BACKGROUND AND APPROACH 2
2.1 Objectives 2
2.2 Selected Wind-Wave and Flow Combinations 2
2.3 Analysis of Wind Data 3
2.4 Numerical Modeling of Wave Conditions 5
2.5 Numerical Modeling of River Flow Conditions 10
2.6 The Role of Wind-Generated Currents 12
2.7 Methodology for Determining Shear Stresses 12
3.0 RESULTS ON ESTIMATED SHEAR STRESSES FOR OU1, FOX RIVER 14
3.1 Shear Stresses Generated by River Flows 14
3.2 Shear Stresses Generated by Wind-Waves and Wind-Driven Currents 18
3.2.1 Wind-Driven Circulation 18
3.3 Combined Wave-Current Shear Stresses Generated by Wind-Waves and River Flows 27
4.0 REVIEW OF PAPERS ON PUMPING AND LIQUEFACTION 33
4.1 Wave Pumping Review 33
4.2 Liquefaction Review 34
5.0 CONCLUSIONS AND RECOMMENDATIONS 35
6.0 REFERENCES 37
7.0 DELIVERABLES 38

APPENDIX A: STWAVE RESULTS FOR RUNS 2 TO 5 ON OU1, FOX RIVER
APPENDIX B: POT ANALYSIS FOR EACH DIRECTION AND SEASON

TABLE OF FIGURES

Figure 1. Model Bathymetry for SSW Grid 6
Figure 2a. Significant Wave Heights Predicted with STWAVE for a SSW Wind at 52.8 mph 8
Figure 2b. Wave Periods Predicted with STWAVE for a SSW Wind at 52.8 mph 9
Figure 3a. Flow Speeds Predicted with ECOMSED for the Daily Average Condition 10
Figure 3b. Flow Speeds Predicted with ECOMSED for the 2-year Return Period Condition 11
Figure 4a. Runs 1 to 3 – River Currents Only Shear Stress Map 15
Figure 4b. Runs 4 and 5 – River Currents Only Shear Stress Map 16
Figure 5. Bed shear stresses within cap areas for River flow only model results 17
Figure 6a. Run 1 - Waves Only Shear Stress Map 19
Figure 6b. Run 2 - Waves Only Shear Stress Map 20
Figure 6c. Run 3 - Waves Only Shear Stress Map 21
Figure 6d. Run 4 - Waves Only Shear Stress Map 22
Figure 6e. Run 5 - Waves Only Shear Stress Map 23
Figure 7a. Run 4 - Flow Speeds from ECOMSED for Wind and River Flow Generated Currents .. 24
Figure 7b. Run 4 - River Flow Plus Wind-Driven Flow Shear Stress Map (i.e. no wave influence) 25
Figure 8. Bed shear stresses within cap areas for wind-wave event results only 26
Figure 9. Bed shear stresses within cap areas for combined river flow and wind results 27
Figure 8a. Run 1 - Combined Wave-Current Shear Stress Map 28
Figure 8b. Run 2 - Combined Wave-Current Shear Stress Map 29
Figure 8c. Run 3 - Combined Wave-Current Shear Stress Map 30
Figure 8d. Run 4 - Combined Wave-Current Shear Stress Map 31
Figure 8e. Run 5 - Combined Wave-Current Shear Stress Map 32

1.0 INTRODUCTION

Baird was retained by Foth Infrastructure & Environment, LLC (Foth) to evaluate bed shear stresses generated by wind-waves and flows in Little Lake Butte des Morts. Little Lake Butte des Morts occupies the upper part of the Lower Fox River from Lake Winnebago to the Appleton Dam, and is referred to as Operable Unit 1 (OU1) of the Lower Fox River Project. The evaluation was performed on a projected post-remedy OU1 bathymetric condition; proposed OU1 optimized Remedy (13 and 16 inch cap placeholders were used in the analysis). The work follows from the project to estimate shear stresses for OU1 under the 100-year flow (with no wind-waves) described in Baird (2006) and based on the ECOMSED model of the Lower Fox River developed and tested by Baird (Baird, 2000). The model results provide information that will be used, in conjunction with other studies, to evaluate the overall stability of the cap materials for a proposed sediment remediation project in Little Lake Butte des Morts.

2.0 BACKGROUND AND APPROACH

2.1 Objectives

The stated objectives of this assignment were as follows:

> Determine the approximate combined shear stresses in Little Lake Butte des Morts under various wave and current conditions. Model outcomes will be considered within the design process of a proposed cap for OU1. The river is always flowing through Little Butte des Morts, therefore, shear stresses created by wind-waves must be considered in combination with river flows. Also, a review of liquefaction and wave pumping issues, specific to OU1, has been completed.

2.2 Selected Wind-Wave and Flow Combinations

It is noted that Foth provided direction on the selection of five conditions required to provide information for Foth to address shear stress in the cap design. The five conditions consisted of:

Run 1 - 2-year return period river flow with 50-year return period wind from SSW

Run 2 - 2-year return period river flow with 50-year return period wind from WSW

Run 3 - 2-year return period river flow with 50-year return period wind from NNW

Run 4 - Average daily flow with a 9-year return period wind from the SSW

Run 5 - Average daily flow with a 2.5-year return period wind from the NNE

Runs 1 to 3 represent three possible combinations of a combined 100-year event or return period on shear stress conditions. Runs 4 and 5 settings were used to simulate more common wind-wave conditions, for purposes of comparison with related studies on OU2-5 (Shaw and Anchor, 2006). Return periods for winds are based on hourly wind data and return periods for flows are based on daily data.

An analysis was completed to evaluate whether there was any interdependency between high flows and high winds speeds. It was determined that these two phenomena were relatively independent. Therefore, it is appropriate to multiply the return periods for the wind and flow to determine the approximate return period of the combined event. Had there been statistical dependency between high winds and flows, the 100-year event would have consisted of larger combined events. It is noted, however, that there are many other possible 100-year event combinations (such as the 100-year wind with a 1.1-year flow condition, the 100-year flow with a 1.1-year wind event, etc.). Some of these combinations may result in higher combined shear stresses than the events selected in Runs 1 to 3 above. The wind speed analysis to review possible interdependency and to determine return period is presented in Section 2.3.

Runs 4 and 5 were used to determine wind-wave outcomes for conditions that were similar to those used for the wind-wave analysis conducted for OU2 to OU5 (Shaw and Anchor, 2006). These runs differed from Runs 1 to 3 in the following ways:

- The return periods for winds were determined assuming no ice cover (in other words, the winds for the entire year were used);
- The return periods for winds were selected to be similar to model runs from the OU2-5 wind-wave analysis (Shaw and Anchor, 2006), for the SSW and NNE wind directions.
- The resulting shear stress combination of wind-waves and flows was not meant to represent a 100-year event;

With respect to water level, Runs 1 to 3 were completed with a water level of 0.2 m (measured at the Appleton Dam and the downstream end of Little Lake Buttes des Morts) above LWD which is representative of a 2-year return period flow condition. The water level for Runs 4 and 5 with the average annual flow were completed with a water level of 0.1 m below LWD, representing a very low water condition.

2.3 Analysis of Wind Data

Wind data was analyzed for two different nearby airports, Appleton-Outagamie County Regional Airport and Green Bay-Austin Straubel International Airport. The Appleton record covered the period from January 1998 to December 2002. A Green Bay record from 1978 to 2002 was obtained to provide a longer dataset to support a more accurate extreme values analysis. A portion of the Green Bay data was recorded at an anemometer elevation of 20 ft (6.1 m), and it was assumed that the balance of the data (for which no elevation was provided) was also recorded at that elevation. The elevation at which the Appleton data was measured but was not reported by the weather station, so it was assumed to be at the standard height of 32.8 ft (10 m) based on direction from Foth. The wind data itself was separated into two separate seasons: full-year and open-water (when ice is not present). An analysis of 25 years of ice data on the southern tip of Green Bay was used in conjunction with an OU1 project ice study (Ashton, 1996) to determine an approximate average ice season; the analysis and data review resulted in the approximate annual average open water season being defined as April 1st through December 20th.

An analysis was undertaken to determine the dependency between river flows and wind speeds and a consistent relationship or dependency between the two datasets was not observed.

An extreme value analysis was undertaken on both datasets, and for both seasons. There was insufficient data at Appleton to determine return periods beyond 10 years with a reasonable level of certainty. The Peaks Over Threshold (POT) approach was implemented with individual events selected on the basis of storm intensity, duration, and direction. Results for both seasons are shown in Tables 1 and 2 (note: 1 mph = 0.447 m/s). Four separate statistical distributions were used to represent the tail of the data in each case, and the final distribution was selected on the basis of goodness of fit measures and engineering judgment. More complete information on the POT analysis for each direction and season is provided in Appendix B.

Table 1
Return Period Events for Various Wind Speeds: Full Year

Return Period	Green Bay Wind Speeds (mph)				Appleton Wind Speeds (mph)			
(years)	SSW	SW	NNE	NE	SSW	SW	NNE	NE
1	29.3	31.0	28.2	29.6	29.7	33.8	22.0	30.1
2	31.7	34.3	30.4	31.0	34.1	36.5	29.0	31.4
5	35.1	38.7	33.5	33.1	40.3	40.0	33.3	33.0
10	38.3	42.0	35.7	34.8	45.6	42.5	36.1	34.2
50	48.9	49.8	41.0	39.0	N/A	N/A	N/A	N/A
100	55.5	53.1	43.3	40.8	N/A	N/A	N/A	N/A

Table 2
Return Period Events for Various Wind Speeds: Open-Water Season

Return Period	Green Bay Wind Speeds (mph)				Appleton Wind Speeds (mph)			
(years)	SSW	SW	NNE	NE	SSW	SW	NNE	NE
1	26.7	27.8	21.7	27.3	29.2	29.2	N/A	28.2
2	30.6	31.1	26.3	29.2	34.1	31.6	N/A	28.8
5	34.8	34.7	29.1	31.3	40.6	35.3	N/A	30.6
10	38.4	37.8	31.0	33.2	45.4	38.6	N/A	32.6
50	49.1	47.1	35.0	38.6	N/A	N/A	N/A	N/A
100	55.1	52.3	36.6	41.7	N/A	N/A	N/A	N/A

Runs 1, 2, and 3 were conducted using winds speeds with a 50-year return period. The wind speeds for the SSW, WSW, and NNW conditions for Runs 1, 2, and 3 are shown in Table 3. Runs 4 and 5 were to use wind speeds for return periods that were found to match two of the modeled OU2-5 conditions (Shaw and Anchor, 1996). The return period of the OU2-5 events was determined for their input winds and correlated to Appleton winds. Run 4 was selected to match the OU2-5 condition of a 37.3 mph wind from the SSW: this corresponded to an 8.2-year return period event with the Green Bay winds, which converted to a 44 mph wind (from the SSW) at Appleton. Run 5 was selected to match the OU2-5 condition of a 31.1 mph wind from the NNE: this corresponded to a 2.5-year return period event with the Green Bay winds, which converted to a 30.2 mph wind (from the SSW) at Appleton.

2.4 Numerical Modeling of Wave Conditions

Wind wave conditions in Little Lake Butte des Morts (Fox River OU1) were simulated using the STWAVE model developed by the US Army Corps of Engineers (USACE, 2001). STWAVE is a phase-averaged, steady-state, half plane two dimensional spectral wave model based on the wave action balance equation, which includes wind generation, refraction, shoaling, breaking, limited implementation of wave diffraction, wave-wave interaction and white-capping that redistribute and dissipate energy in a growing wave field. For wave generation, the steady-state assumption means that the winds have remained steady sufficiently long that waves are not limited by the duration of the winds, a reasonable assumption for the fetch-limited conditions in the Little Lake Butte des Morts. The water level used for the lake surface during the STWAVE model runs was +0.2 m (~7.9 inches), related to low water datum.

The model is run on a regularly spaced grid. Different grids were prepared for the model, to properly simulate wind conditions from SSW, WSW, NNW and NNE; the X-Axis of the model grid is oriented parallel to the desired wind direction. 10m-grid resolution was used for all the grids. The model grids were prepared using the post remedy bathymetry (proposed OU1 plan using 13 and 16 inch, cap placeholder designs) related to low water datum. Wisconsin State Plane South in feet (provided to Baird by Foth in April 2007). Horizontal coordinate system was re-projected to match the horizontal coordinate system of earlier model runs (WTM). Figure 1 shows the bathymetry grid used for SSW.

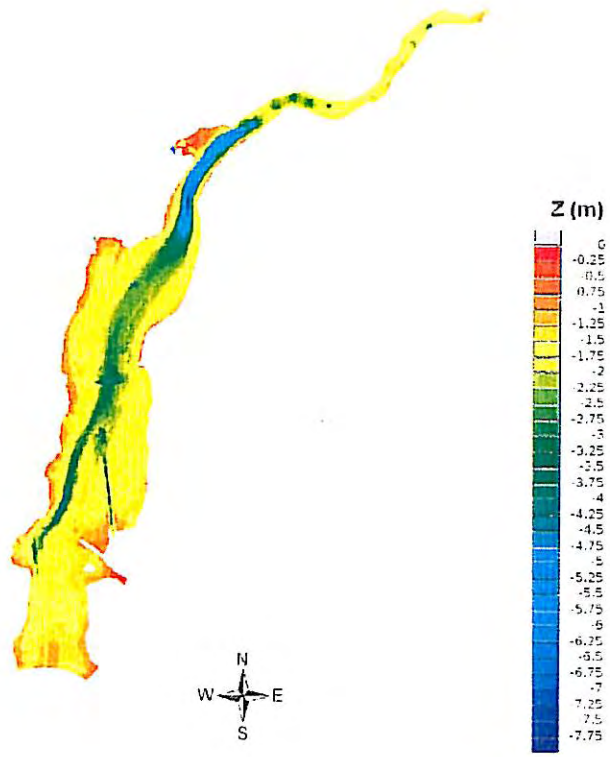

Figure 1. Model Bathymetry for SSW Grid

Five different wind conditions were simulated using the respective bathymetry grids. The wind conditions are shown in Table 3 below. Output from the model consists of wave height, period and direction at each point in the model grid, providing a map of these parameters throughout the model domain.

Table 3
Wind Speed and Direction with Combined Flow Condition for STWAVE Simulations

Run	Wind Direction	Wind Speed (mph)	Wind Speed (m/s)	Return Period (wind, yrs)	Flow Condition (cms)	Flow Description
1	SSW	52.8	23.6	50	360	2 Yr Return Flow
2	WSW	50.6	22.6	50	360	2 Yr Return Flow
3	NNW	37.6	16.8	50	360	2 Yr Return Flow
4	SSW	44.1	19.7	8.2	122	Mean Flow
5	NNE	30.2	13.5	8.2	122	Mean Flow

The predicted wave heights and periods for Run 1 (SSW wind at 52.8 mph) are shown in Figures 2a and 2b below. The wave height and period maps for the other runs are presented in Appendix A.

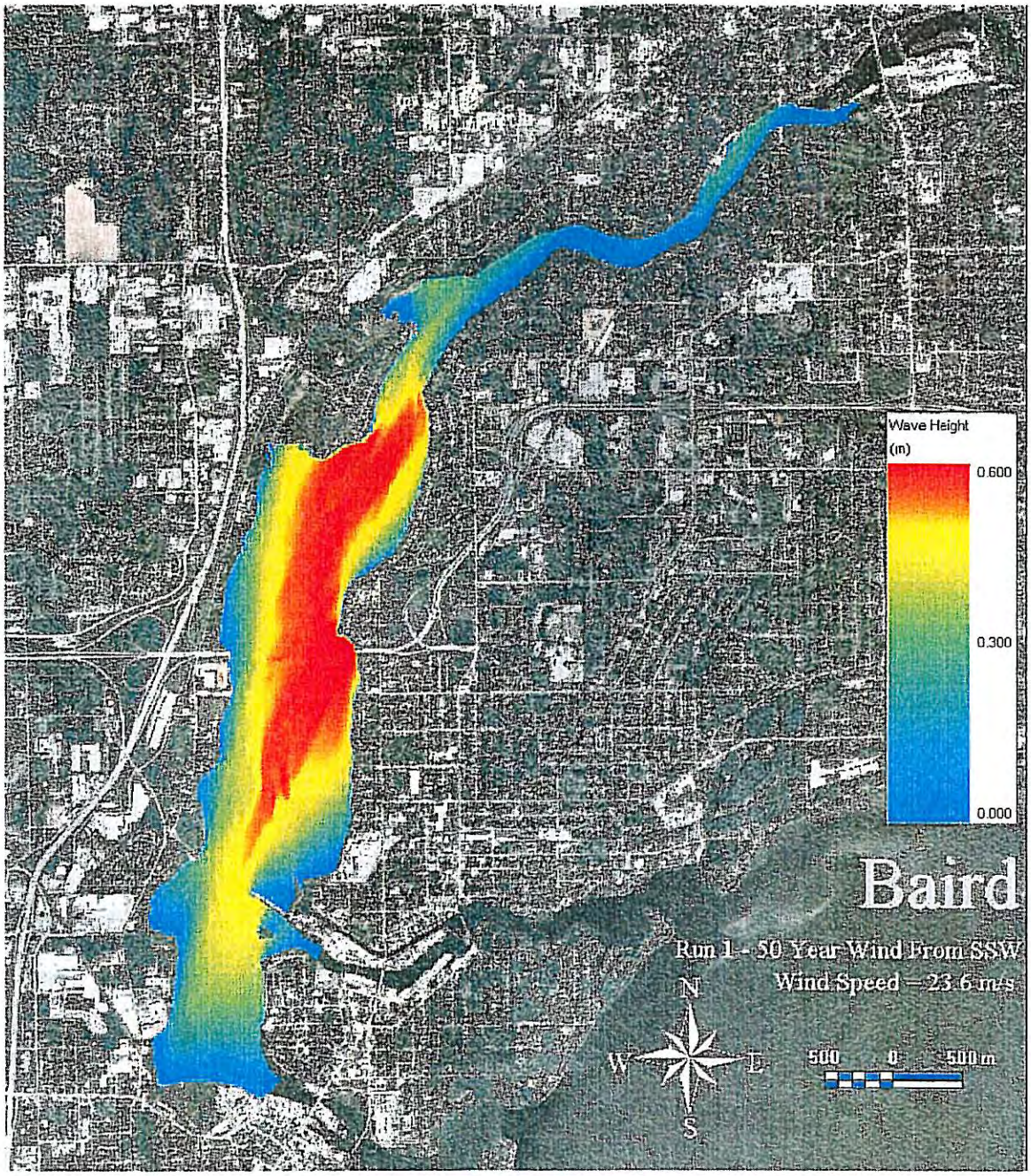

Figure 2a. Significant Wave Heights Predicted with STWAVE for a SSW Wind at 52.8 mph

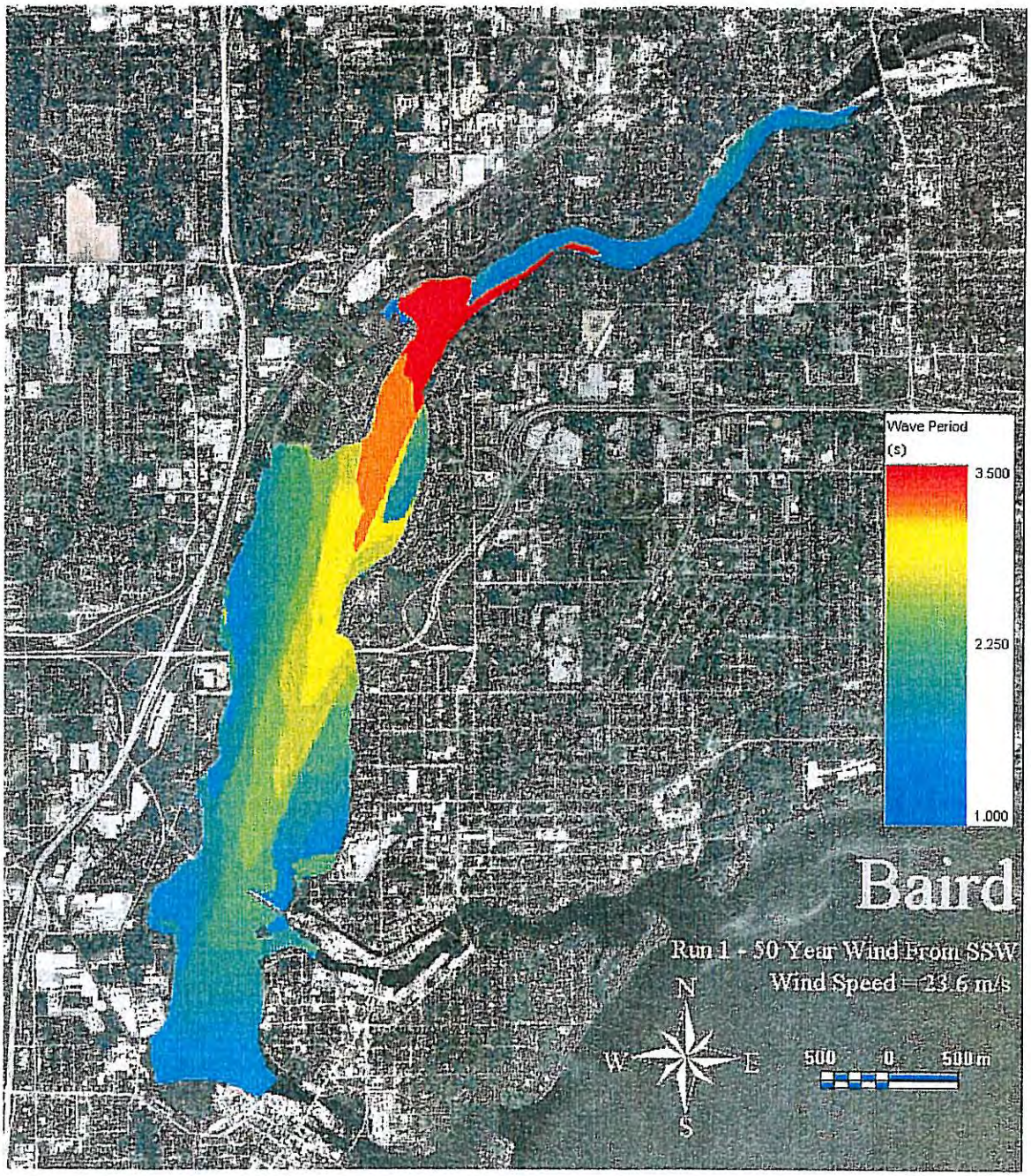

Figure 2b. Wave Periods Predicted with STWAVE for a SSW Wind at 52.8 mph

2.5 Numerical Modeling of River Flow Conditions

A discussion of revisions to the ECOMSED model for the estimates of flow speeds and directions are provided in Baird (2006). The model bathymetry was revised again for this investigation based on information provided by Foth related to revisions to the cap design since the writing of the Baird (2006) report in October 2006. For this study, the daily average (4,300 cfs or 122 m^3/s) and 2-year return period (12,710 cfs or 360 m^3/s) flows were simulated with ECOMSED model for use with Runs 4/5 and Runs 1-3, respectively (i.e. to add to the 100-year return period flow results from Baird, 2006). The flow speeds for two events are shown in Figures 3a and 3b.

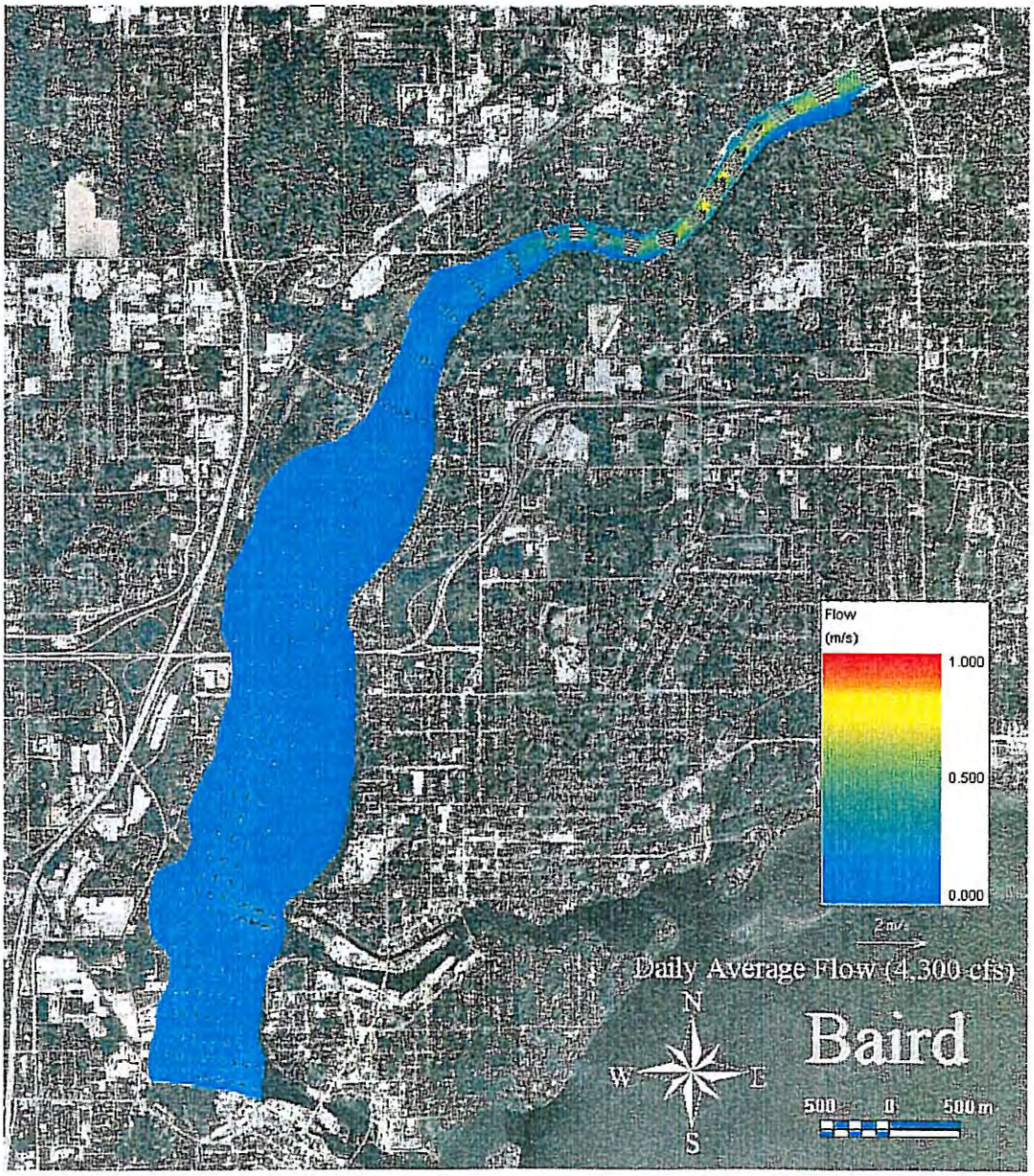

Figure 3a. Flow Speeds Predicted with ECOMSED for the Daily Average Condition

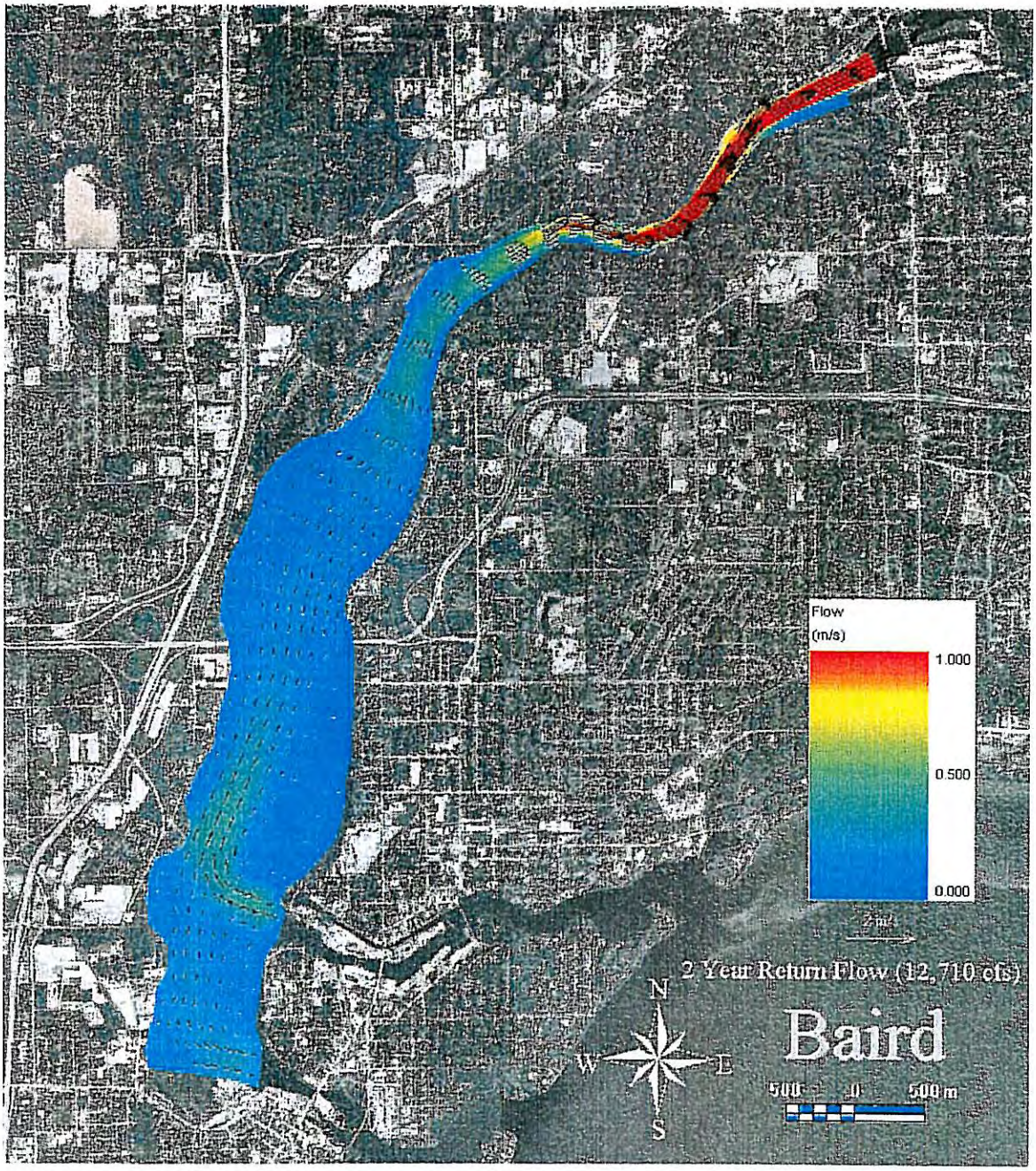

Figure 3b. Flow Speeds Predicted with ECOMSED for the 2-year Return Period Condition

2.6 The Role of Wind-Generated Currents

The section of the Lower Fox River between Lake Winnebago and the Appleton Dam is effectively a lake. Therefore, in addition to the orbital velocities generated by wind-waves and the river flow, there will also be circulation generated by wind shear stresses on the surface of the lake. The wind-driven circulation pattern was considered for Run 1 only to evaluate the importance of this component of the flow on the lake. The results are presented in Section 3.2.

2.7 Methodology for Determining Shear Stresses

Three sets of shear stress maps were developed for each of the model runs: wave-generated shear stresses; river flow generated shear stresses; and combined wave-current generated shear stresses. All three shear stress maps were generated at the 10 m by 10 m grid resolution of the STWAVE model by linear interpolation of the coarser and curvilinear grid of the ECOMSED model (the latter is described in Baird, 2006).

The bed shear stress generated by waves and current was calculated by using the van Rijn (1993) equation:

$$\tau_{b,cw} = \alpha \cdot \tau_{b,c} + \tau_{b,w}$$

in which $\tau_{b,cw}$ is the bed shear stress produced by the combination of waves and currents, $\tau_{b,c}$ is the bed shear stress produced by currents only, $\tau_{b,w}$ is the bed shear stress produced by waves only, and the coefficient α is the bed shear stress reduction factor (<= 1) to account for the current reduction at the bottom due to the present waves. The equation for the coefficient α is

$$\alpha = \left[\frac{\ln(30\delta / k_a)}{\ln(30\delta / k_s)}\right]^2 \left[\frac{-1+\ln(30h / k_s)}{-1+\ln(30h / k_a)}\right]^2$$

in which:

δ - thickness of wave-related near bed layer (=$3\delta_w$ and < $0.033k_a$) (m),

δ_ω - thickness of wave boundary layer ($=0.072\hat{A}_\delta\left(\frac{\hat{A}_\delta}{k_s}\right)^{-0.25}$)(m)

h - water depth (m)

k_s - bed roughness (m)

k_a - apparent bed roughness (m)

$\hat{A}_\delta$ - wave orbital excursion ($=\frac{H}{2\sinh(kh)}$) (m)

H - wave height (m)

k - wave number ($=2\pi / L$) (1/m)

L - wave length ($=\left(gT^2 / 2\pi\right)\tanh(kh)$) (m)

T - wave period (s)

The bed shear stress produced by current only was calculated by:

$$\tau_{b,c} = \rho g \frac{\overline{u}}{C^2}$$

in which:

ρ - fluid density (kg/m^3)
g – acceleration of gravity (m/s^2)
$\overline{u}$ - depth-averaged velocity (m/s)
C – Chezy coefficient (m$^{0.5}$/s)

$$C = \begin{cases} 18\log\left(\dfrac{11.4h}{\nu C/\overline{u}}\right) & \textit{for hydraulic smooth flow} \\ 18\log\left(\dfrac{12h}{k_s + 1.05\nu C}/\overline{u}\right) & \textit{for transitional flow} \\ 18\log\left(\dfrac{12h}{k_s}\right) & \textit{for hydraulic rough flow} \end{cases}$$

ν - kinematic viscosity coefficient

The bed shear stress produced by waves only was calculated by:

$$\tau_{b,w} = 0.5\rho f_w \hat{U}_\delta^2$$

in which:

$\tau_{b,w}$ – instantaneous wave-related bed shear stress (N/m^2)
f_w – friction coefficient (-)

$$= \begin{cases} 2\left(\dfrac{\hat{U}_\delta \hat{A}_\delta}{\nu}\right)^{-0.5} & \text{for Laminar flow} \\ 0.09\left(\dfrac{\hat{U}_\delta \hat{A}_\delta}{\nu}\right)^{-0.2} & \text{for smooth turbulent flow} \\ \exp\left[-6 + 5.2\left(\dfrac{\hat{A}_\delta}{k_s}\right)^{-0.19}\right] & \text{for rough turbulent flow } \left(f_{w,\max} = 0.3 \text{ for } \dfrac{\hat{A}_\delta}{k_s} \le 1.57\right) \end{cases}$$

$\hat{U}_\delta$ - peak orbital velocity just outside boundary layer (m/s) = $\dfrac{\pi H}{T\sinh(kh)}$

3.0 RESULTS ON ESTIMATED SHEAR STRESSES FOR OU1, FOX RIVER

As explained in Section 2.7, three shear stress maps were produced for each of the five model runs corresponding to: shear stresses from river flow alone; shear stresses from wind-wave generated orbital velocities; and combined wave-current generated shear stresses. It is not appropriate to simply superimpose the wave and flow generated shear stresses due to the wave-current interaction in the boundary layer.

In all of the shear stress bed maps the color mapping scheme is the same as that used in Baird (2006), with the exception that the results are presented in Pa and not dynes/cm^2. The color-mapping scheme is described in Table 4 below and it provides an indication of the range of cap sizes required in different areas.

Table 4
Color Mapping Scheme in the Shear Stress Plots

Cap Materials	Grain Size	Inches	Critical Shear Stress for Erosion (Pa)	(Dynes/cm^2)	Color
Medium Sand	< 0.5 mm	< 0.020	0.25	2.5	Navy Blue
Very Coarse Sand	< 2 mm	< 0.079	1.3	13	Greenish Yellow
Fine Gravel	< 8 mm	< 0.315	7.1	71	Green/Blue/Teal
Median Gravel	< 16 mm	< 0.630	14.2	142	Pink/Red

Note: 10 dynes/cm^2 = 1 Pa

The three shear stress maps for each of the five runs have also been provided as GIS files as part of the deliverable for this project (see Section 7.0).

3.1 Shear Stresses Generated by River Flows

Two river flows were considered for the five model runs: the 2-year return period flow (Runs 1 to 3) and the average daily flow (Runs 4 and 5). The river flows were selected to simulate close to a 100-year combined event, with greater impact being placed on the wind event. An analysis into the dependency between the flow and wind datasets was completed and there was almost no dependency observed; therefore combining the 2-year flow and the 50-year wind resulted in an approximate 100-year combined event. Later, as will be explained, it was discovered that lower flow events result in lower water levels on Little Lake Buttes des Morts and therefore, higher wave driven shear stresses due to shallower water depths. Figures 4a and 4b show the shear stress map results for the 2-year return flow and average daily flow, respectively. The shear stresses for river flows alone are low for both these cases and almost everywhere with the cap zone they are less than 1 Pa or 10 dynes/cm^2 for the 2-year event and less than 0.25 Pa for the average daily flow event.

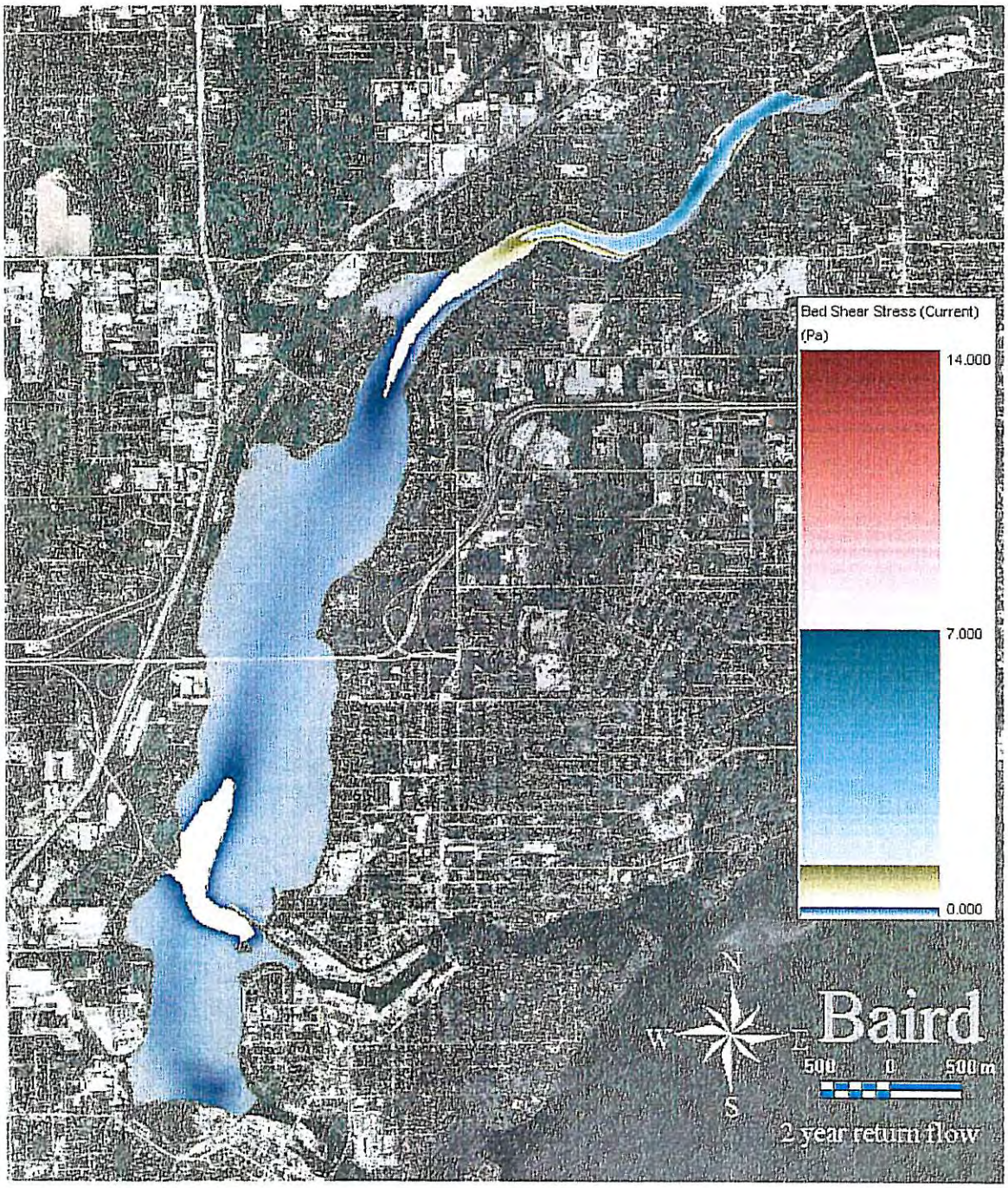

Figure 4a. Runs 1 to 3 – River Currents Only Shear Stress Map

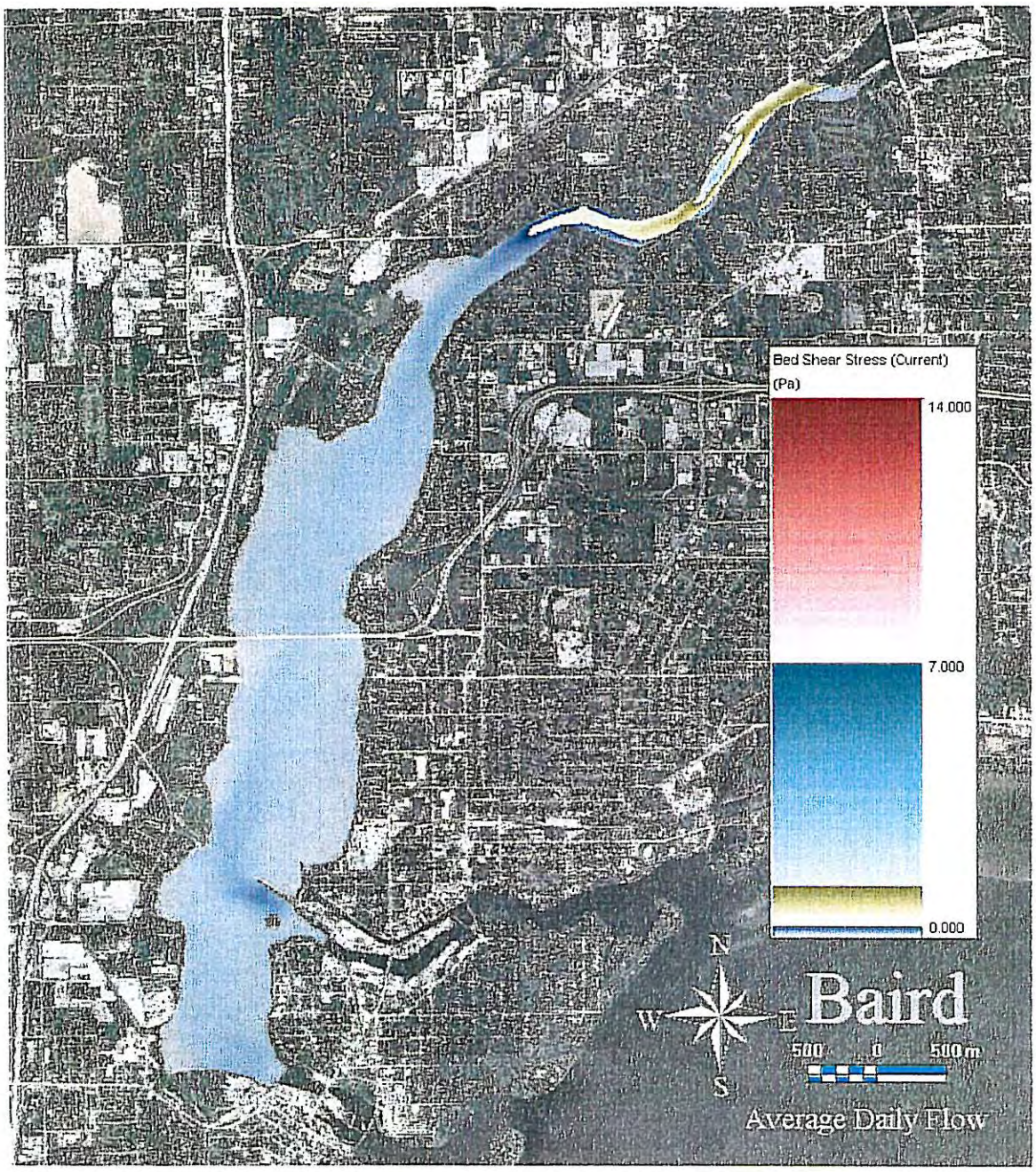

Figure 4b. Runs 4 and 5 – River Currents Only Shear Stress Map

The low shear stresses through the main part of Little Lake Butte des Morts (OU1) are a result of the fact this is a relatively wide lake where the flow is diffused.

Specifically through the proposed cap areas the shear stresses are in the range of 0.13 and 3.46 dynes/cm^2 for the 2-year return period flow, and between 0.04 and 0.65 dynes/cm^2 for the daily average flows. A summary table is presented in Table 5, and a statistical plot is shown in Figure 5.

Table 5
Bed Shear Stresses in cap areas for River Flow only model results

Flow Selection	Bed Shear Stress (Dynes/cm^2)							
	Cap 13				Cap 16			
	Min	Max	Mean	Std Dev	Min	Max	Mean	Std Dev
2-Year Return (Runs 1-3)	0.13	3.46	0.77	0.473	0.35	1.36	0.84	0.196
Daily Avg. (Runs 4-5)	0.04	0.65	0.18	0.179	0.16	0.32	0.22	0.040

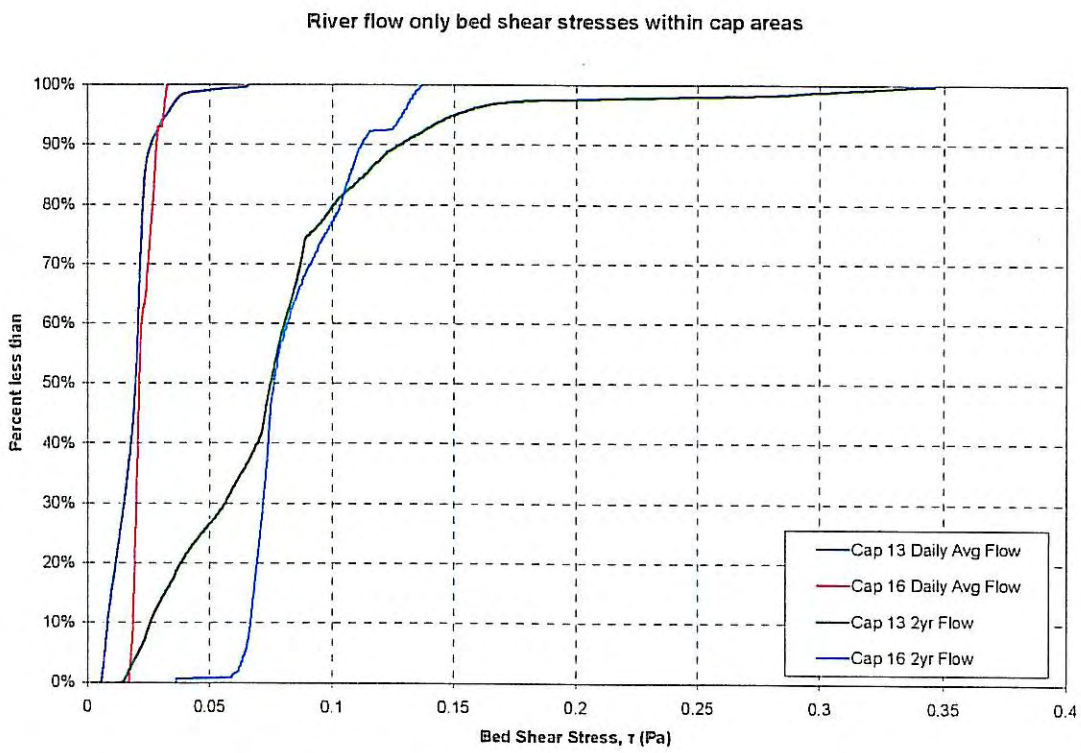

Figure 5. Bed shear stresses within cap areas for River flow only model results

3.2 Shear Stresses Generated by Wind-Waves and Wind-Driven Currents

The shear stress maps for the wave alone condition for the five model runs are shown in Figures 6a to 6e. As expected the most widespread high shear stresses are encountered in Runs 1 and 4, and these two results are quite similar (the wind speeds are not that different, Run 1 was 52.8 mph and Run 4 was 44.1 mph, both from the SSW). For these two runs the wave-only shear stresses within the proposed cap areas were always less than approximately 3.5 Pa or 35 dynes/cm^2. The NNE wind event of Run 5 produced wave-only shear stresses in similar range as Runs 1 and 4, but as expected, more towards the south end of Little Lake Butte des Morts. The WSW and NNW wind directions of Runs 2 and 3 respectively produced the highest wave-only shear stresses on the east side of the lake and generally less than 1.3 Pa.

3.2.1 Wind-Driven Circulation

Wind-driven circulation was predicted for the Run 1 condition only using ECOMSED. Figure 7a shows the predicted flow vectors for Run 1 with the 50-year SSW wind-generated currents combined with the 2-year river flow. The flow velocities of Figure 7a can be compared to those presented in Figure 3b for the 2-year river flow alone. It is evident that flow speeds along the shallower edges of the river have been significantly increased by the addition of the wind-driven circulation. Figure 7b shows the combined river and wind-generated flow shear stress map, and again, shear stresses are increased along the edges of the river, although remain less than about 1 Pa (10 dynes/ cm^2).

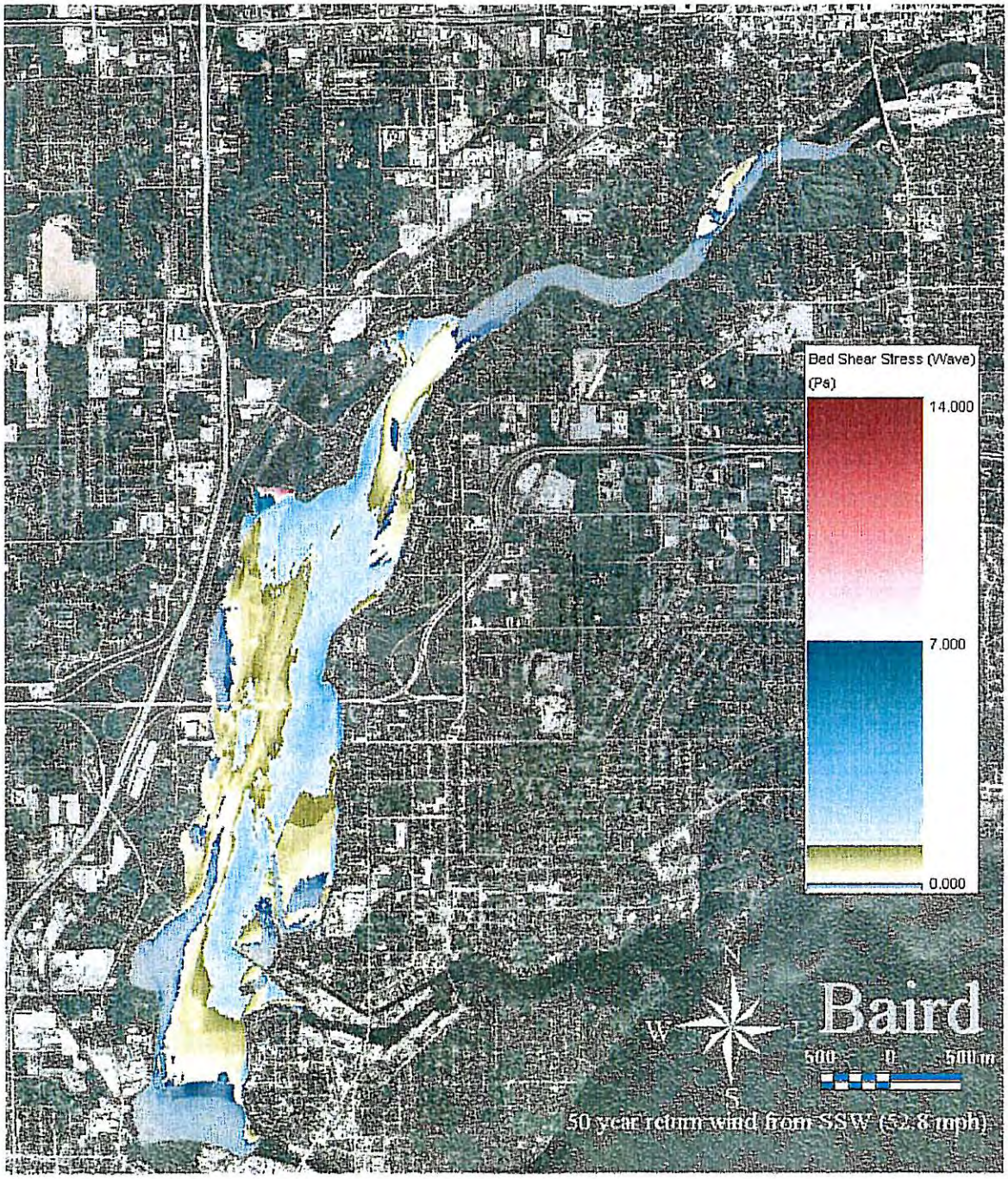

Figure 6a. Run 1 - Waves Only Shear Stress Map

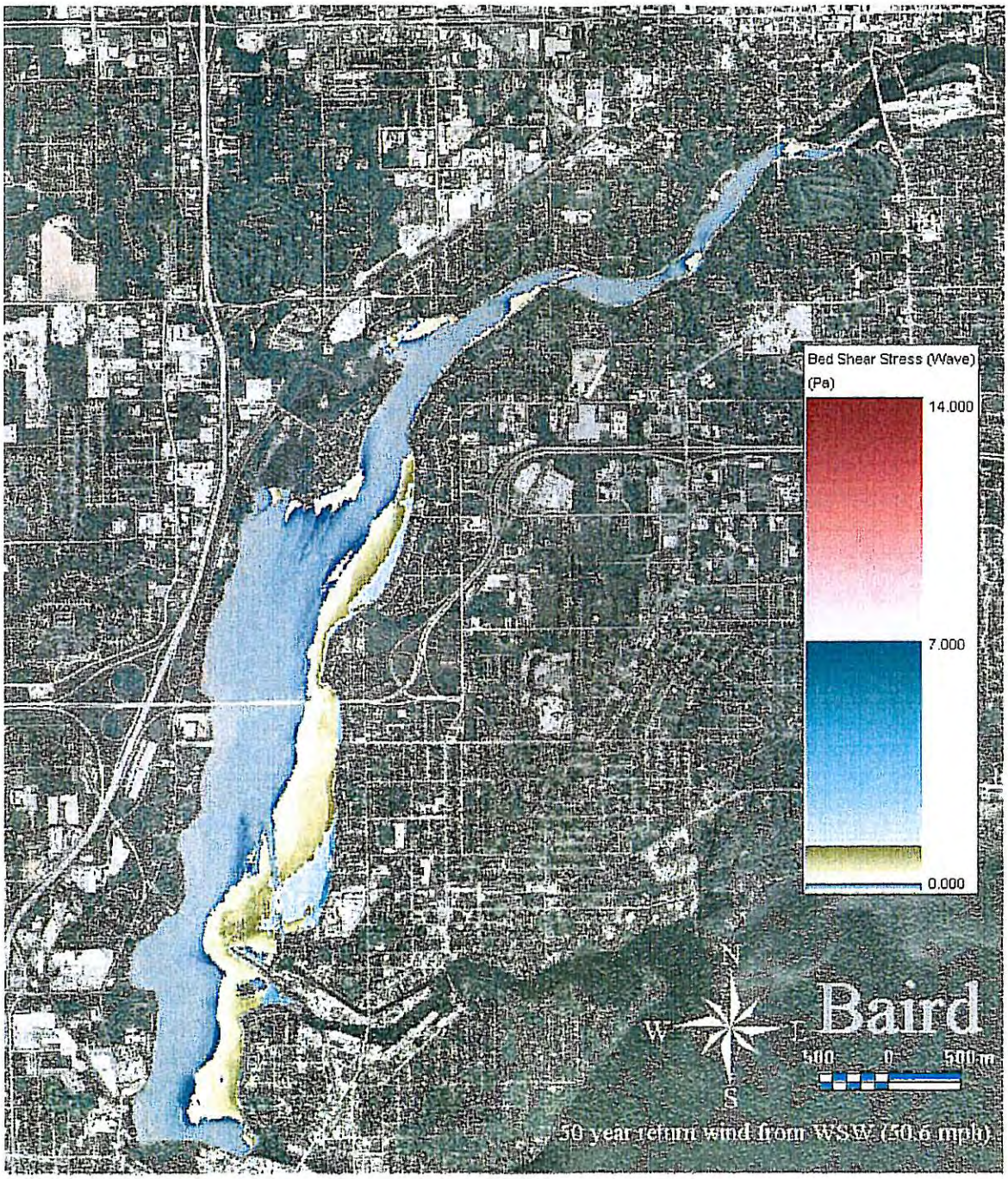

Figure 6b. Run 2 - Waves Only Shear Stress Map

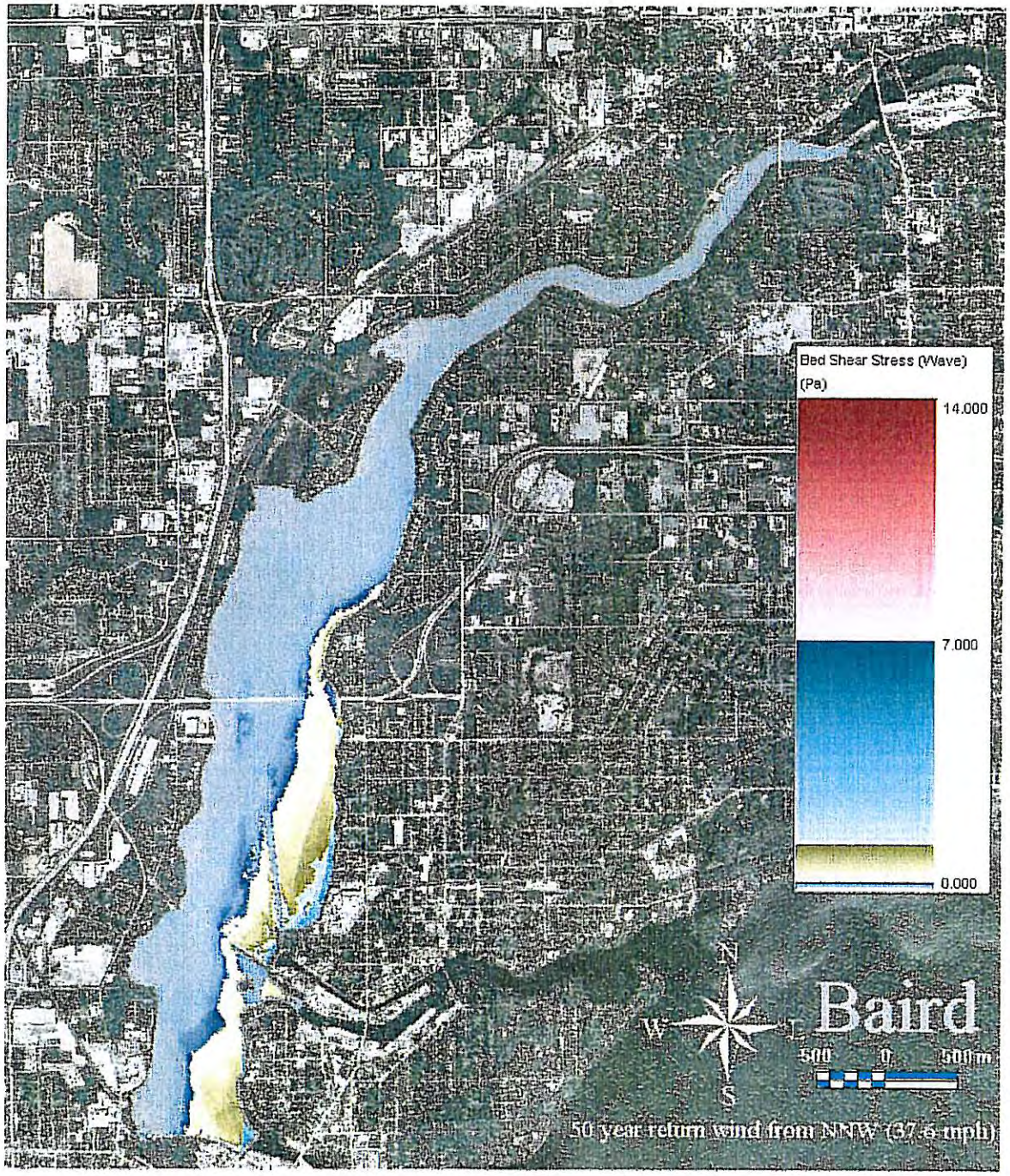

Figure 6c. Run 3 - Waves Only Shear Stress Map

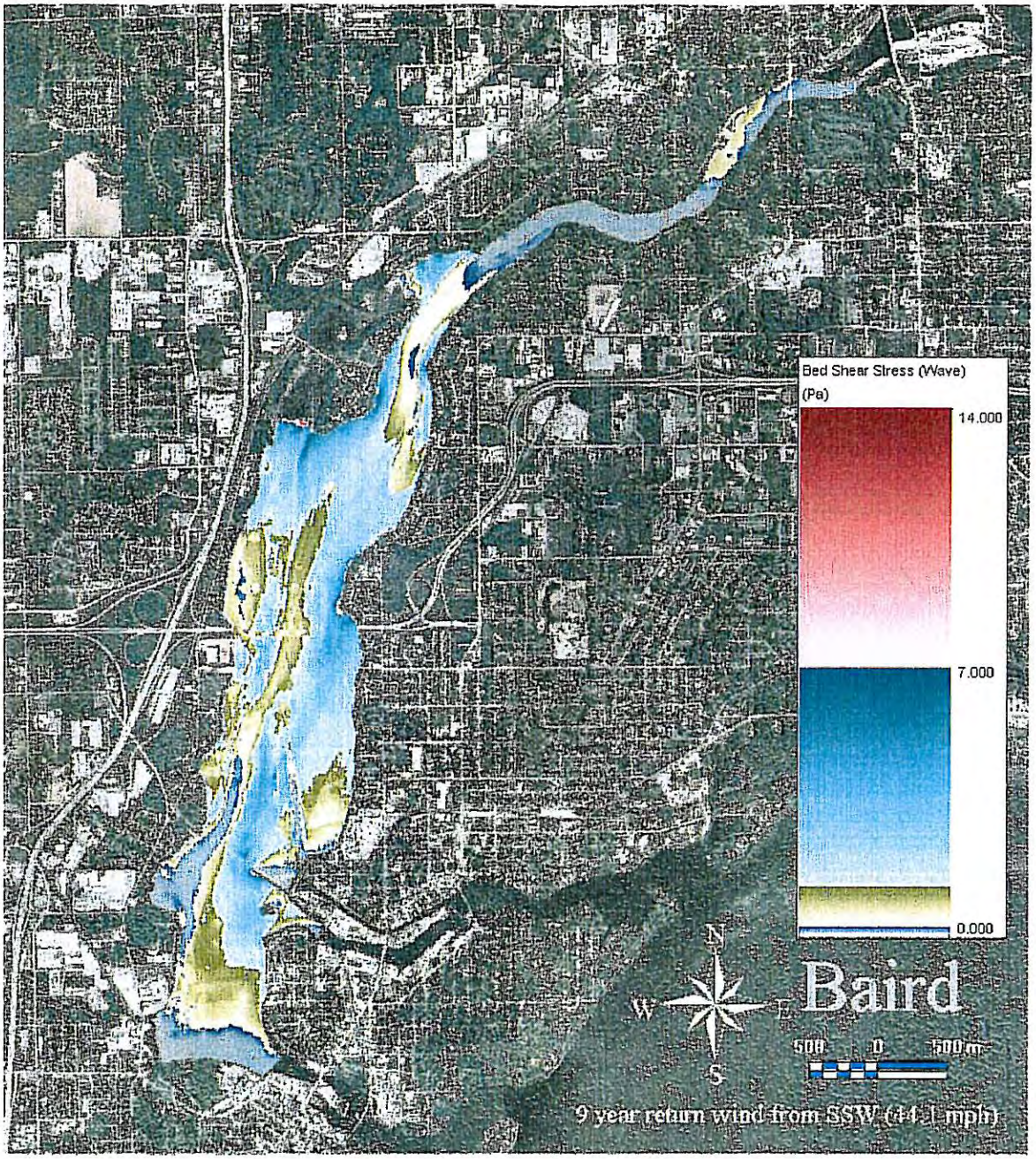

Figure 6d. Run 4 - Waves Only Shear Stress Map

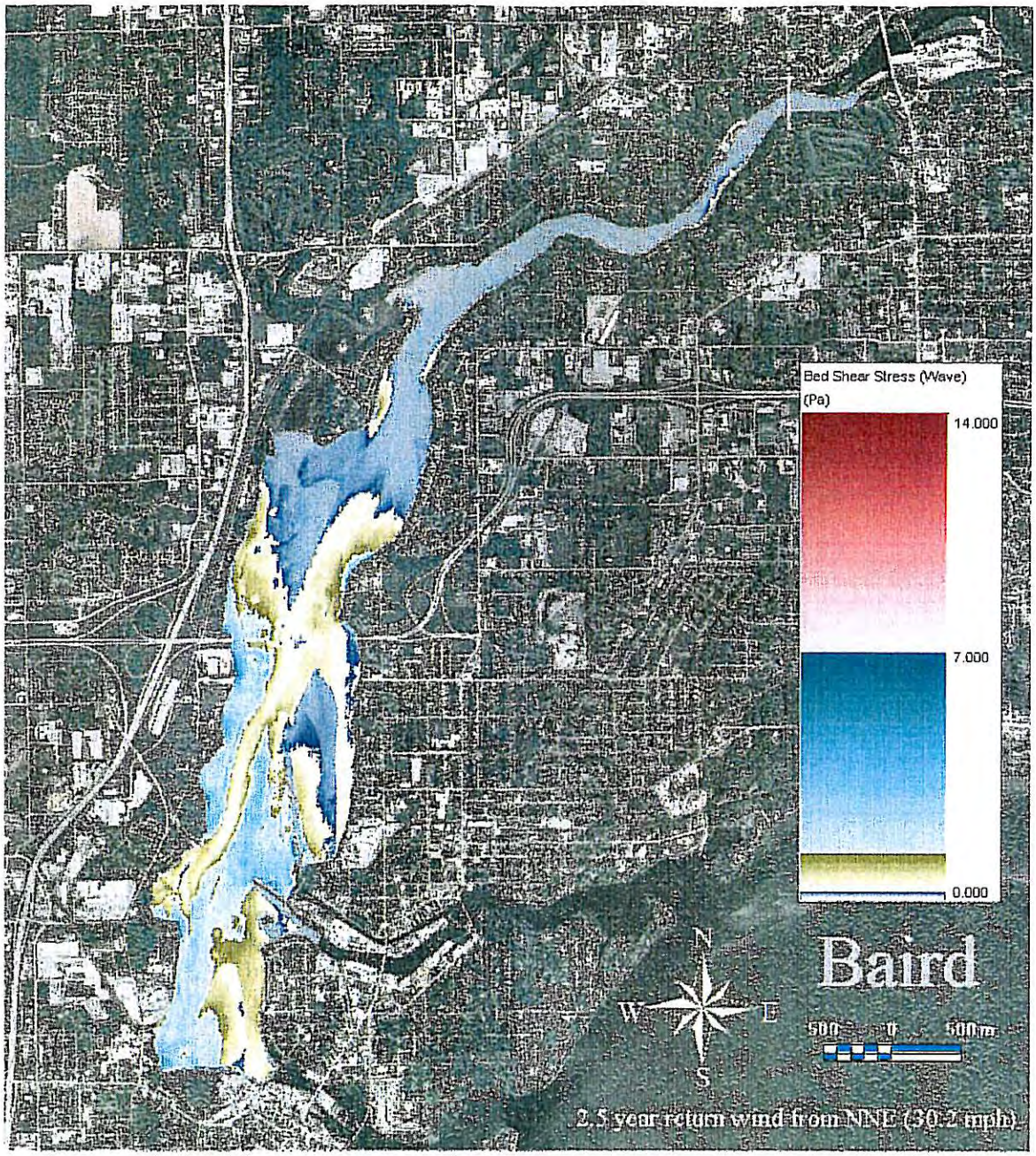

Figure 6e. Run 5 - Waves Only Shear Stress Map

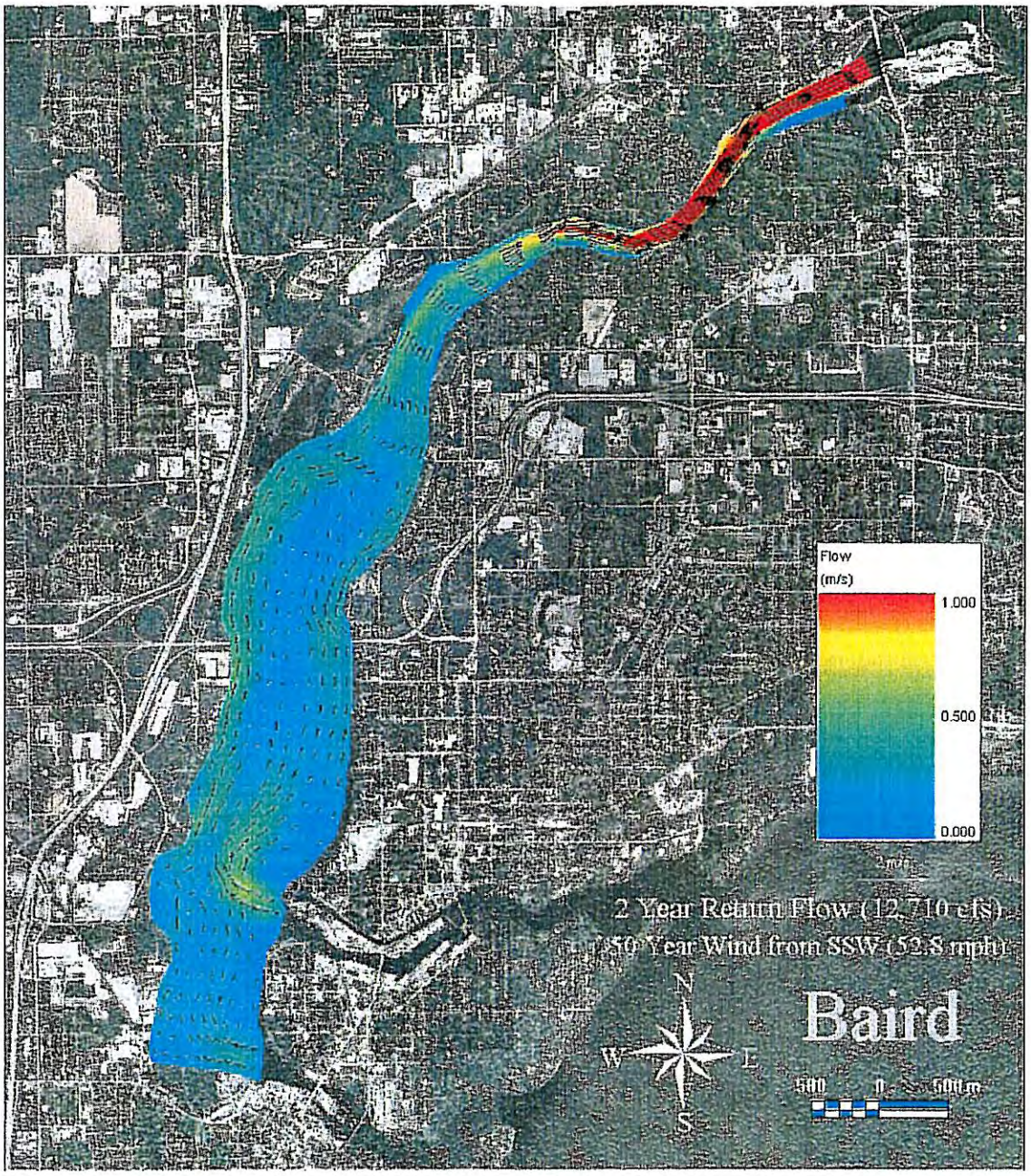

Figure 7a. Run 4 - Flow Speeds from ECOMSED for Wind and River Flow Generated Currents

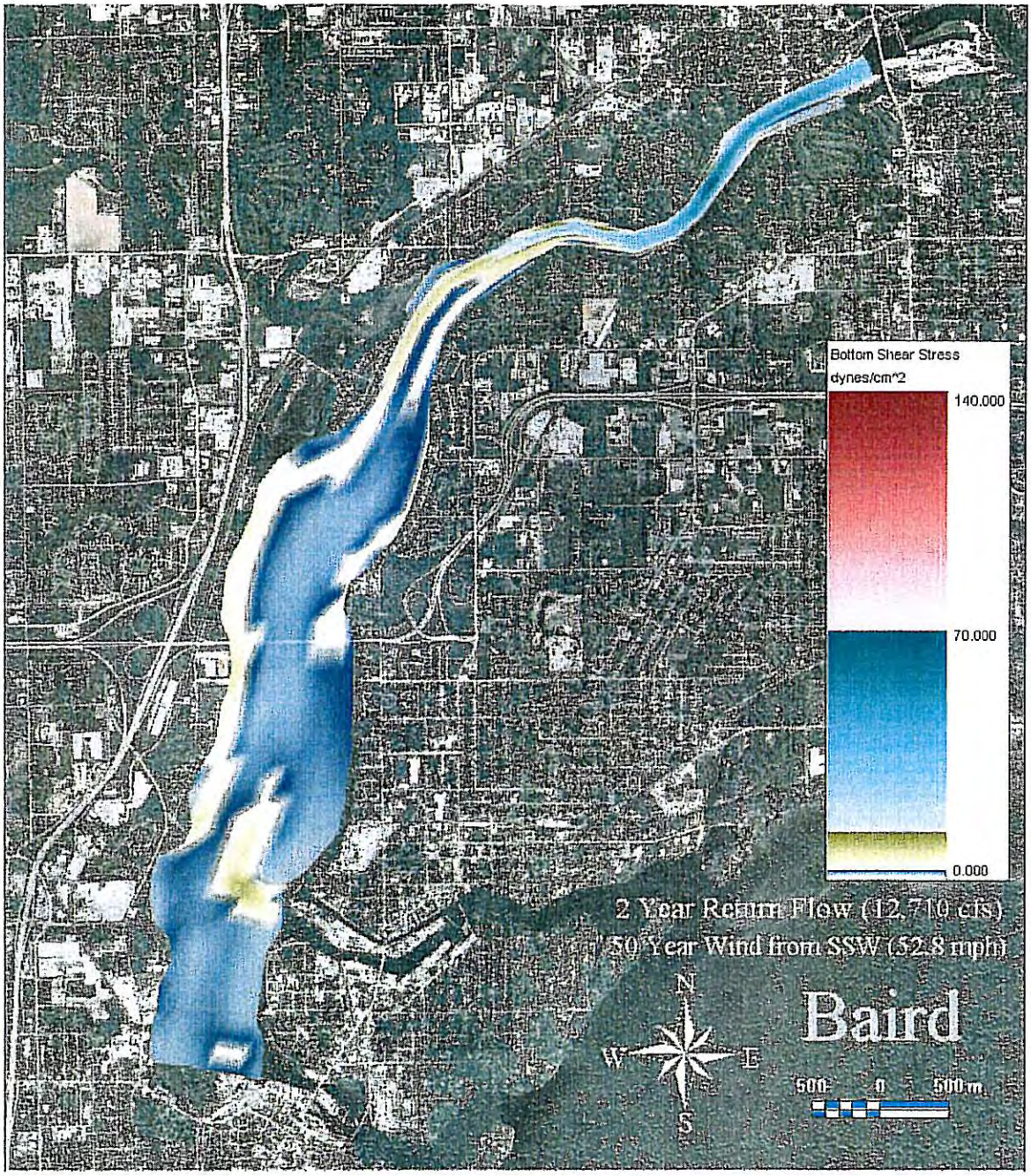

Figure 7b. Run 4 - River Flow Plus Wind-Driven Flow Shear Stress Map (i.e. no wave influence)

Numerically, the results indicate that the wind waves are more dominant than the river flow. For the runs with the wind waves only, the bed shear stresses were generally less than 3.0 Pa (30 dynes/cm^2) through the cap areas, however in an isolated area of Run 4, the maximum was up to 4.8 Pa (48 dynes/cm^2). A summary table of the results through the Cap 13 and 16 areas is provided in Table 6, and statistically presented in Figure 8.

Table 6
Bed shear stresses in cap areas for wind wave only events

Dataset	Bed Shear Stress in Cap 13 (Pa)				Bed Shear Stress in Cap 16 (Pa)			
Wind Wave Cond.	Min	Max	Mean	Std Dev	Min	Max	Mean	Std Dev
50 yr SSW (Run 1)	0.04	3.64	1.10	0.520	0.74	1.99	1.50	0.215
50 yr WSW (Run 2)	0.00	0.55	0.04	0.062	0.01	0.13	0.06	0.019
50 yr NNW (Run 3)	0.00	0.49	0.02	0.040	0.00	0.01	0.00	0.001
9 yr SSW (Run 4)	0.12	4.82	1.53	0.653	0.87	2.58	1.73	0.250
2.5 yr NNE (Run 5)	0.00	3.41	0.58	0.608	0.00	0.27	0.06	0.056

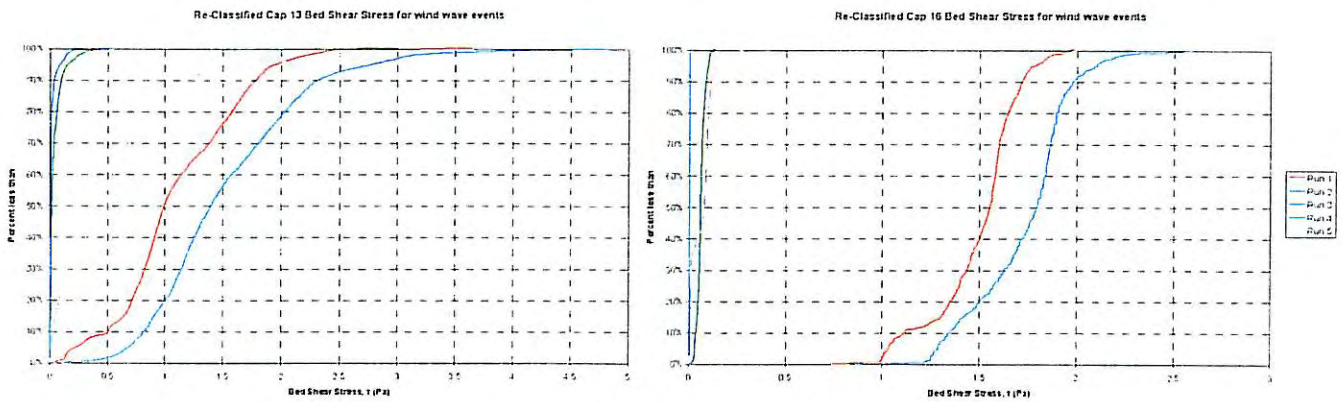

Figure 8. Bed shear stresses within cap areas for wind-wave event results only

It is worth noting that the bed shear stresses for Run 4 are greater than those in Run 1 despite the fact that the Run 4 condition included a lower wind speed event. On the basis of the equations described in Section 2.7, the bed shear stress generated by a combined wave and current climate is a function of wave related variables (height, period, and direction), flow velocity (speed and direction), and water depth. The wave information was calculated using STWAVE while the flow velocity and water depth was extracted from the ECOMSED model. Looking at the wave-alone case, the wave-induced bed shear not only depends on the wave height and period, but also on the water depth. The bed shear stress induced by waves decreases greatly as water depth increases (this is because the bottom orbital velocities decrease with increasing depth). The ECOM model result shows that the water level in Little Lake Butte des Morts depends upon the flow conditions from Lake Winnebago. The water levels in Little Lake Buttes des Morts increase to about 1.0 m above LWD during the 2-year return flow event, and for a 0.2 m water level at the Appleton Dam. The water levels in the lake increase to only 0.11m above LWD during the mean-flow conditions, with a -0.1 m water level at the Appleton Dam (the latter being the assumed downstream boundary condition for Runs 4 and 5). As a result, the greater water depth for Run 1 results in less wave-induced bed shear stress than was

observed in Run 4. The 50-year wind event with average flow conditions would result in higher combined shear stresses than any of the Runs 1 to 5.

3.3 Combined Wave-Current Shear Stresses Generated by Wind-Waves and River Flows

The combined shear stresses generated by wave-current interaction between the orbital velocities generated by wind-waves and the river flow are presented for the five model runs in Figures 8a to 8e (note that wind-generated currents were not considered in this analysis).

A comparison of the results of Runs 1, 4 and 5 show that the highest shear stresses occur in different areas for different combinations of events. However, for the selected events, shear stresses are almost always less than 3.5 Pa or 35 dynes/cm^2 through the cap area with a very small section of Run 4 having an estimated bed shear stress of approximately 4.8 Pa or 48 dynes/cm^2. A summary table of the results through the Cap 13 and 16 areas is provided in Table 7, and statistically presented in Figure 9.

Table 7
Bed shear stresses in cap areas for combined flow events

Dataset			Bed Shear Stress in Cap 13 (Dynes/cm^2)				Bed Shear Stress in Cap 16 (Dynes/cm^2)			
Flow Cond.	Wind Cond.	Run #	Min	Max	Mean	Std. Dev.	Min	Max	Mean	Std. Dev.
2 Year	50 yr SSW	1	0.55	36.62	11.78	5.23	7.99	20.59	15.71	2.18
2 Year	50 yr WSW	2	0.13	5.84	1.15	0.77	0.42	2.13	1.45	0.28
2 Year	50 yr NNW	3	0.13	5.25	0.92	0.59	0.36	1.36	0.84	0.19
Daily Avg.	9 yr SSW	4	1.77	48.24	15.44	6.52	8.82	25.97	17.47	2.49
Daily Avg.	2.5 yr NNE	5	0.18	34.12	5.96	6.04	0.17	2.88	0.86	0.56

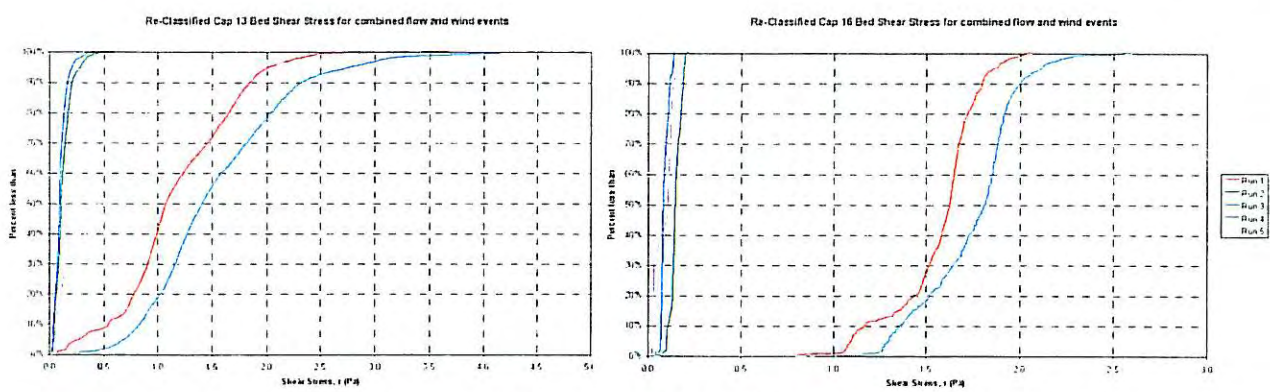

Figure 9. Bed shear stresses within cap areas for combined river flow and wind results

It is noticeable that the trend of Run 4 having higher bed shear stresses than Run 1 through the cap area continues. This is once again caused by higher water levels in Run 1. Furthermore, it demonstrates that the wave component is more dominant than the flow component, particularly with lower water levels. A run with a 50-year return period wind from the SSW combined with an average flow condition would result in higher shear stresses than any of the combinations considered in Runs 1 to 5.

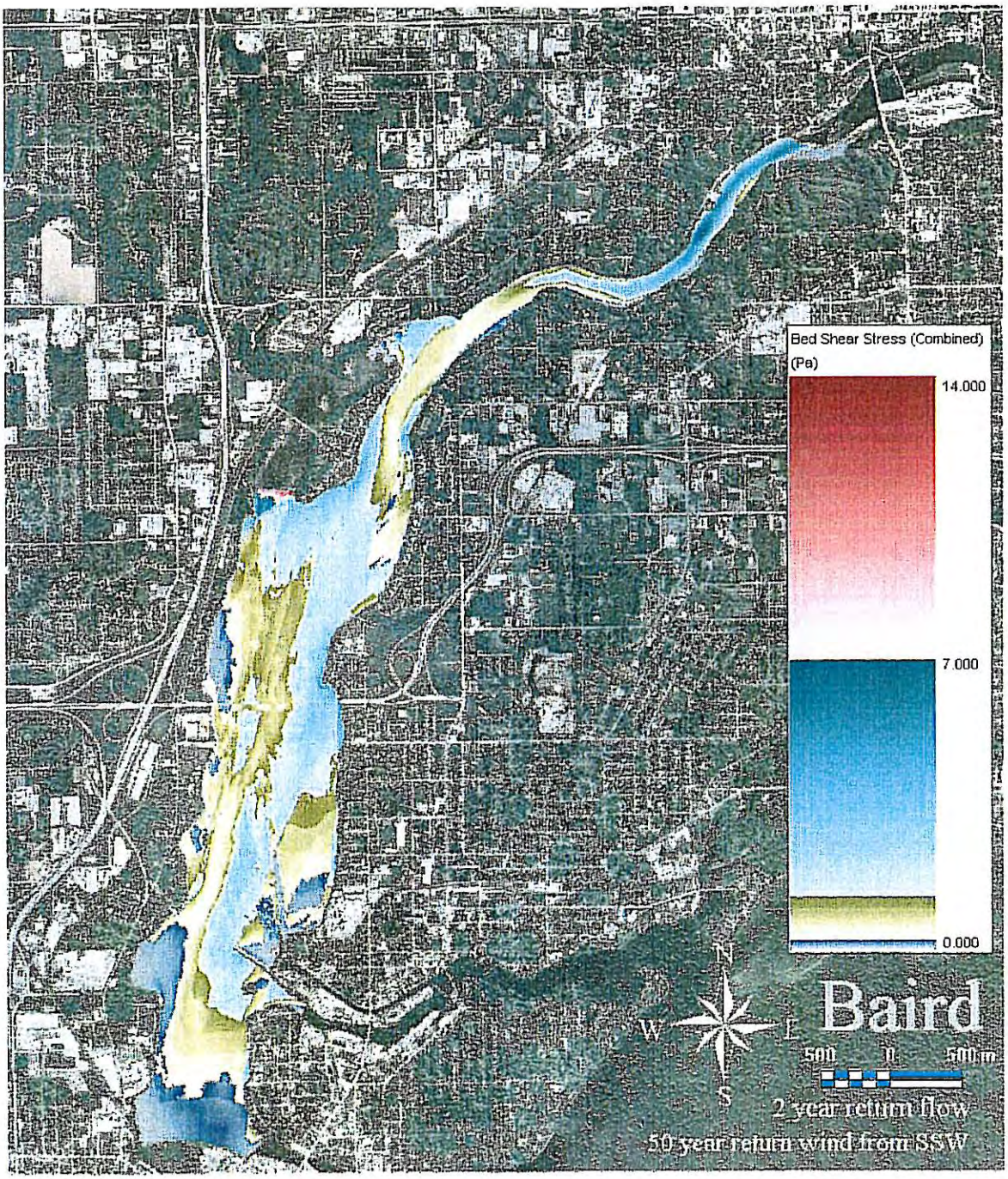

Figure 8a. Run 1 - Combined Wave-Current Shear Stress Map

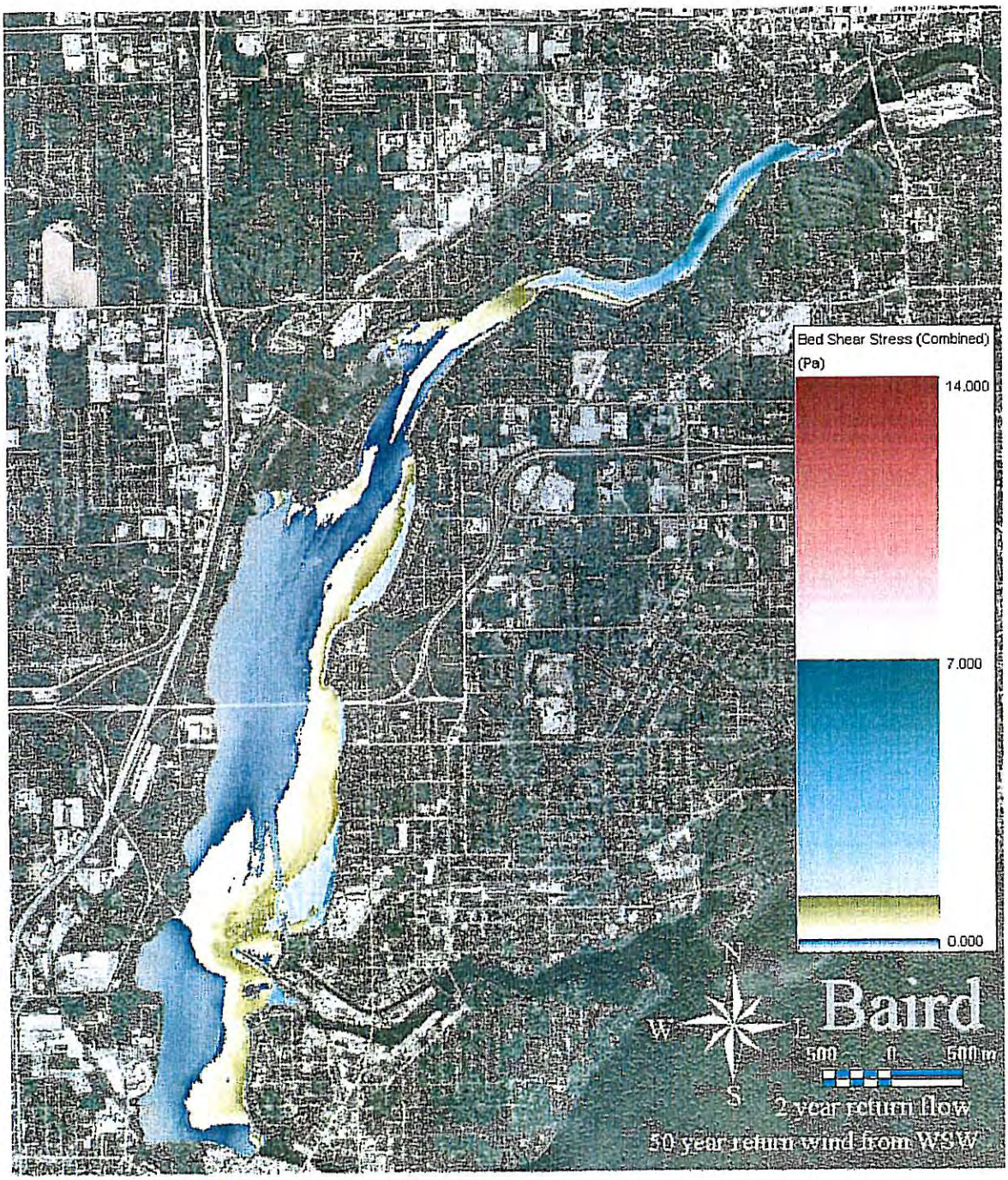

Figure 8b. Run 2 - Combined Wave-Current Shear Stress Map

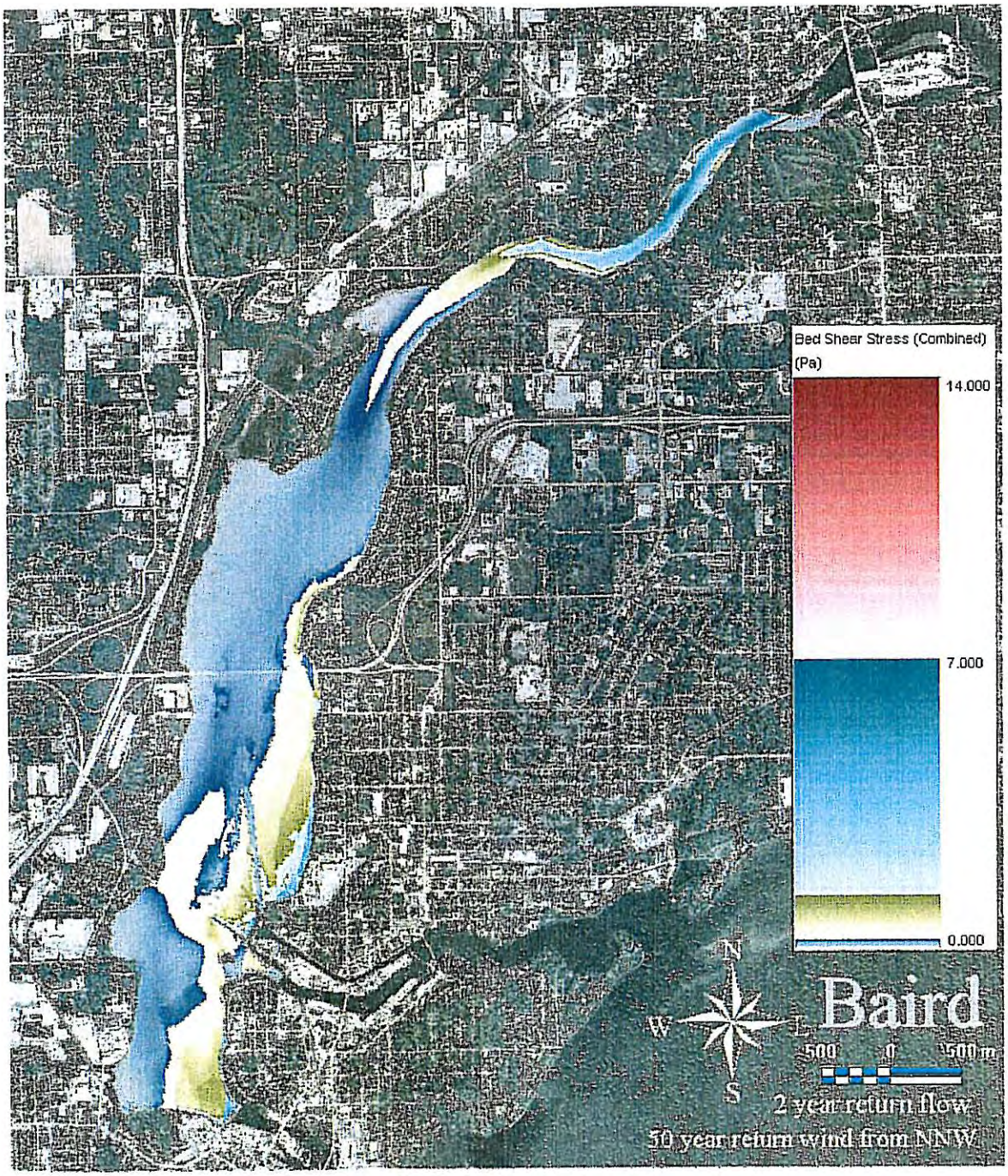

Figure 8c. Run 3 - Combined Wave-Current Shear Stress Map

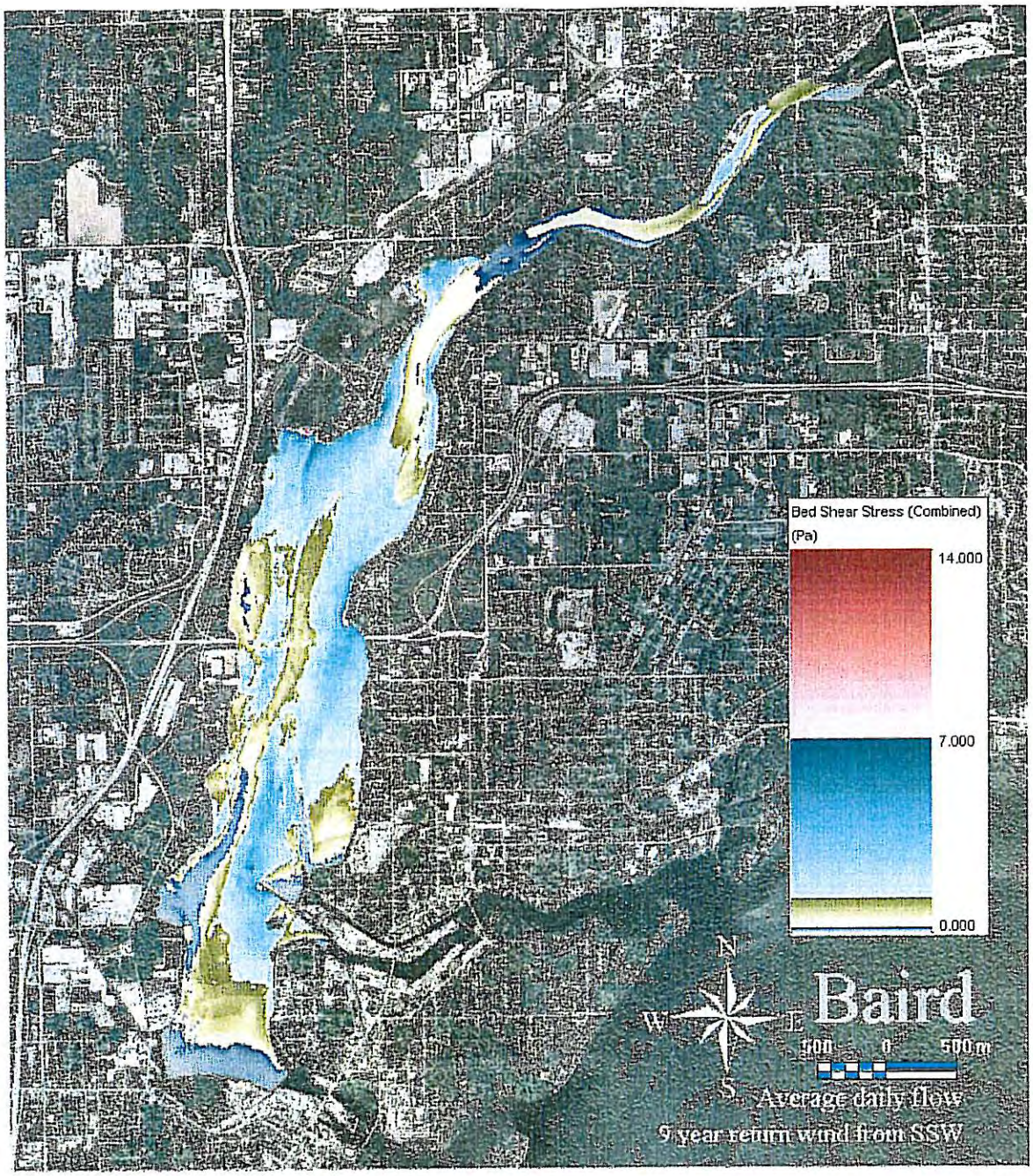

Figure 8d. Run 4 - Combined Wave-Current Shear Stress Map

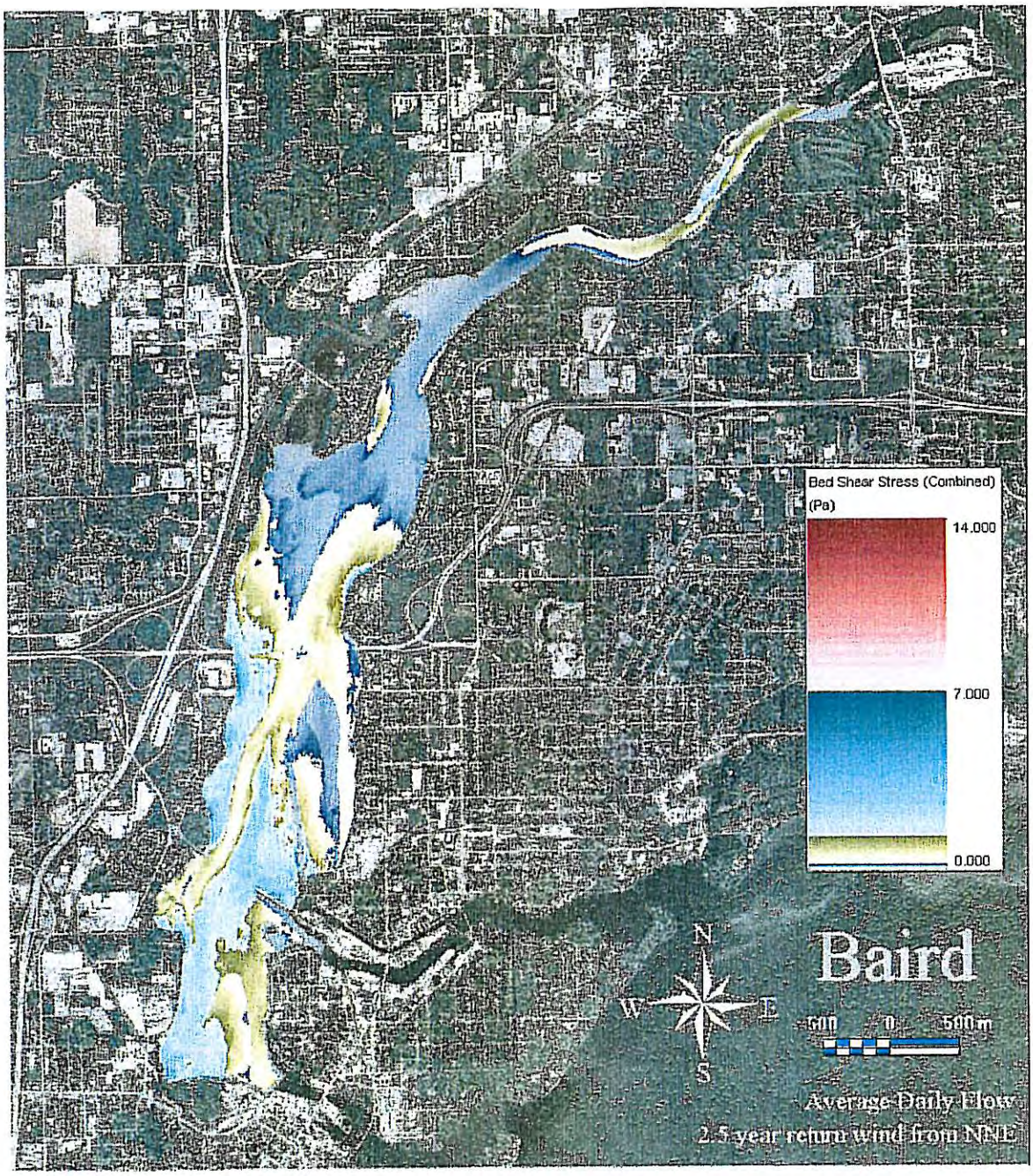

Figure 8e. Run 5 - Combined Wave-Current Shear Stress Map

4.0 REVIEW OF PAPERS ON PUMPING AND LIQUEFACTION

In order to consider other implications of wind-waves on the proposed OU1 cap, Baird reviewed relevant literature identified by Foth on the processes of wave pumping and liquefaction. These processes may affect the design of the cap for OU1. However, specific design recommendations regarding these processes were not intended to be within the scope of this work. Instead, the objective was to provide opinion on the relevance of these processes to the cap design process.

The processes of wave pumping and liquefaction are related to the pore-pressures in submarine soil. As a wave passes, the increase in pressure above the crest of the wave pumps additional pressure into the soil matrix below the crest. Sometimes, as the trough of a wave passes, there is insufficient time for the pressure to dissipate, resulting in a buildup of pressure until eventually the pressures are greater than the overburden pressure; at this point the soil acts as a fluid and may flow downhill or allow supported structural elements to sink into it. A secondary way for soils to liquefy under waves is for momentary liquefaction to occur, this is as a result of a wave trough passing: the sudden reduction in water pressure at the bottom reduces the overburden pressure sufficiently to allow a temporary liquefaction of a relatively small area of soil. Liquefaction not resulting from waves (such as earthquakes) is not considered here.

4.1 Wave Pumping Review

The two papers that were reviewed on wave pumping were:

- Habel and Bagtzoglou (2005)
- Precht and Heuttel (2003)

Habel and Bagtzoglou (2005) indicate that the flux through a porous bed is a function of the ratio of wave length to water depth and soil permeability. For the 50-year wind conditions the predicted peak wave period was approximately 2.5 s for the longer fetch events (SSW), and approximately 2.2 s for the shorter fetch events (WSW). The average water depth in the areas of interest is in the range of 2 m. These conditions give a wave length of 8.7 m for the SSW events and 7.2 m for the WSW events. These correspond to a wave length to water depth ratio of 4.35 and 3.55, respectively. If one assumes a permeability for the proposed cap corresponding to sandy gravel ($K = 1 \times 10^{-11}$ m^2), the potential flux at the bed interface may be estimated from Figure 5 of Habel and Bagtzoglou (2005). This approach yields fluxes in the range of approximately 4 to 8 x 10^{-6} m/s. It is likely there will be flux between the river bed and the underside of a 13-inch fine to medium gravel cap as currently envisaged, however filter layers could be used to minimize the risk of it occurring. More detailed consideration of potential flow between the native sediment and the overlying water would require information on the anticipated filtering design and more detailed analysis is beyond the scope of this review. The Precht and Heuttel (2003) paper primarily focuses on conditions where ripples are created on the surface of a sandy deposit. This will likely not occur for the proposed cap of OU1 as the material will be selected to be stable under all conditions.

4.2 Liquefaction Review

The documents reviewed on liquefaction were:

- Nataraja and Gill (1983)
- Madsen (1978)
- De Wit (1995)
- De Wit and Kranenburg (1997)

Wave-induced liquefaction is caused by either temporal or spatial gradients in pore-water pressures within the matrix of a soil generated by wave-induced pressures. Liquefaction can result in the loss of soil strength, resulting in a flow of the soil mass down a slope, or supported structures sinking into the weakened sediment. Although the waves on Little Lake Butte des Morts are not large, the oscillations in wave pressures could result in liquefaction that would allow the cap armor to sink into the supporting soft sediments. Madsen (1978) presents an equation to evaluate the potential for failure conditions in cohesionless sediment. For a water depth of approximately 2 m, the 50-year wind event resulted in a wave period of 3 s and wave height of 60 cm in the cap zone; for this wave condition it is clear that liquefaction failure of coarse sandy sediment is not possible, and certainly not possible for an anticipated cap sediment size of greater than 25 mm. Furthermore, in a case where there are no foundations of concern, liquefaction only becomes an issue where there is sufficient slope of the material enabling it to be transported away from its initial position. This requires relatively steep slopes such that auto-suspension and/or underwater avalanching conditions can be generated (Nairn, 1990). For sandy beds (i.e. with a median grain size in the range of 0.2 mm) this would require slopes significantly steeper than approximately 1 (vertical): 2.5 (horizontal) together with a flow speed of approximately 1 m/s. This range of bed slopes and flow speeds do not exist in OU1, and the anticipated cap sediment size is much coarser. Possible interaction between wave-induced pore-water flows and the native material under the cap may be another issue to consider, however, this is more a question of appropriate filtering design between the layers.

De Wit and Kranenburg (1997) studied liquefaction in cohesive sediments caused by waves. They undertook a series of physical modeling studies, with the primary emphasis on China, Caland, and Westwald clays. They found that liquefaction occurs in these clayey materials when the pore pressure reaches approximately the soils yield stress value. Following from this, they observed that the required wave height to induce liquefaction increased with consolidation time. This means that after placing the cap, the probability of liquefaction occurring decreases with time, down to some minima. The level of consolidation that occurs as a result of placing the cap is dependant upon the soil type and properties beneath the cap and the final cap design. Therefore, consideration of the potential for liquefaction of the cohesive sediment underlying the cap is dependent on the change of the cohesive soil characteristics associated with the construction of the cap, and specifically, the degree of consolidation. This type of geotechnical assessment is beyond the scope of this preliminary review.

5.0 CONCLUSIONS AND RECOMMENDATIONS

The conclusions of this report include and build on the conclusions and recommendations of the Baird (2006) report that evaluated river-current only shear stresses for the 100-year return period flow event.

- Baird (2006) found that the bed shear stresses in Little Lake Butte des Morts (Fox River OU1) under the condition of the 100-year return flow are generally less than 1.3 Pa (13 dynes/cm^2) and this is associated with the critical shear stress for erosion for very coarse sand (< 2 mm). This indicates that very coarse sand is likely stable under the 100-year return river flow alone (i.e. no waves or wind) for areas with shear stress equal to or less than 13 dynes/cm^2.
- Baird (2006) also found that there is no significant impact of water level change, at the Appleton Dam, on the bed shear stress generated by river flows in Little Lake Butte des Morts.
- The current study evaluated selected combinations of possible combined 100-year (events) return period conditions associated with river currents, orbital velocities generated by wind-waves, and to a limited extent, steady flows generated by wind stresses.
- A wind record and extreme value analysis was completed with winds from the Green Bay and Appleton wind stations. The analysis determined that there was limited or no dependency between extreme flows and extreme winds. Therefore, the 100-year combined event can be approximated as a direct multiple of wind speed return period and river flow return period (e.g. 50-year wind and 2-year flow or 33-year flow and 3-year wind).
- Three possible 100-year conditions were selected consisting of 50-year return period winds from the SSW, WSW and NNW combined with the 2-year return period river flow condition. The US Army Corps of Engineers STWAVE model was applied to predict the wave conditions for the selected wind events on OU1.
- Two additional runs were completed to evaluate two conditions similar to the approach used to derive the wind-wave and flow design shear stresses for OU2 to OU5 (Shaw and Anchor, 2006). Through the cap areas, the event from the SSW resulted in comparable bed shear stresses as the SSW 100-year return period events.
- Combined shear stresses were calculated using the approach of Van Rijn (1993) and it is noted that, in conditions where waves and currents are occurring simultaneously, it is necessary to compute the combined shear stresses considering wave-current interaction in the boundary layer.
- For the selected conditions that were evaluated, the combined wave-current shear stresses were found to be almost everywhere less than 3.5 Pa (35 dynes/cm^2) through both cap areas 13 and 16, with the maximum predicted shear stress of 4.8 Pa (48 dynes/cm^2). The mean values in the cap areas were at most 1.7 Pa (17 dynes/cm^2) for the SSW conditions, other directions had lower bed shear stresses. The 90th and 95th percentiles were at most 2.3 Pa (23 dynes/cm^2) and 2.8 Pa (28 dynes/cm^2), respectively. Throughout both the Cap 13 and 16 areas, the predicted maximum bed shear stresses correspond to the stability of a coarse sand or fine gravel. The GIS files for all of the shear stress maps have been provided with this report (see Section 3).
- It is noted that there may be other 100-year return period combinations of wind speed and flow conditions that generate higher shear stresses, and therefore, represent the true 100-year bed shear stress condition. On this reach of the Fox River, owing to the width of the lake and the diffused river flow, wave-generated shear stresses dominate. Also, as determined through this analysis, lower flow

conditions together with high wind speeds result in the highest bed shears stresses due to the greater influence of wave-generated shear stresses for Little Lake Buttes des Morts and due to the significant influence of shallow water (associated with low flows) on increasing wave-driven shear stresses. Therefore, it is possible the 100-year wind condition with an average flow condition may result in the true 100-year shear stress condition. It is also possible that different parts of the cap may experience a 100-year shear stress condition from different wind conditions. The two most severe wind conditions for the cap area appear to be SSW (for the central and north end) and NNE (for the south end).

- The influence of wind-generated circulation on the flows in Little Lake Butte des Morts was predicted with ECOMSED for Run 1 with currents alone. This simulation showed that although flow speeds and related shear stresses vary both spatially and temporally through the model runs, they are generally significantly increased along the 200 to 300 m wide band at the edge of the river. However, the wind-generated flow shear stresses remain less than 1 Pa (10 dynes/cm^2). This influence was ***not*** included in the combined wave-current shear stress estimate for Run 1. If additional runs are completed with higher wind speeds (such as the 100-year wind speed), it would be advisable to consider the influence of wind-generated currents, particularly for analysis in shallow areas where the impact is much greater.
- Liquefaction concerns will be mitigated to some extent through the consolidation of the underlying sediment associated with the loading that will occur with placement of the cap. The extent of consolidation associated with placement of the cap would need to be evaluated by a geotechnical engineer. Wave-pumping was also reviewed in a preliminary manner and it was determined that there could be flow extending down below a medium-sized gravel cap thickness of 13 inches as currently envisaged. Details on filtering between the cap and the underlying native sediment would need to be considered in a more detailed evaluation of both liquefaction potential and wave pumping.

6.0 REFERENCES

Ashton, G. (2006). *Effects of Ice on Sediments in Little Lake Butte des Morts, Fox River above Appleton, Wisconsin*. Appendix A in "OU1 Final Plan: Lower Fox River Operable Unit 1", presented by GW Partners to Agencies and Oversight Team, Lower Fox River Project, November 2006.

Baird (2000). *ECOMSED Model Application: Upstream Lower Fox River From Lake Winnebago to DePere Dam*, Technical Report.

Baird (2006). *Numerical Model Assessment of Bed Shear Stress for the 100-year Return Flow, Little Lake Butte des Morts, Fox River*. Report submitted to Foth & Van Dyke and Associates Inc.

De Wit, P.J. (1995). Liquefaction of Cohesive Sediments Caused by Waves. Ph.D. Dissertation, Delft University of Technology. The Netherlands. 197 pp.

De Wit, P.J. and Kranenburg, C. (1997). The Wave-Induced Liquefaction of Cohesive Sediment Beds. Estuarine, Coastal and Shelf Science. 45, 261-271.

Habel, F., and Bagtzoglou, A.C. (2005). Wave Induced Flow and Transport in Sediment Beds. J. of the American Water Resources Association (JAWRA) 41(2):461-476.

Madsen, O.S. (1978). Wave-induced Pore Pressures and Effective Stresses in a Porous Bed. *Geotechnique* 28, No. 4, 377-393.

Nairn, R.B. (1990). Prediction of Cross-Shore Sediment Transport and Beach Profile Evolution. Ph.D. Thesis, Imperial College, London. 391 p.

Nataraja, M.S. and Gill, H.S. (1983). Ocean Wave-Induced Liquefaction Analysis. ASCE J. of Geotechncal Engineering, Vol. 109, No. 4, 573-590.

Precht, E. and Heuttel, M. (2003). Advective Pore-Water Exchange Driven by Surface Gravity Waves and its Ecological Implications. Limnol. Oceangr., 48(4): 1674-1684.

Shaw and Anchor (2006). *Final Basis of Design Report. Lower Fox River and Green Bay Site. Brown, Outagamie, and Winnebago Counties, Wisconsin*. Prepared for Fort James Operating Company, Inc. and NCR Corporation by Shaw Environmental and Infrastructure, Inc. and Anchor Environmental, LLC. June 16, 2006.

USACE (2001). "STWAVE: Steady-State Spectral Wave Model", *User's Manual for STWAVE*, Version 3.0. Coastal and Hydraulic Laboratory, ERDC.

Van Rijn, L.C. (1993). Principles of Sediment Transport in Rivers, Estuaries and Coastal Seas. Aqua Publications, Amsterdam, The Netherlands.

7.0 DELIVERABLES

- Current Only Bed Shear Stress for a 2 year return flow (Runs 1 to 3).shp
- Current Only Bed Shear Stress for average daily flow (Runs 4 and 5).shp
- Wave Only Bed Shear for 50 year return wind from SSW (Run 1).shp
- Wave Only Bed Shear for 50 year return wind from WSW (Run 2).shp
- Wave Only Bed Shear for 50 year return wind from NNW (Run 3).shp
- Wave Only Bed Shear for 9 year return wind from SSW (Run 4).shp
- Wave Only Bed Shear for 2.5 year return wind from NNE (Run 5).shp
- Bed shear stress for combined 2 year return flow and 50 year return wind from SSW (Run 1).shp
- Bed shear stress for combined 2 year return flow and 50 year return wind from WSW (Run 2).shp
- Bed shear stress for combined 2 year return flow and 50 year return wind from NNW (Run 3).shp
- Bed shear stress for combined daily average flow and 9 year return wind from SSW (Run 4).shp
- Bed shear stress for combined daily average flow and 2.5 year return wind from NNE (Run 5).shp

APPENDIX A

STWAVE RESULTS

FOR RUNS 2 TO 5 ON OU1, FOX RIVER

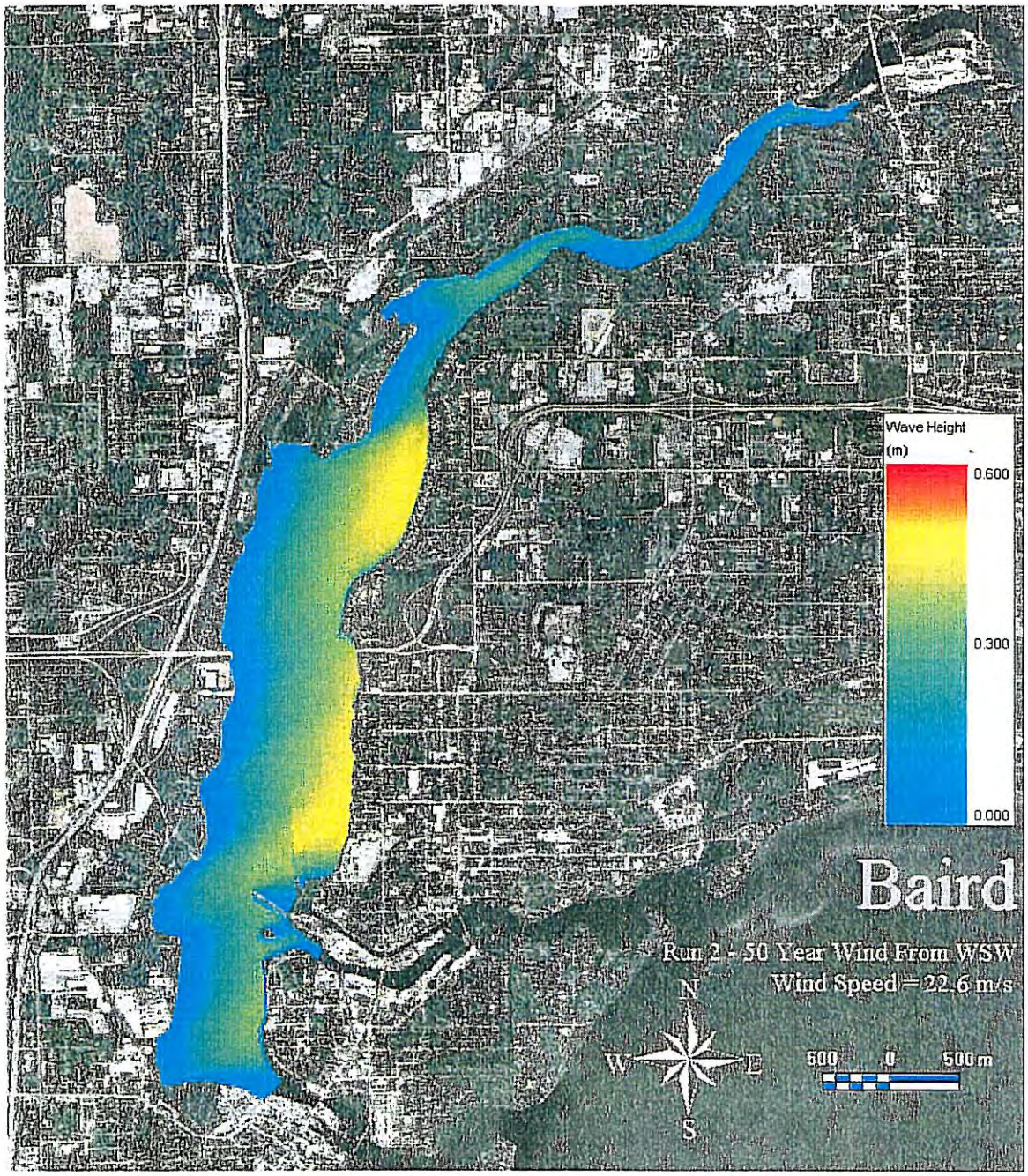
Wave Height
(m)
0.600
0.300
0.000
Baird
Run 2 - 50 Year Wind From WSW
Wind Speed = 22.6 m/s
N
W
E
S
500
0
500 m

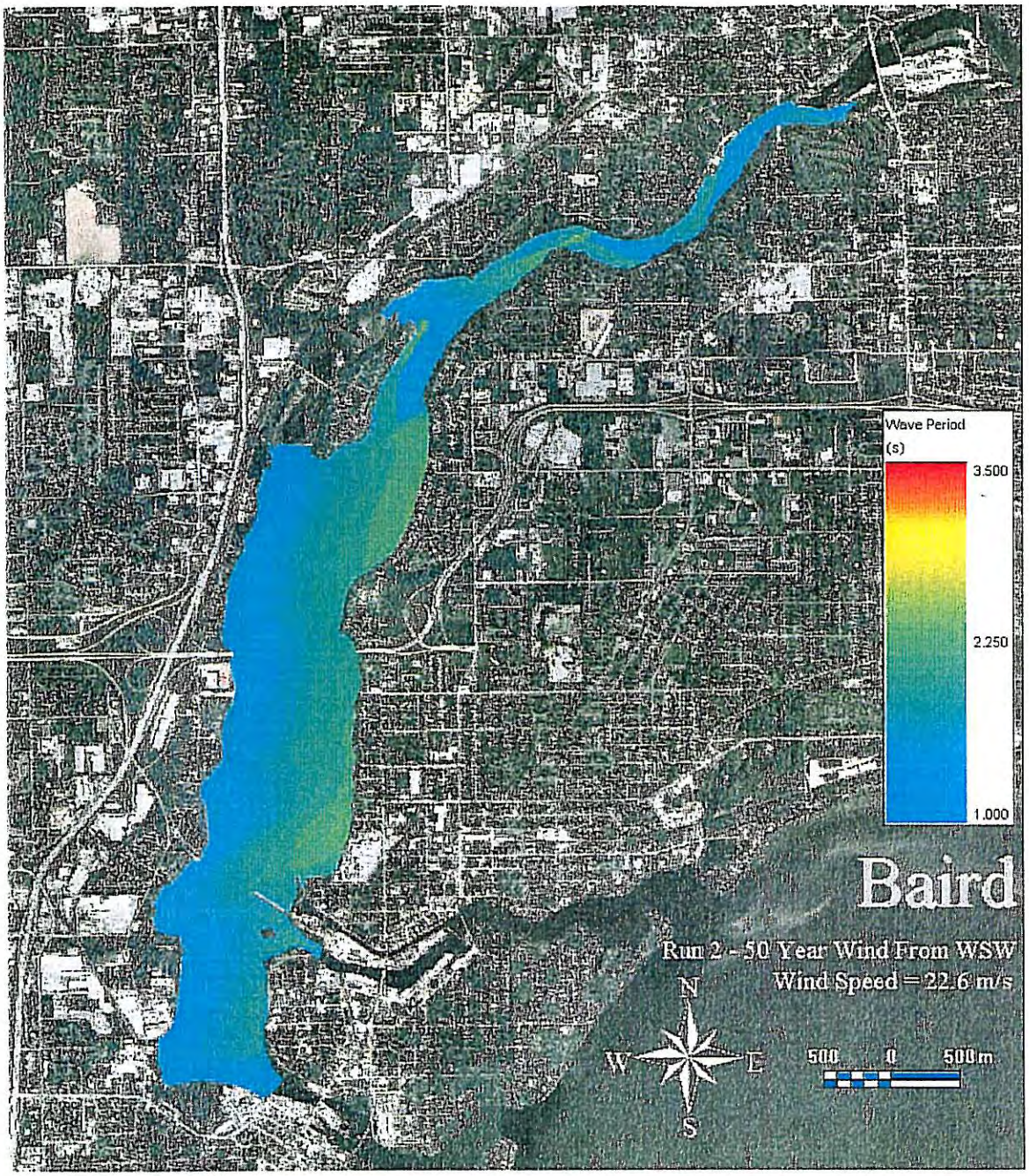
Wave Period
(s)
3.500
2.250
1.000
Baird
Run 2 - 50 Year Wind From WSW
Wind Speed = 22.6 m/s
N
W
E
S
500
0
500 m

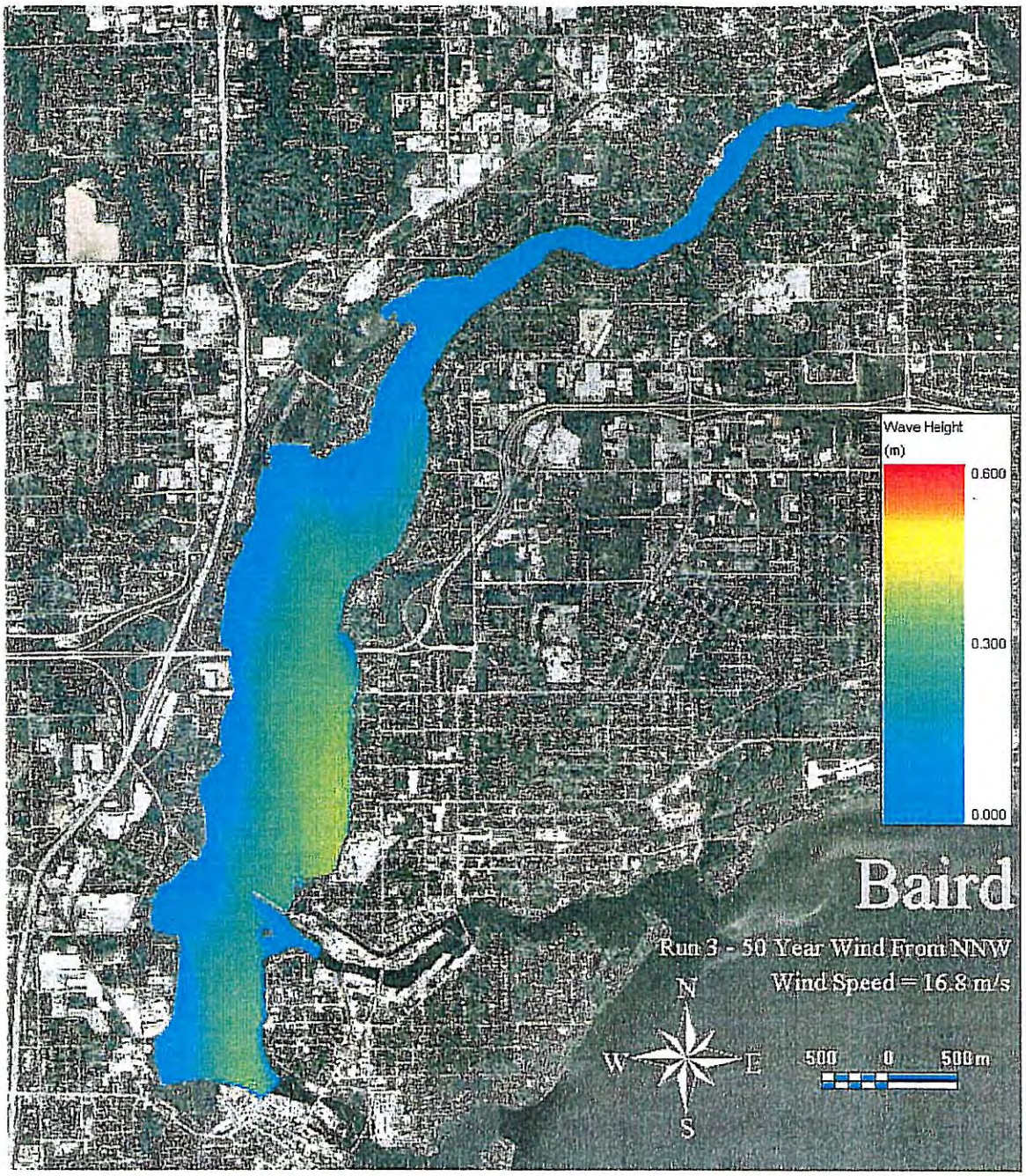
Wave Height
(m)
0.600
0.300
0.000
Baird
Run 3 - 50 Year Wind From NNW
Wind Speed = 16.8 m/s
N
W
E
S
500
0
500 m

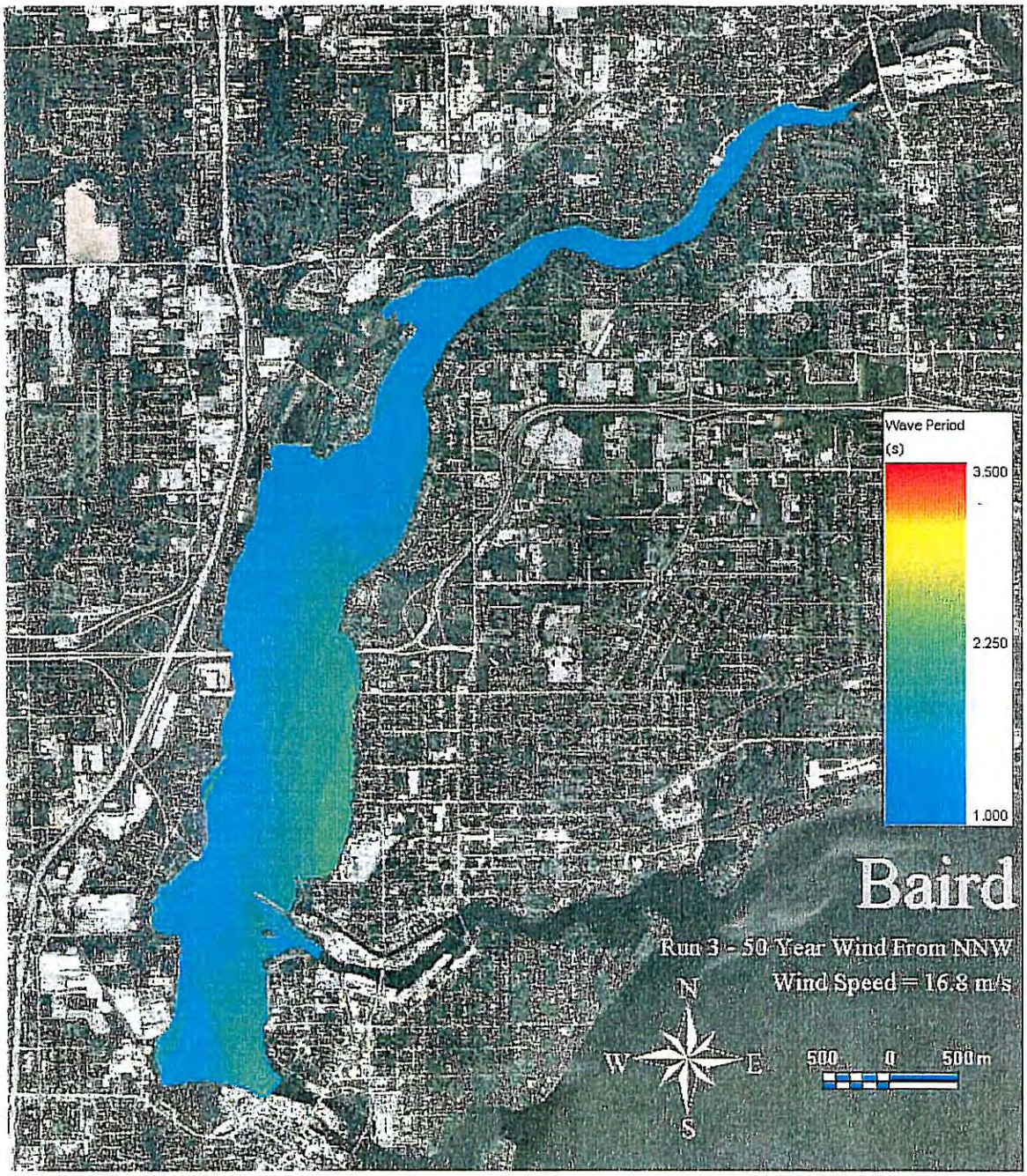
Wave Period
(s)
3.500
2.250
1.000
Baird
Run 3 - 50 Year Wind From NNW
Wind Speed = 16.8 m/s
N
W
E
S
500
0
500 m

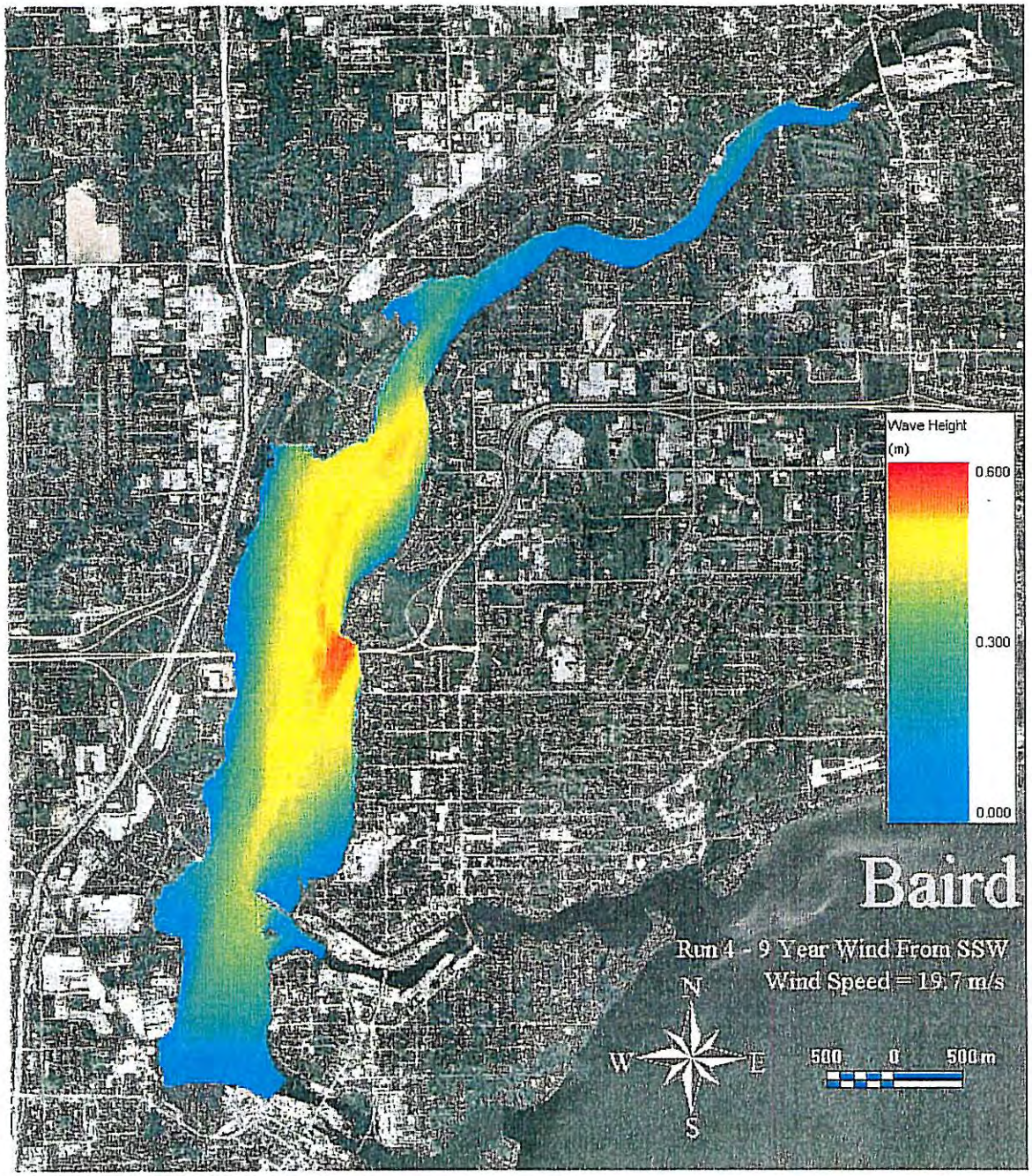
Wave Height
(m)
0.600
0.300
0.000
Baird
Run 4 - 9 Year Wind From SSW
Wind Speed = 19.7 m/s
N
W
E
S
500
0
500 m

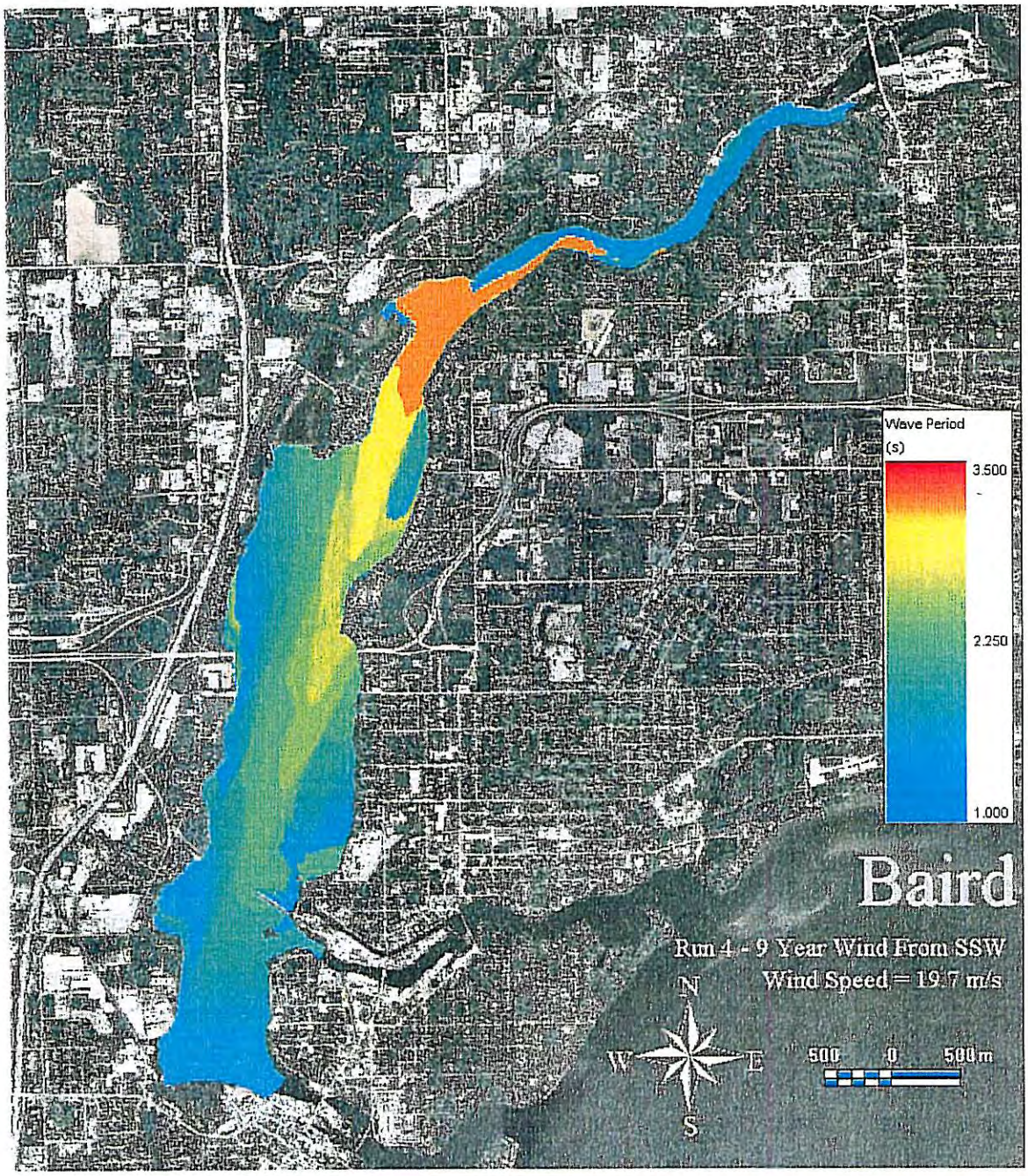
Wave Period
(s)
3.500
2.250
1.000
Baird
Run 4 - 9 Year Wind From SSW
Wind Speed = 19.7 m/s
N
W
E
S
500
0
500m

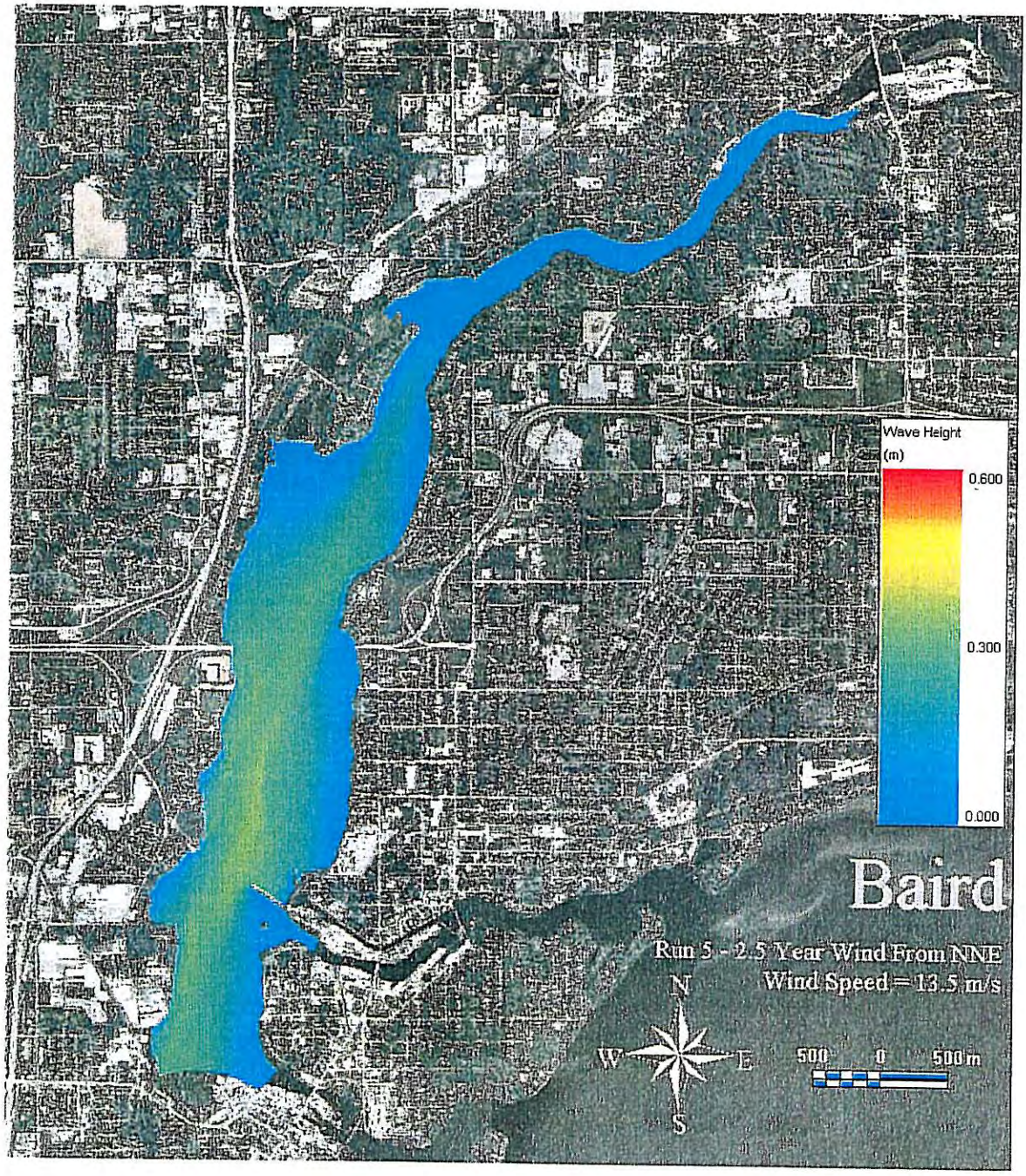
Wave Height
(m)
0.600
0.300
0.000
Baird
Run 5 - 2.5 Year Wind From NNE
Wind Speed = 13.5 m/s
N
W
E
S
500
0
500 m

APPENDIX B

PEAK OVER THRESHOLD ANALYSIS FOR EACH DIRECTION AND SEASON

Peak over Threshold Extreme Value Analysis

Data Set: Green Bay Winds 1978 - 2002 Full year: 180-225deg only

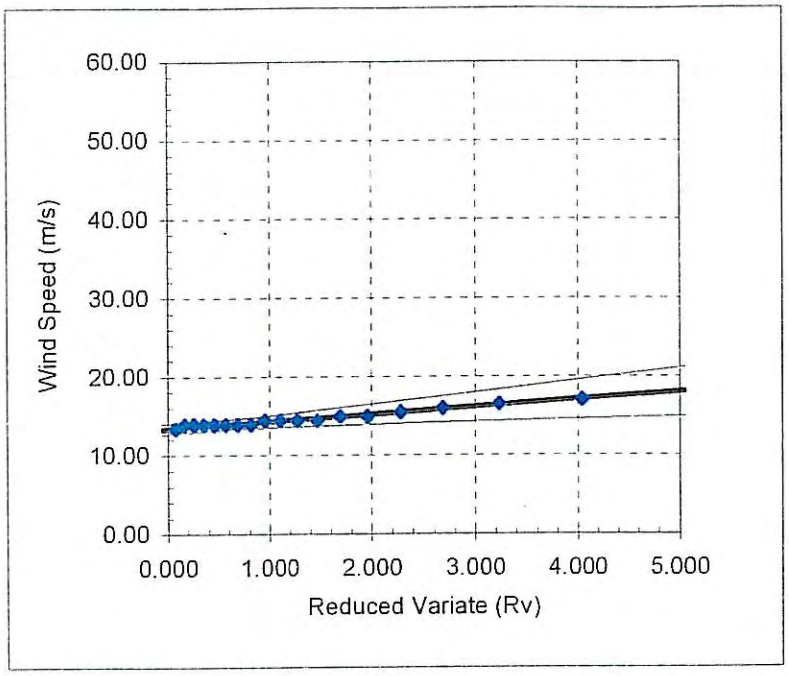

Fisher-Tippet II

Total Years of Data:	24
Total Storm Events:	32
Total No. Events Selected:	32
Events per year:	1.33

Sample Statistics

Mean:	14.50
Maximum:	23.14
Minimum:	13.36
s:	1.96
Sample skewness:	-0.34

FTII Parameters

Shape:	3.00
Scale:	0.928
Location:	13.374

Goodness of Fit

Correlation:	0.995

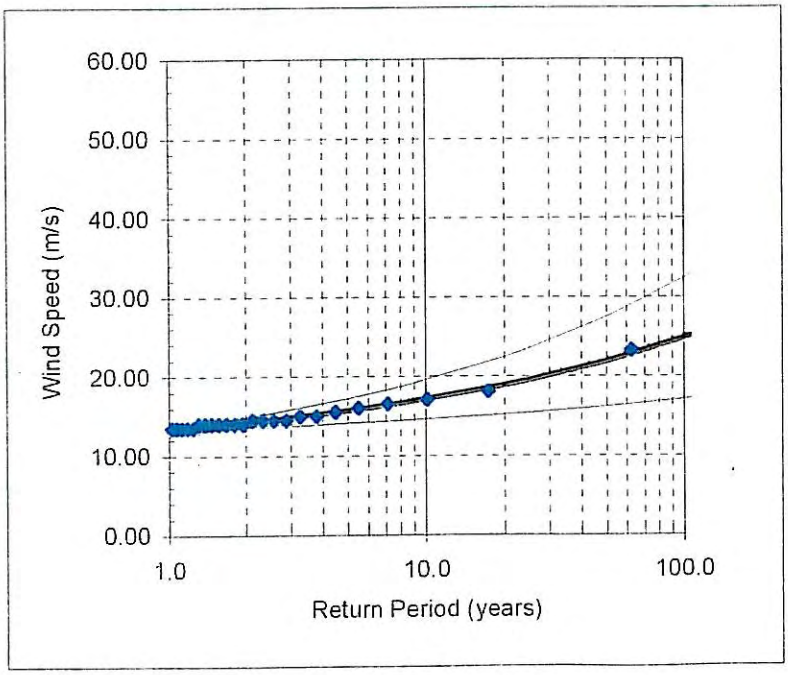

Return Period

		Confidence Limit	
Tr	X(T)	Upper	Lower
1	13.09	13.8	12.4
2	14.17	14.9	13.5
5	15.69	17.2	14.2
8.2	16.67	18.8	14.5
20	18.85	22.5	15.2
25	19.50	23.6	15.4
50	21.85	27.5	16.2
100	24.79	32.4	17.1
200	28.49	38.7	18.3
500	34.90	49.4	20.4

Date: 15-Jun-07

Baird

Peak over Threshold Extreme Value Analysis

Data Set: Green Bay Winds 1978 - 2002 Full Year: 225-280

Three-Parameter Weibull Distribution

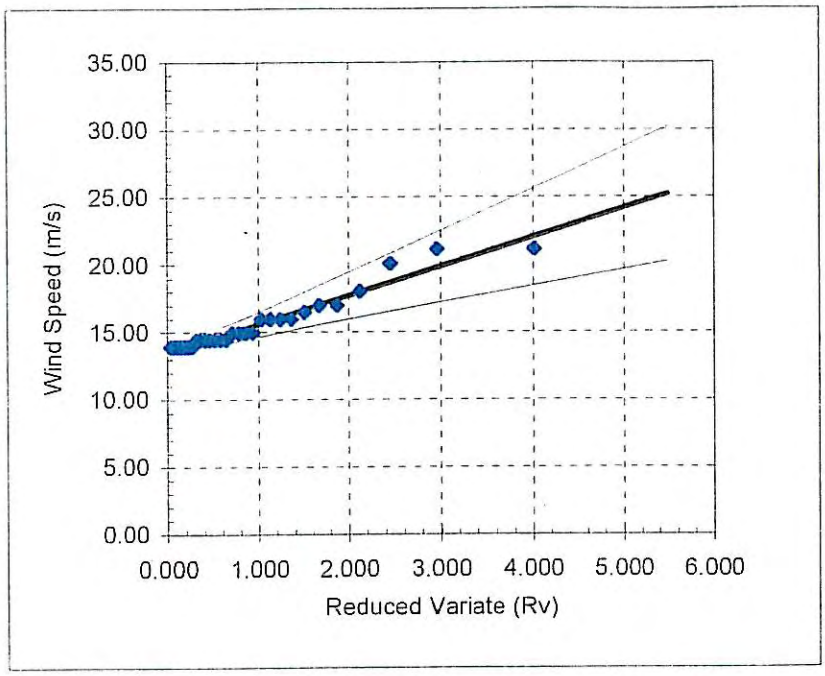

Total Years of Data:	24
Total Storm Events:	29
Total No. Events Selected:	29
Events per year:	1.21

Sample Statistics

Mean:	15.58
Maximum:	21.08
Minimum:	13.88
s:	2.10
Sample skewness:	-1.04

Weibull Parameters

Shape:	1.00
Scale:	2.149
Location:	13.435

Goodness of Fit

Correlation:	0.974

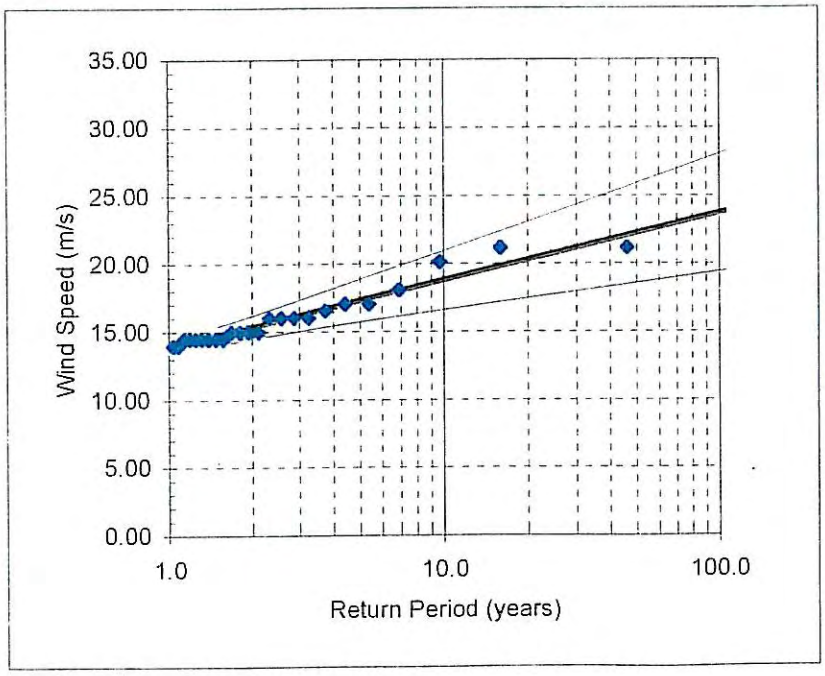

Return Period

		Confidence Limit	
Tr	X(T)	Upper	Lower
1.5	14.71	15.4	14.0
2	15.33	16.2	14.5
3.73	16.67	18.0	15.4
10	18.79	21.0	16.6
15	19.66	22.2	17.1
20	20.28	23.1	17.5
25	20.76	23.8	17.7
50	22.25	25.9	18.6
100	23.74	28.1	19.4
200	25.23	30.2	20.2

Baird

Peak over Threshold Extreme Value Analysis

Data Set: Green Bay Winds 1978 - 2002 Full Year: 340-20 Deg.

Three-Parameter Weibull Distribution

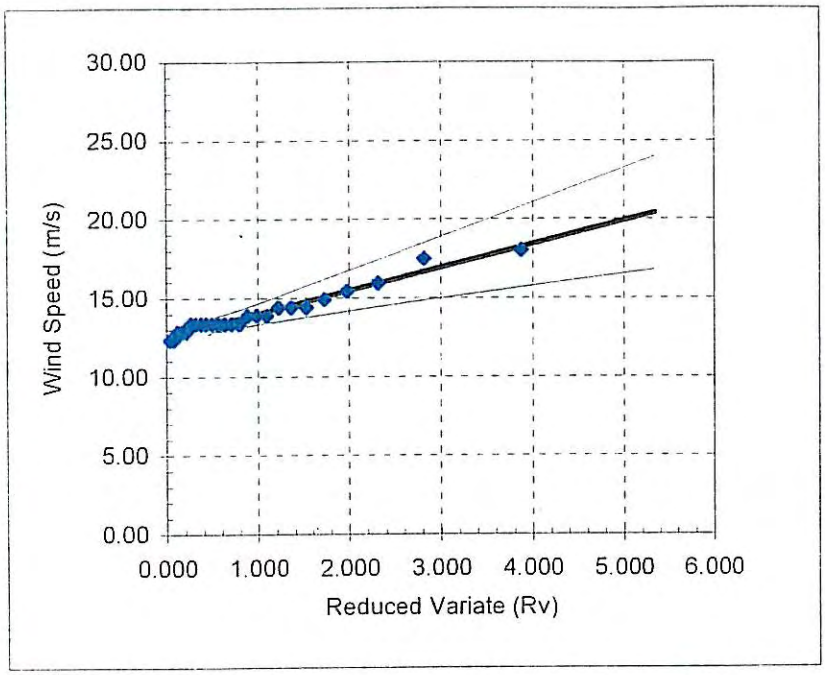

Total Years of Data:	24
Total Storm Events:	25
Total No. Events Selected:	25
Events per year:	1.04

Sample Statistics

Mean:	14.00
Maximum:	17.99
Minimum:	12.33
s:	1.42
Sample skewness:	-0.56

Weibull Parameters

Shape:	1.00
Scale:	1.471
Location:	12.532

Goodness of Fit

Correlation:	0.981

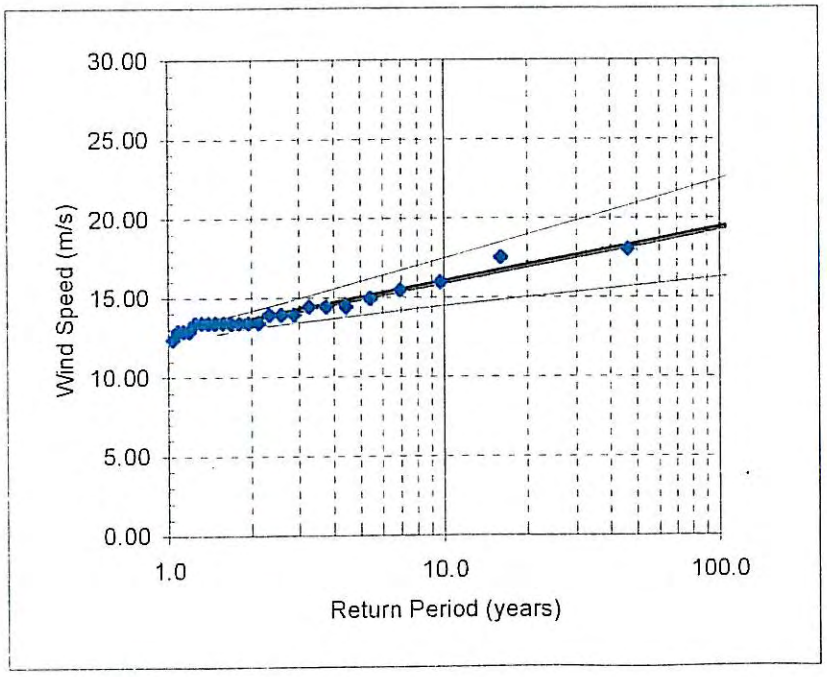

Return Period

		Confidence Limit	
Tr	X(T)	Upper	Lower
1.5	13.19	13.7	12.7
2	13.61	14.2	13.1
2.5	13.94	14.6	13.3
10	15.98	17.5	14.5
15	16.58	18.4	14.8
20	17.00	19.0	15.0
25	17.33	19.5	15.2
50	18.35	21.0	15.7
100	19.37	22.5	16.3
200	20.39	24.0	16.8

Baird

Peak over Threshold Extreme Value Analysis

Data Set: Green Bay Winds 1978 - 2002 Full Year: 20-60 Deg.

Three-Parameter Weibull Distribution

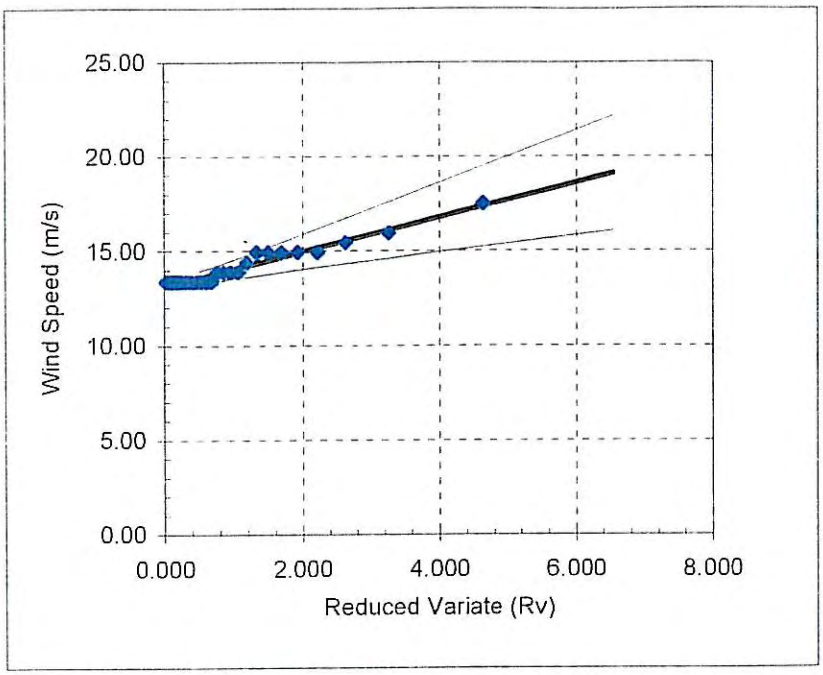

Total Years of Data:	24
Total Storm Events:	27
Total No. Events Selected:	27
Events per year:	1.13

Sample Statistics

Mean:	14.08
Maximum:	17.48
Minimum:	13.36
s:	1.03
Sample skewness:	-0.11

Weibull Parameters

Shape:	0.90
Scale:	0.915
Location:	13.125

Goodness of Fit

Correlation:	0.977

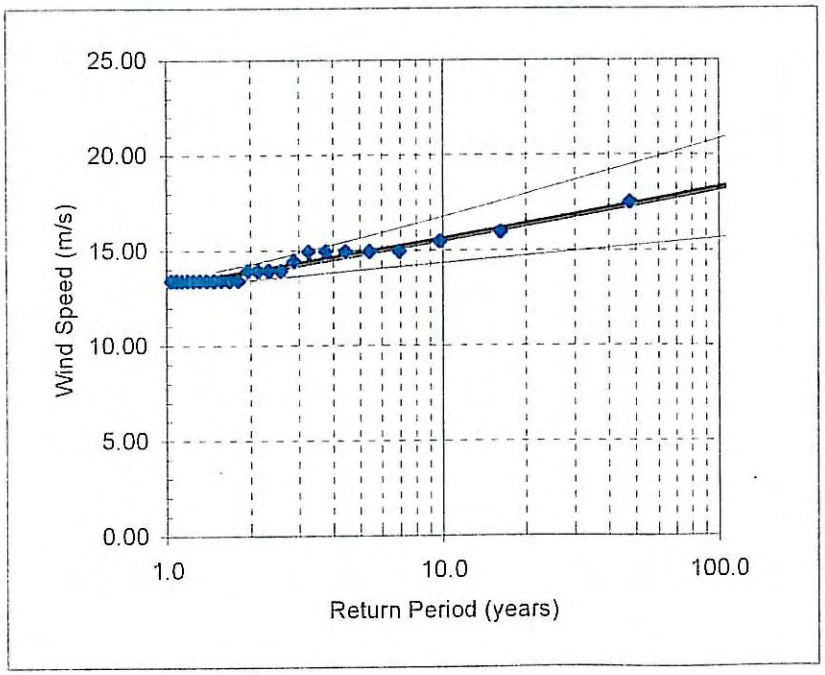

Return Period

		Confidence Limit	
Tr	X(T)	Upper	Lower
1.5	13.57	13.9	13.2
2	13.85	14.3	13.4
5	14.80	15.6	14.0
10	15.57	16.8	14.3
15	16.03	17.5	14.6
20	16.36	18.0	14.7
26.2	16.67	18.5	14.9
50	17.43	19.6	15.3
100	18.26	20.9	15.7
200	19.10	22.1	16.1

Date: 15-Jun-07

Baird

Peak over Threshold Extreme Value Analysis

Data Set: Appleton Winds 1998 - 2004 Full Year: 180-225deg only

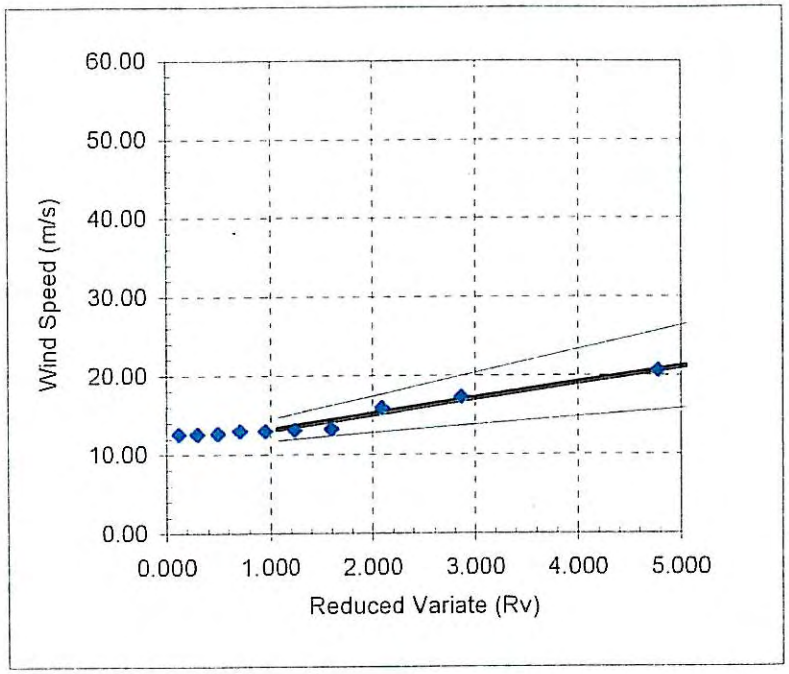

Fisher-Tippet II

Total Years of Data:	5
Total Storm Events:	16
Total No. Events Selected:	16
Events per year:	3.20

Sample Statistics

Mean:	13.28
Maximum:	20.564
Minimum:	11.176
s:	2.54
Sample skewness:	-2.84

FTII Parameters

Shape:	6.00
Scale:	1.976
Location:	11.169

Goodness of Fit

Correlation:	0.978

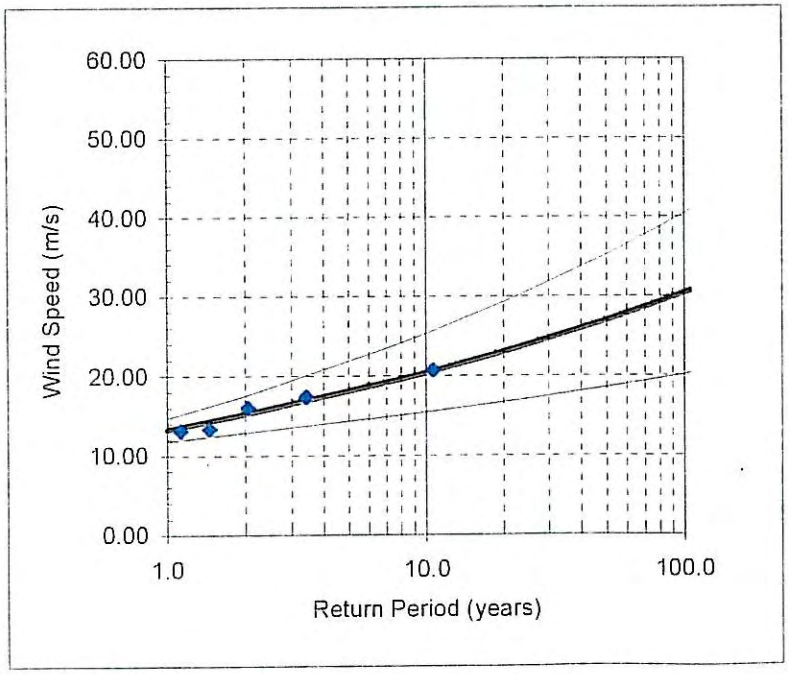

Return Period

		Confidence Limit	
Tr	X(T)	Upper	Lower
1	13.28	14.7	11.8
2	15.24	17.6	12.9
8.2	19.69	24.2	15.1
10	20.38	25.3	15.5
20	23.00	29.3	16.7
25	23.90	30.7	17.1
50	26.92	35.3	18.6
100	30.31	40.4	20.2
200	34.12	46.3	22.0
500	39.86	55.0	24.7

Date: 15-Jun-07

Baird

Peak over Threshold Extreme Value Analysis

Data Set: Appleton Winds 1998 - 2002 Full Year: 225-280

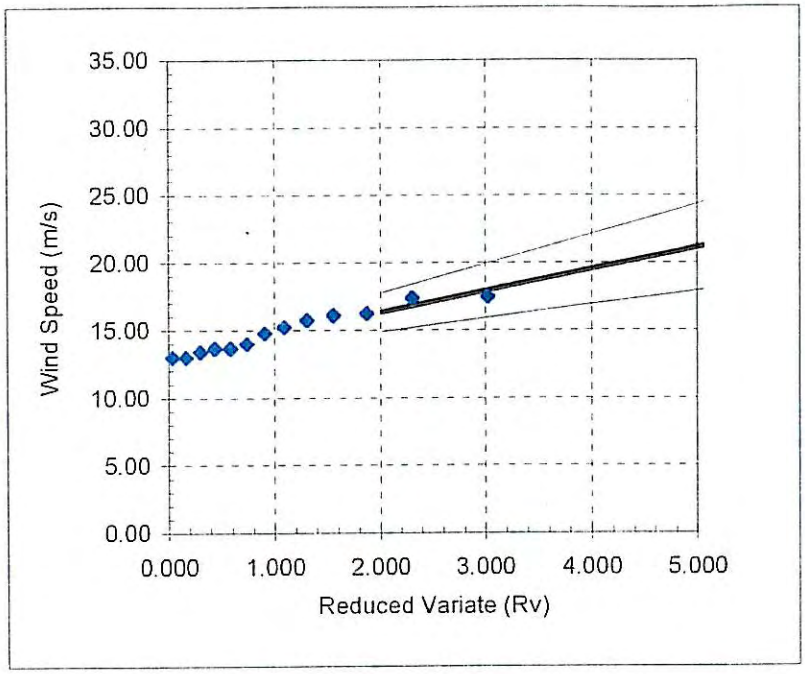

Fisher-Tippet I (Gumbel)

Total Years of Data:	5
Total Storm Events:	20
Total No. Events Selected:	20
Events per year:	4.00

Sample Statistics

Mean:	13.95
Maximum:	17.435
Minimum:	12.07
s:	1.79
Sample skewness:	-1.13

FT I Parameters

Scale:	1.600
Location:	13.113

Goodness of Fit

Correlation:	0.974

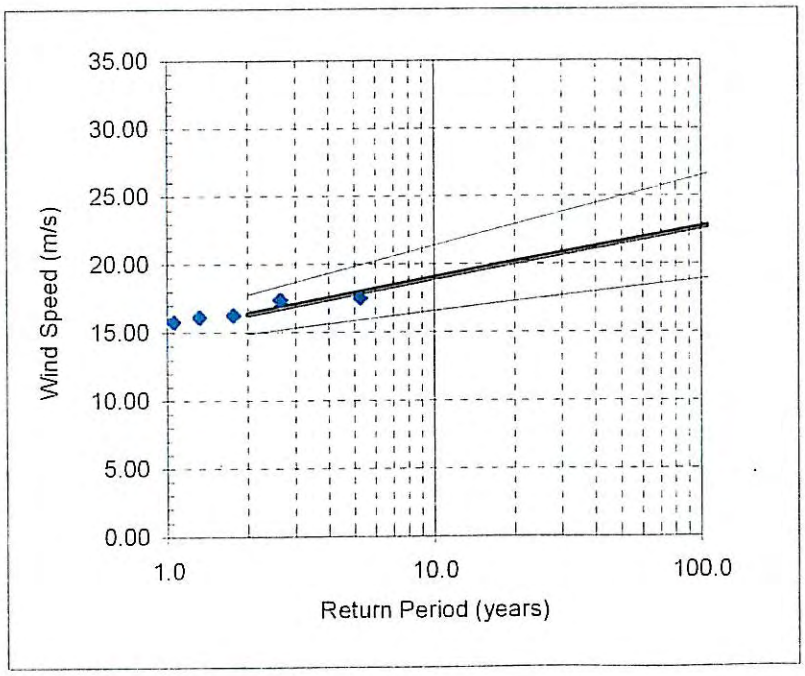

Return Period

		Confidence Limit	
Tr	X(T)	Upper	Lower
2	16.33	17.78	14.89
3.7	17.37	19.18	15.56
10	19.00	21.40	16.59
20	20.11	22.94	17.29
25	20.47	23.44	17.51
50	21.59	24.97	18.20
100	22.70	26.50	18.89
200	23.81	28.04	19.58
500	25.28	30.06	20.49
1000	26.38	31.60	21.17

Date: 15-Jun-07

Baird

Peak over Threshold Extreme Value Analysis

Data Set: Appleton Winds 1998 - 2004 Full Year: 340-20deg only

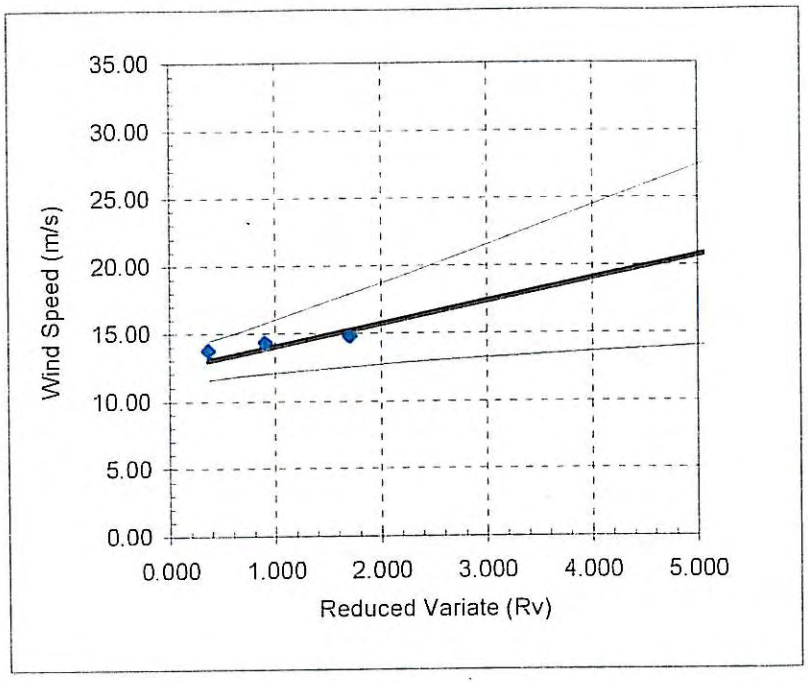

Fisher-Tippet I (Gumbel)

Total Years of Data:	5
Total Storm Events:	5
Total No. Events Selected:	5
Events per year:	1.00

Sample Statistics

Mean:	13.14
Maximum:	14.752
Minimum:	11.288
s:	1.58
Sample skewness:	-4.10

FT I Parameters

Scale:	1.666
Location:	12.375

Goodness of Fit

Correlation:	0.932

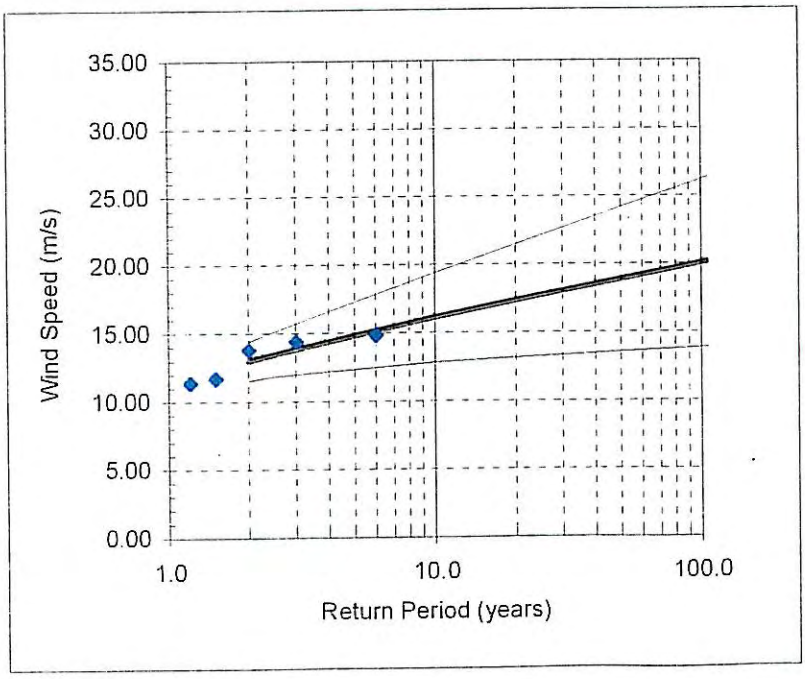

Return Period

Tr	X(T)	Confidence Limit Upper	Confidence Limit Lower
2	12.99	14.43	11.54
2.5	13.49	15.14	11.85
10	16.12	19.41	12.84
20	17.32	21.47	13.18
25	17.70	22.13	13.28
50	18.88	24.17	13.58
100	20.04	26.21	13.87
200	21.20	28.24	14.15
500	22.73	30.93	14.52
1000	23.88	32.97	14.80

Date: 15-Jun-07

Baird

Peak over Threshold Extreme Value Analysis

Data Set: Appleton Winds 1978 - 2002 Full Year:20-60

Three-Parameter Weibull Distribution

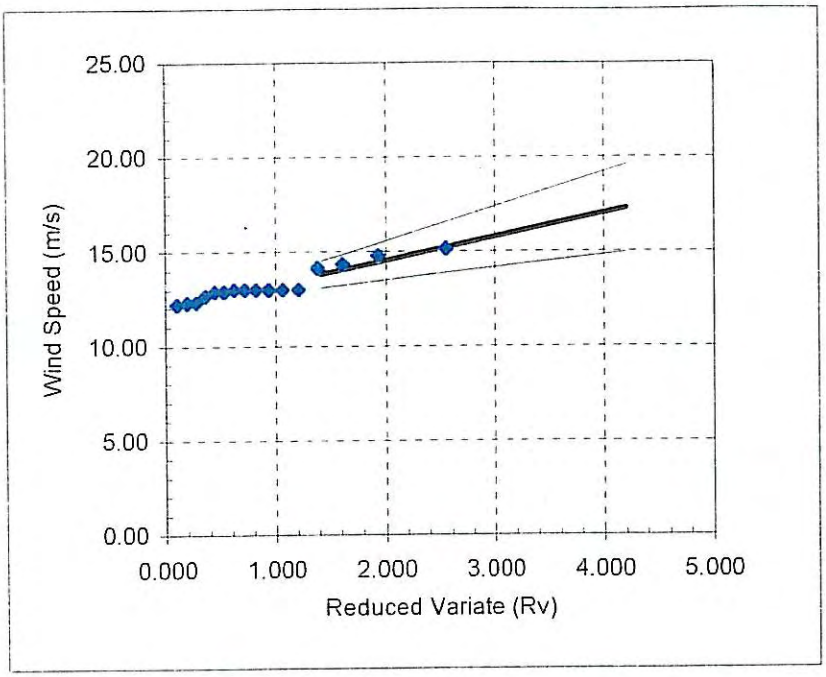

Total Years of Data:	5
Total Storm Events:	16
Total No. Events Selected:	16
Events per year:	3.20

Sample Statistics

Mean:	13.19
Maximum:	15.09
Minimum:	12.18
s:	0.88
Sample skewness:	-0.17

Weibull Parameters

Shape:	1.30
Scale:	1.241
Location:	12.049

Goodness of Fit

Correlation:	0.957

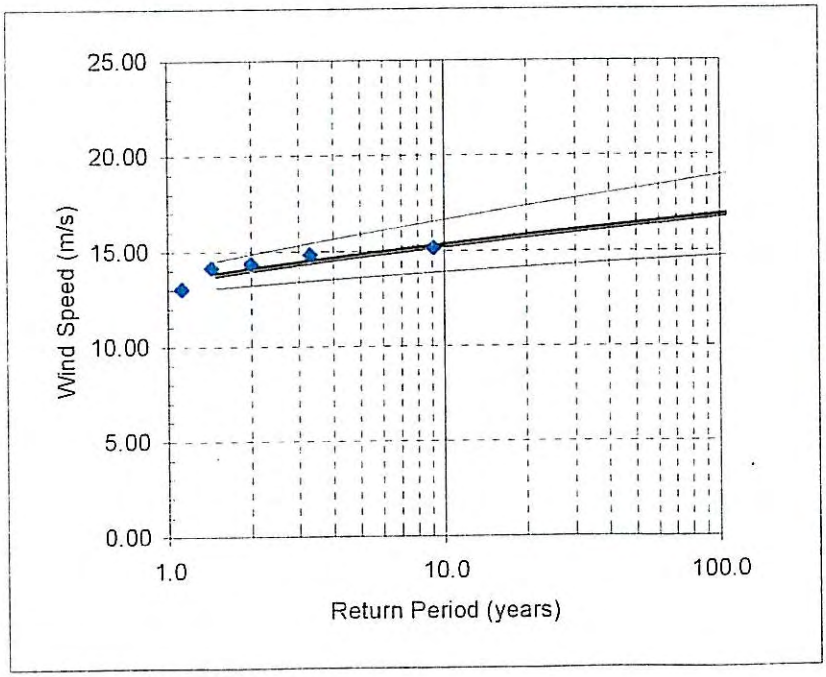

Return Period

		Confidence Limit	
Tr	X(T)	Upper	Lower
1.5	13.80	14.5	13.1
2	14.05	14.9	13.2
5	14.77	15.9	13.6
10	15.28	16.7	13.9
15	15.57	17.1	14.1
20	15.76	17.4	14.2
25	15.92	17.6	14.2
50	16.38	18.3	14.5
78	16.67	18.7	14.6
200	17.26	19.6	14.9

Baird

Peak over Threshold Extreme Value Analysis

Data Set: Green Bay Winds 1978 - 2002 Ice Removed: 180-225deg only **Fisher-Tippet II**

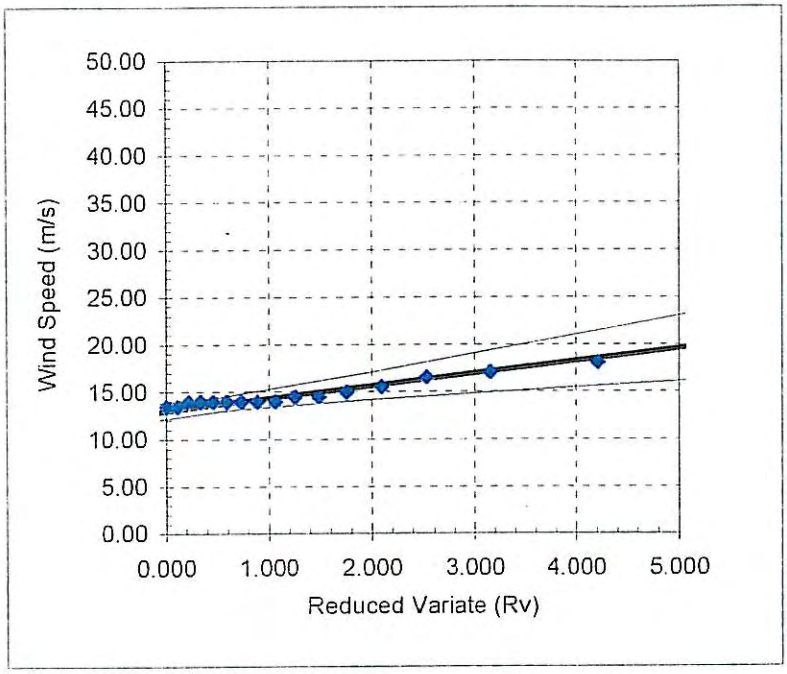

Total Years of Data:	24
Total Storm Events:	26
Total No. Events Selected:	26
Events per year:	1.08

Sample Statistics

Mean:	14.53
Maximum:	23.14
Minimum:	13.36
s:	2.14
Sample skewness:	-0.51

FTII Parameters

Shape:	4.00
Scale:	1.307
Location:	13.020

Goodness of Fit

Correlation:	0.985

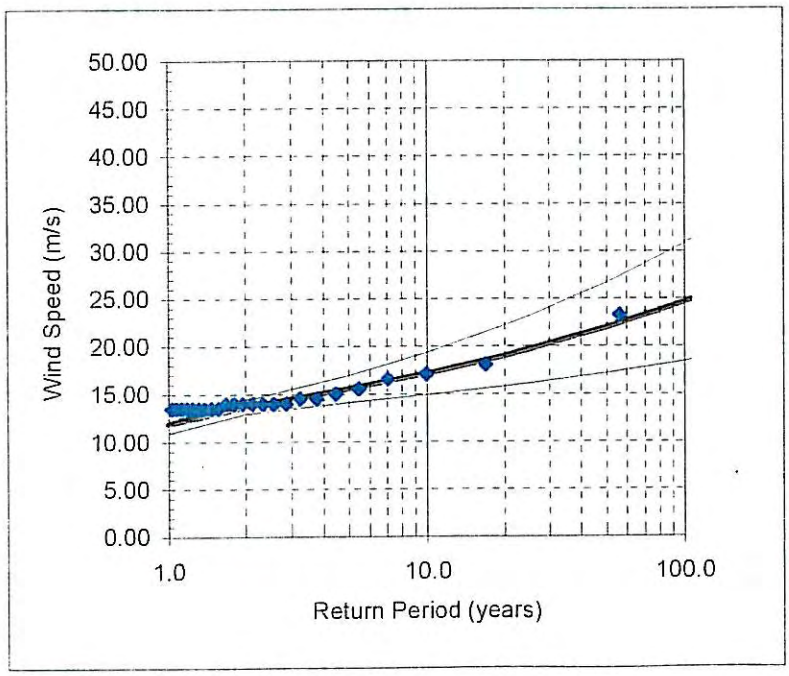

Return Period

		Confidence Limit	
Tr	X(T)	Upper	Lower
1	11.92	12.9	10.9
2	13.69	14.4	13.0
5	15.57	17.0	14.1
10	17.16	19.4	14.9
20	19.01	22.2	15.8
25	19.66	23.2	16.1
50	21.94	26.7	17.2
100	24.64	30.8	18.5
200	27.84	35.7	20.0
500	33.01	43.7	22.4

Date: 15-Jun-07

Baird

Peak over Threshold Extreme Value Analysis

Data Set: Green Bay Winds 1978 - 2002 Ice removed: 225-280

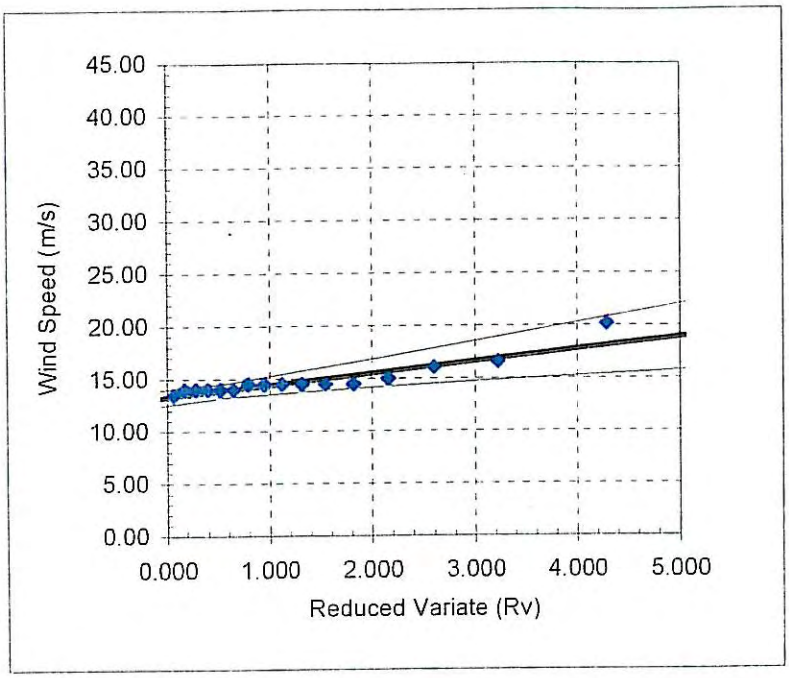

Fisher-Tippet II

Total Years of Data:	24
Total Storm Events:	27
Total No. Events Selected:	27
Events per year:	1.13

Sample Statistics

Mean:	14.41
Maximum:	21.08
Minimum:	12.85
s:	1.98
Sample skewness:	-0.85

FTII Parameters

Shape:	4.00
Scale:	1.124
Location:	13.246

Goodness of Fit

Correlation:	0.959

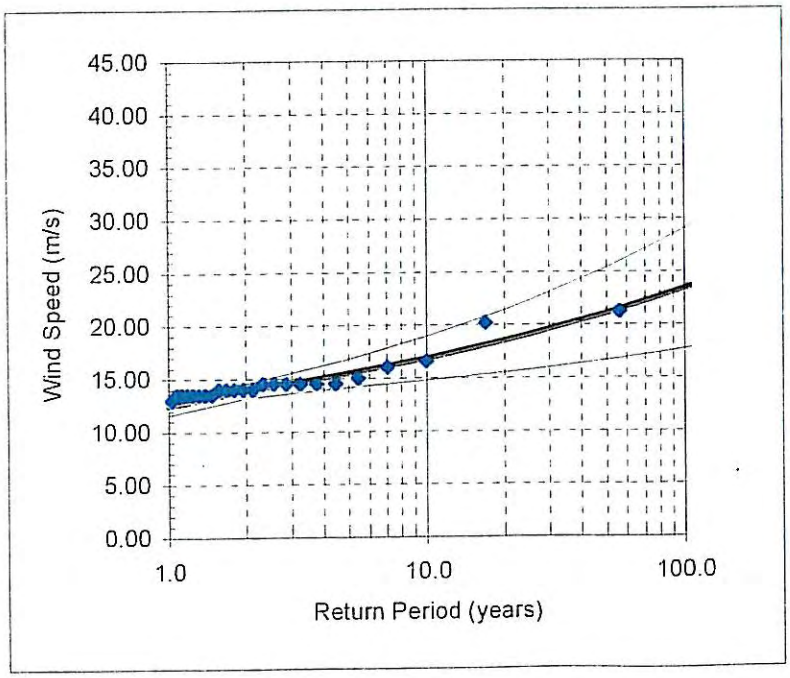

Return Period

		Confidence Limit	
Tr	X(T)	Upper	Lower
1	12.44	13.3	11.6
2	13.88	14.6	13.2
5	15.51	16.8	14.2
10	16.89	18.9	14.8
20	18.49	21.4	15.5
25	19.06	22.3	15.8
50	21.03	25.4	16.7
100	23.37	29.0	17.7
200	26.15	33.4	18.9
500	30.64	40.4	20.9

Date: 15-Jun-07

Baird

Peak over Threshold Extreme Value Analysis

Data Set: Green Bay Winds 1978 - 2002 Ice Removed: 340-20 Deg.

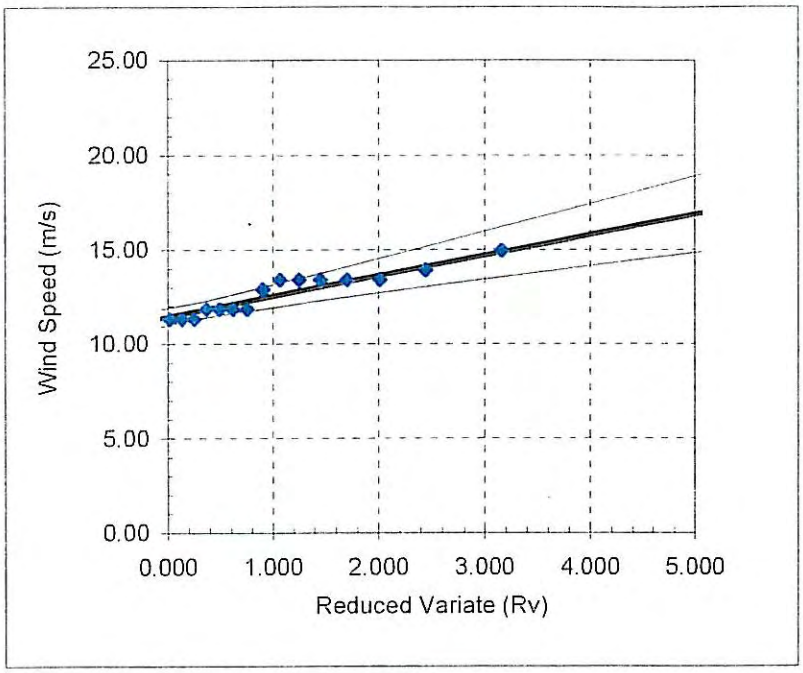

Fisher-Tippet I (Gumbel)

Total Years of Data:	24
Total Storm Events:	23
Total No. Events Selected:	23
Events per year:	0.96

Sample Statistics

Mean:	12.02
Maximum:	14.9
Minimum:	10.79
s:	1.25
Sample skewness:	-0.21

FT I Parameters

Scale:	1.083
Location:	11.447

Goodness of Fit

Correlation:	0.960

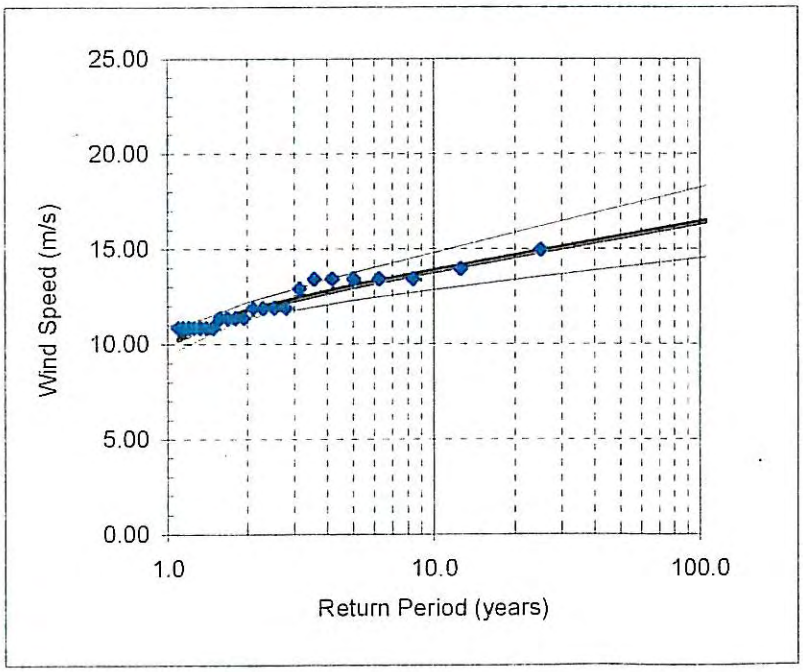

Return Period

Tr	X(T)	Confidence Limit Upper	Confidence Limit Lower
1.1	10.27	10.83	9.71
2	11.78	12.21	11.35
5	13.02	13.74	12.30
10	13.84	14.82	12.86
20	14.62	15.86	13.38
25	14.86	16.19	13.54
50	15.63	17.22	14.04
100	16.38	18.24	14.53
200	17.14	19.26	15.02
500	18.13	20.60	15.66

Date: 15-Jun-07

Baird

Peak over Threshold Extreme Value Analysis

Data Set: Green Bay Winds 1978 - 2002 Ice Removed: 20-60 Deg.

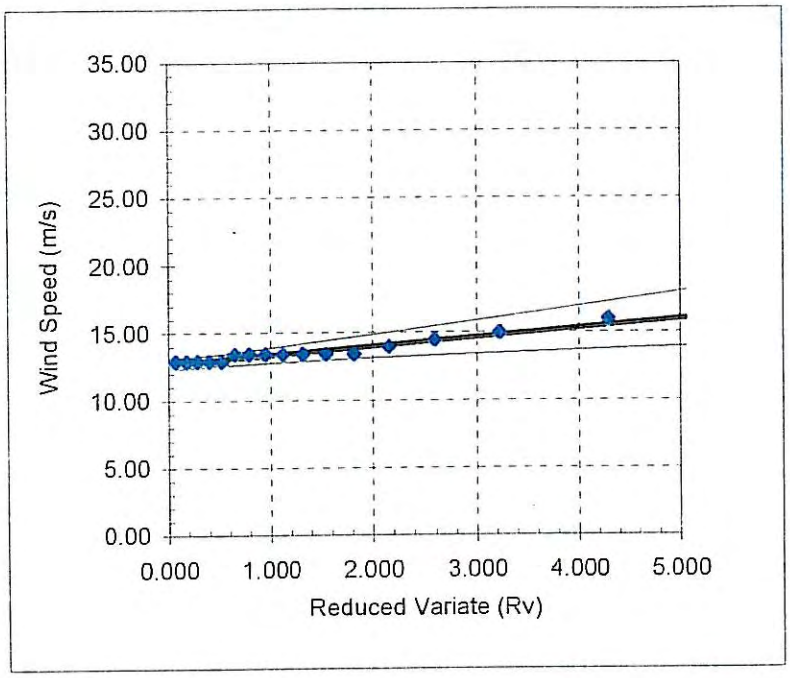

Fisher-Tippet II

Total Years of Data:	24
Total Storm Events:	27
Total No. Events Selected:	27
Events per year:	1.13

Sample Statistics

Mean:	13.21
Maximum:	17.48
Minimum:	11.82
s:	1.28
Sample skewness:	-0.55

FTII Parameters

Shape:	4.00
Scale:	0.662
Location:	12.677

Goodness of Fit

Correlation:	0.983

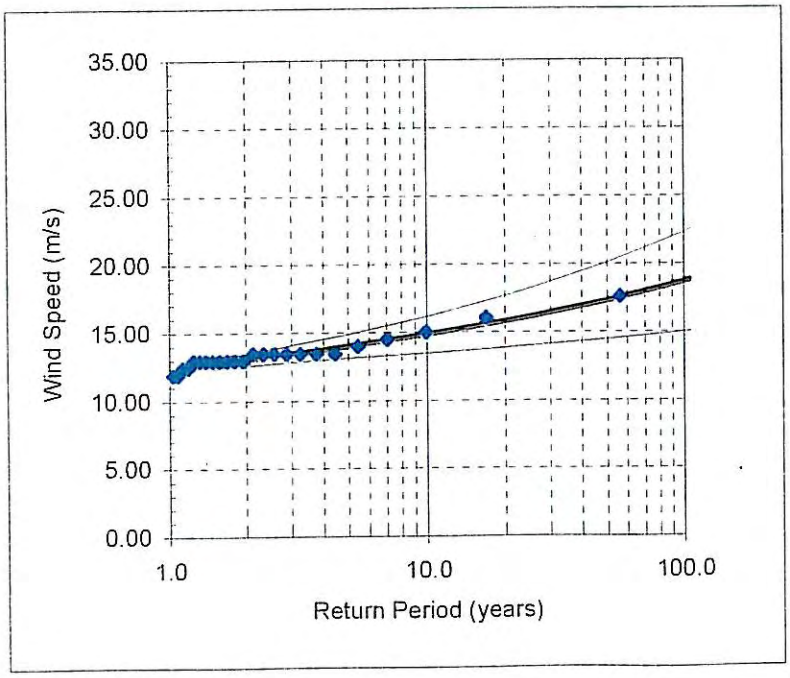

Return Period

		Confidence Limit	
Tr	X(T)	Upper	Lower
1.5	12.75	13.2	12.3
2	13.05	13.5	12.6
5	14.01	14.9	13.1
10	14.82	16.2	13.5
20	15.76	17.7	13.9
25	16.10	18.2	14.0
50	17.27	20.1	14.4
100	18.65	22.3	15.0
200	20.28	25.0	15.6
500	22.93	29.3	16.6

Date: 15-Jun-07

Baird

Peak over Threshold Extreme Value Analysis

Data Set: Appleton Winds 1998 - 2004 Ice Removed: 180-225deg only **Three-Parameter Weibull Distribution**

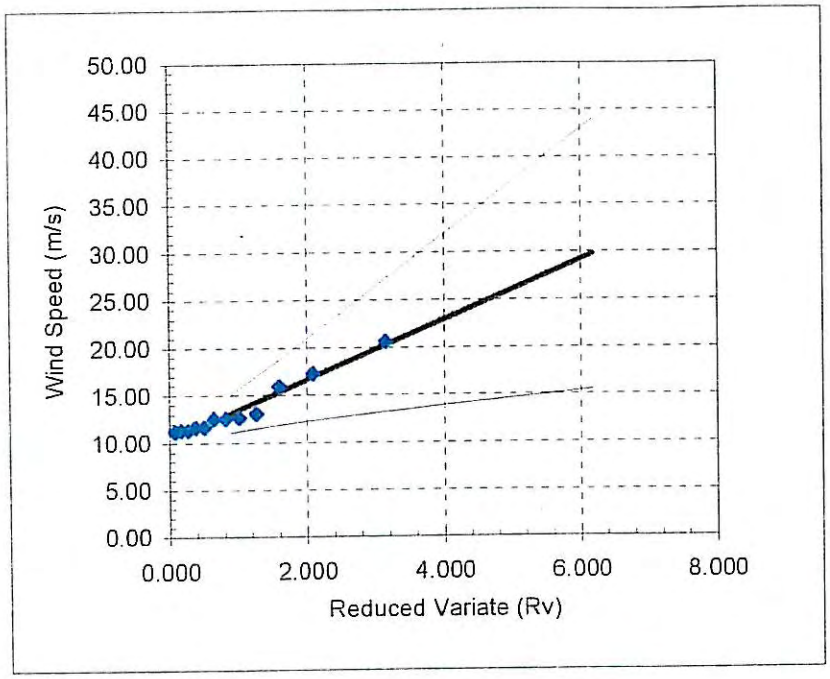

Total Years of Data:	5
Total Storm Events:	12
Total No. Events Selected:	12
Events per year:	2.40

Sample Statistics

Mean:	13.44
Maximum:	20.56
Minimum:	11.18
s:	2.93
Sample skewness:	-5.01

Weibull Parameters

Shape:	1.00
Scale:	3.149
Location:	10.308

Goodness of Fit

Correlation:	0.980

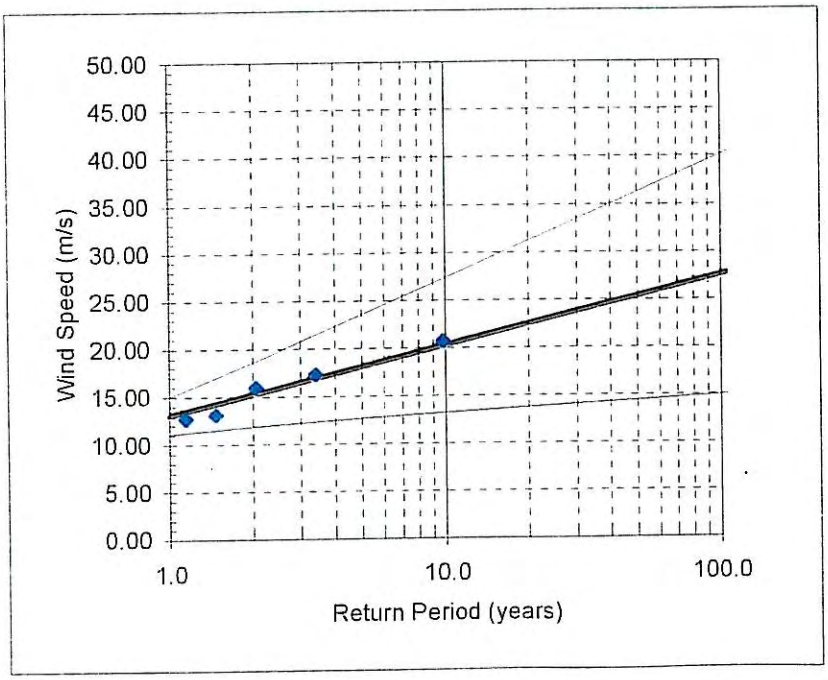

Return Period

		Confidence Limit	
Tr	X(T)	Upper	Lower
1	13.06	15.0	11.1
2	15.25	18.6	11.9
5	18.13	23.6	12.7
10	20.31	27.4	13.2
15	21.59	29.6	13.5
20	22.50	31.2	13.8
25	23.20	32.5	13.9
50	25.38	36.3	14.5
100	27.56	40.2	15.0
200	29.75	44.0	15.5

Baird

Peak over Threshold Extreme Value Analysis

Data Set: Appleton Winds 1978 - 2002 Ice removed: 225-280

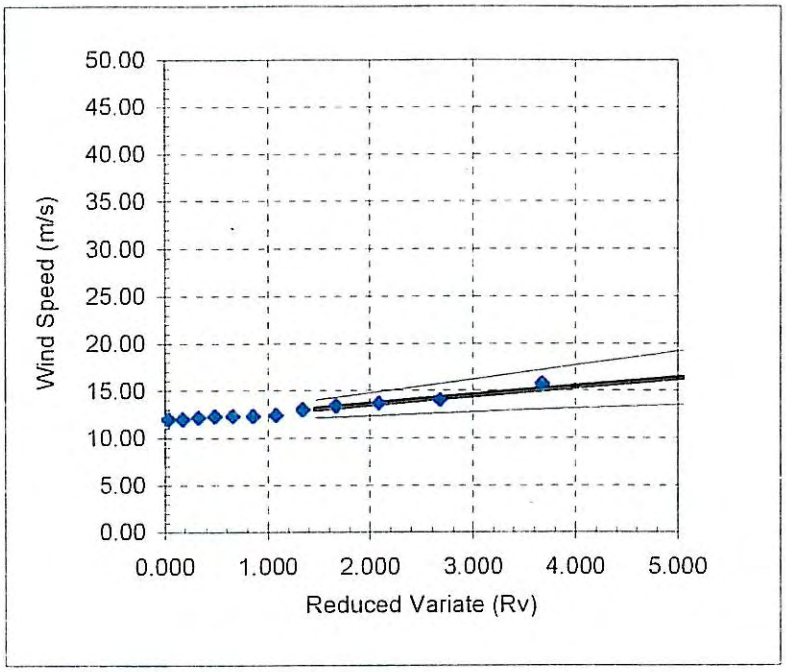

Fisher-Tippet II

Total Years of Data:	5
Total Storm Events:	20
Total No. Events Selected:	20
Events per year:	4.00

Sample Statistics

Mean:	12.70
Maximum:	17.435
Minimum:	11.4
s:	1.53
Sample skewness:	-0.51

FTII Parameters

Shape:	4.00
Scale:	0.919
Location:	11.728

Goodness of Fit

Correlation:	0.989

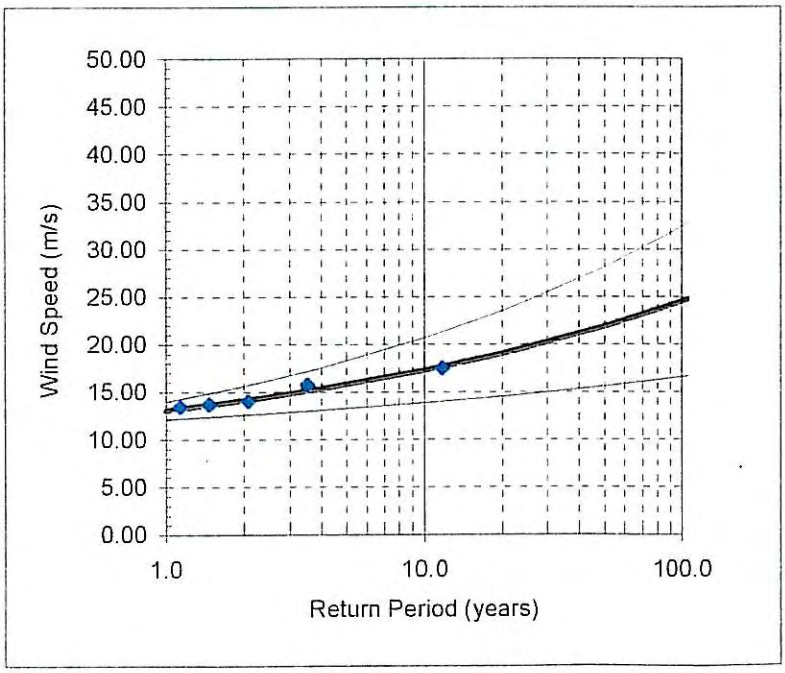

Return Period

		Confidence Limit	
Tr	X(T)	Upper	Lower
1	13.07	14.0	12.1
2	14.13	15.7	12.6
3.7	15.20	17.4	13.1
10	17.27	20.7	13.9
20	19.03	23.5	14.5
25	19.67	24.6	14.8
50	21.87	28.1	15.6
100	24.49	32.4	16.6
200	27.61	37.4	17.8
500	32.64	45.6	19.7

Date: 15-Jun-07

Baird

Peak over Threshold Extreme Value Analysis

Data Set: Appleton Winds 1978 - 2002 Ice removed: 20-60

Three-Parameter Weibull Distribution

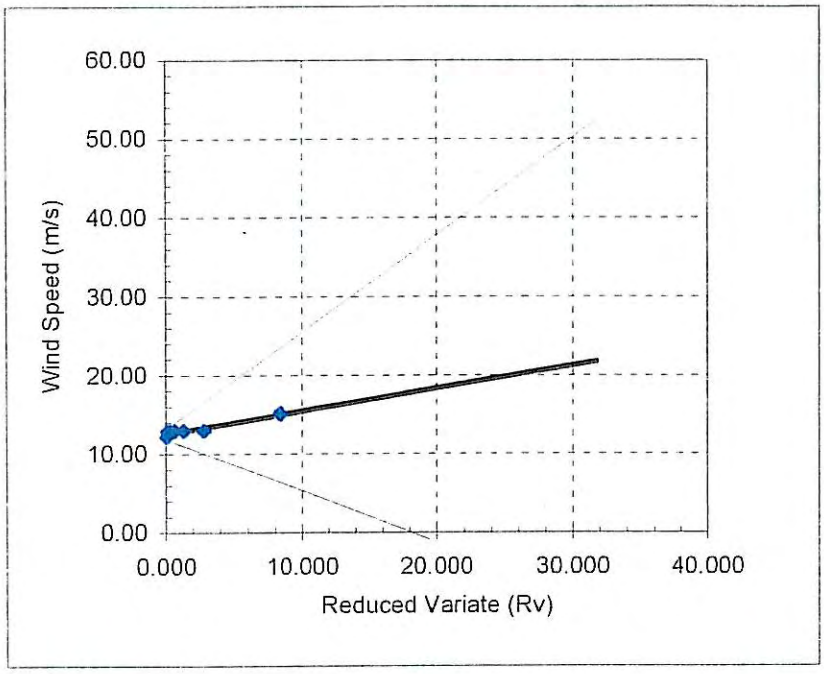

Total Years of Data:	5
Total Storm Events:	7
Total No. Events Selected:	7
Events per year:	1.40

Sample Statistics

Mean:	13.12
Maximum:	15.09
Minimum:	12.18
s:	0.91
Sample skewness:	-0.21

Weibull Parameters

Shape:	0.50
Scale:	0.289
Location:	12.568

Goodness of Fit

Correlation:	0.950

Error - k out of range

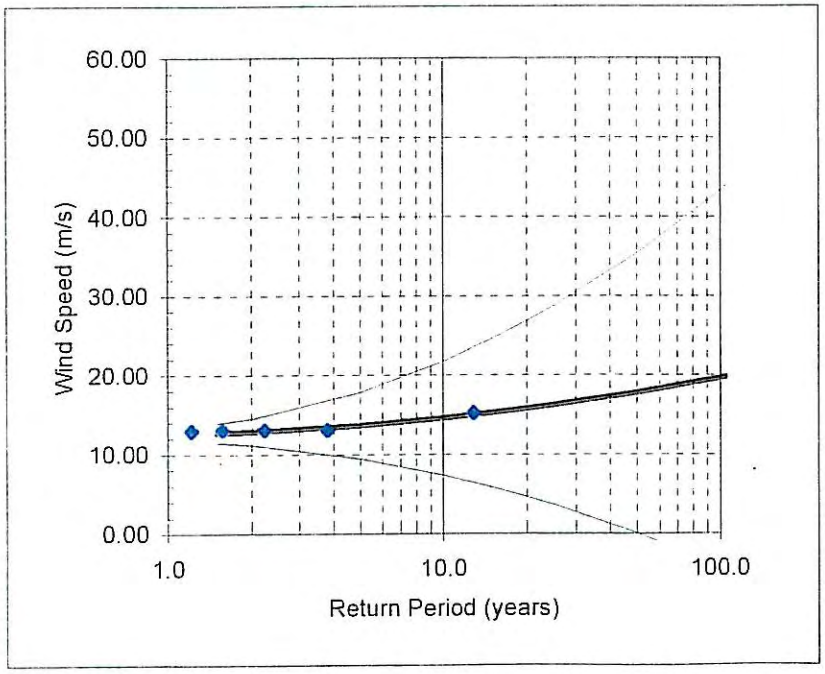

Return Period

		Confidence Limit	
Tr	X(T)	Upper	Lower
1.5	12.73	14.0	11.5
2	12.87	14.6	11.2
5	13.66	17.9	9.5
10	14.58	21.8	7.4
15	15.24	24.6	5.9
20	15.77	26.9	4.7
25	16.22	28.8	3.7
50	17.78	35.5	0.1
100	19.62	43.3	-4.1
200	21.74	52.4	-8.9

Baird

Appendix E

Effects of Ice on Sediments in LLBdM, Lower Fox River above Appleton, Wisconsin (Ashton 2006)

Effects of Ice on Sediments in Little Lake Butte des Morts, Lower Fox River above Appleton, Wisconsin

By:
George D. Ashton, PhD
86 Bank Street
Lebanon, NH 03766

November 8, 2006

Summary of Findings

No evidence was found of ice jamming associated with breakup of the ice cover in OU1 on the Fox River just upstream from Appleton, Wisconsin. There is a possibility of some very limited frazil production and accumulation during very cold periods at the very upstream end of the pool termed Little Lake Butte des Morts, and these accumulations possibly could extend to the upstream region of interest. Other ice processes that conceivably might pose a hazard to capping were examined including the simple blockage of the flow cross section by the ice cover thickness. These blockages only increase the shear stress on the bottom, relative to the same discharge under open water conditions, at low discharges and are much less than the bottom shear stresses at high discharges associated with 100 year return flows. Velocities even at very high flows are less than those associated with ice jamming. The overall conclusion is that ice does not change the selection of capping materials in the regions D and E.

Background

As part of the effort to remediate sediments in OU1 extending from the Menasha and Neenah channels at the upstream end of the pool to the dam downstream located at Appleton, Wisconsin, there was concern as to the possible effects of ice on sediments and the remediation measures planned. This report discusses the nature of the ice cover at the site and associated processes that could conceivably interact with the sediments or the capping of those sediments in the central region of the Little Lake Butte des Morts extending from downstream of the Menasha channel confluence on downstream to where the Lake narrows approximately 2.5 miles downstream. The conclusions below are based on review of data of stream flows and winter temperatures for the site, on a site visit on 27 October 2006, on published literature dealing with ice and sediments, and on some 35 years of personal experience examining river and lake ice behavior.

The formation of ice in rivers is complex. Nevertheless approximate calculations are made to assess the general behavior of ice at the site to evaluate any possible interactions with sediments.

Fox River Near OU1 – Appleton, Wisconsin

The Lower Fox River extends from the outlet of Lake Winnebago to its mouth at Green Bay. The flow from Lake Winnebago in winter is dominated by measures taken to control the water level in Lake Winnebago. This includes a winter drawdown beginning in mid-October and extending until the end of February with the intent of providing storage for later runoff into Lake Winnebago. When the drawdown target is achieved the stage at the outlet of Lake Winnebago is held constant until the ice cover in the Lake Winnebago pool breaks up. The stage in Lake Winnebago is then increased beginning about mid-April to provide a navigation stage. More detail on the operating schedules and objectives are contained in USACE (1994).

The region of concern is a reach of river that is similar to a lake (and named "Little Lake Butte des Morts") with through flow until the river narrows about 3 miles downstream. Flows enter into the pool at its upstream end in two channels, the Neenah and the Menasha channel with the flows split between the two channels. The pool formed by the dam downstream at Appleton is quite wide (typically 3000 to 4000 feet) for two miles downstream of the Menasha channel confluence and then narrows to about 1500 feet beginning at the downstream end of the remediation region E2 and further narrows gradually over the last few miles to the dam at Appleton. There is awareness of possible ice problems downstream of Lake Winnebago contained in the operational strategy for the river and to "help prevent frazil ice development, experience has shown that flows must be limited to about 4,000 cfs (113 cms) when the air temperature falls below 25 degrees Fahrenheit, until such time as a complete ice cover has developed on the river." (USACE 1994). Those frazil problems are associated primarily with stretches of the river downstream of the Appleton dam and extending to the outlet at Green Bay. Examination of the detailed flow records at the USGS gaging station at Appleton, WI showed that, at least since 1994, that strategy has been implemented with flows during the freezeup period from 15 December – 31 December no greater than 4420 cfs except for two periods: during the period 14-16 December 1999 when the average daily flow on 15 December was 5,130 cfs; and during 14-18 December 2004 when the average daily flow on 15 December was 5550 cfs. (Note: In December 1999 the air temperature was quite warm until just after 15 December when the flows were reduced; similarly in 2004 the temperatures abruptly decreased just after 18 December when flows were similarly reduced; this is consistent with the intent, namely to maintain flows at about 4,000 cfs during ice formation periods.)

The region of concern in this report is the central region of the pool. The overall bathymetry (See Foth & Van Dyke Figure 6-2: Post Remedy Water Depth, dated October 2006) is a central deeper portion along the axis of the lake generally about 6 to 10 feet deep. The region of proposed capping (See Foth & Van Dyke Figure 6-1: OU1 Final Optimized Remedy, dated October 2006) involves a proposed 10 inch cap in the central portion about 8000 feet long and a proposed 13 inch cap along the west side of that central portion for about half that length and in water depths of 3 to 6 feet. There is a smaller, narrow area about 2000 feet long near the west side opposite the dredged channel leading to the Menasha lock that will involve capping with a 13 inch deep cap in the areas where the water depth is 3 to 6 feet and two small areas in slightly deeper water where a 10 inch cap is proposed. All of these areas of concern in this report are well away from the shoreline and hence not affected by possible near-shore ice processes.

OU1 Site Visit

A visit was made to OU1 on 27 October 2006. On the morning of 27 October, the writer, together with Matthew Oberhofer of Foth and Van Dyke, traveled around the river from the mid-pool highway bridge south along the west side, through Neenah and Menasha and then north along the east side and on downstream to the dam at Appleton, Wisconsin. Observations were made of vegetation and structures along the shores with the objective of detecting any damage due to ice effects. None was observed. Notably there were observed extensive small docks for recreational boat mooring, generally consisting of 8 to 12 inch diameter timber piles permanently installed. This is evidence of little or no damage due to ice that would result from major jamming or ice movement. The extended width of the river caused by the dam at Appleton results in the pool above the Appleton Dam characterized as a lake-like environment with relatively slow velocities compared to that in the narrower reaches just upstream of the dam at Appleton and extending on downstream to Green Bay, WI, although even those downstream reaches are a series of pools behind low head dams.

In a previous visit to the Lower Fox River in October 2005 a number of people with experience on the river during winter were interviewed. The overall behavior of the river during winter was characterized by these. Typically the river becomes ice covered in mid-December and melting begins in February to sometimes mid- to late March.

OU1 Climate and Hydraulics

The Fox River near Green Bay, WI is characterized by a quite cold winter with from as few as 8 to as many as 50 days during which the daily minimum air temperature is below 0°F with a long term average of 24.3 days per winter. Mean monthly temperatures (period 1971-2000) at Green Bay, WI are tabulated below. (Note: The meteorological record for Green Bay is used because of its ready availability and long term record; the site is about 30 miles south of Green Bay).

December	January	February	March
21.2°F	15.6°F	20.5°F	31.3°F

The long term average mean air temperature (average of daily high and lows) decreases to 32°F in late November and increases to 32°F about the last week of March. In terms of freezing degree days (1 freezing degree day is 1°F below 32°F for a day), this means the average freezing degree days accumulated December thru March is 1230 °F – days (684 °C-days). This latter value is useful to estimate the maximum ice thickness to be expected at the end of the winter. An examination of longer term records showed that there have been a few years when it was very cold relative to this long term average; notably in the last 50 years, both 1976 and 1978 experienced very cold winters and the estimated accumulated freezing degree day totals for those winters were about 2200 °F – days (1222 °C – days).

The hydraulics at the site is variable but, as pointed out above, considerably controlled upstream in association with control of the water levels in Lake Winnebago. Average monthly stream flows as measured at Appleton, WI as measured by the USGS for the period 1986- 2005 are

December	January	February	March
4060 cfs	3690 cfs	3750 cfs	5050 cfs

These are fairly constant flows through the winter for a river this far north and are due to the control at the outlet of Lake Winnebago. However, there are excursions of the flow that are quite a bit higher. The daily discharge records at the USGS station at Appleton were examined for the period 15 December to 31 March for the years of record from the winter of 1986-87 through the winter of 2005-2006 and the peak flows during that period extracted.

The maximum peak average daily flows for the period 15-31 December, and for January, February, and March periods over the period of 21 years are:

15-31 December	January	February	March
6860 cfs	7590 cfs	7000 cfs	11,100 cfs

The five highest ranked peak flows are shown in Table 1 together with the air temperatures experienced before, during and after the peak flow. These are all associated with warm temperatures and little ice production during the period of high flows.

Table 1
Highest Peak Flows December 15-March 31
Period 1986-2006

			Air Temperatures		
Winter	**Peak Flow (cfs)**	**Date**	**Before**	**During**	**After**
2003-04	11100	6 Mar	Warm*	Warm	Cool**
1989-90	9500	21 Mar	Unavailable at time of report		
1996-97	9330	29 Mar	Warm	Warm	Very Warm
1988-89	8800	32 Mar	Unavailable at time of report		
1997-98	8640	31 Mar	Very Warm	Warm	Very Warm

* Warm – average daily air temperatures above 32 °F
** Cool – average daily air temperatures below 32 °F but above 15 °F

Note: At the time of writing detailed air temperatures had not been obtained for the years 1988-1990. However the long term average daily high temperature at the end of March is 45°F and the long term average daily low temperature is 28°F so it is very unlikely that the air temperatures associated with a high discharge would be very cold.

The record was then examined to determine the highest flows that would be experienced during the mid-winter with the results shown in Table 2.

Table 2
Highest Peak Flows December 15-31, January & February
Period 1986-2006

December 15-31	6860 cfs	21 December 1992
January	7590 cfs	13 January 1987
February	7000 cfs	25 February 1994

While a more detailed statistical analysis was not performed, it is clear that flows as high as 7500 cfs may be expected during mid-winter and flows as high as 11,100 cfs may be expected in March (although these seem to be associated with warm periods and probably either during or after breakup). It is also possible that a 100 year return period flow of 24,000 cfs could occur near the end of the winter season, but would most likely be associated with quite warm temperatures and significant melting of the ice cover with rise in the hydrograph to such an extreme flow. In this report we will use 12,000 cfs as representative of an extreme flow in association with an ice cover on Little Lake Butte des Morts.

Flow Velocities

Using the results of hydrodynamic modeling done previously for the site for a design flow of 408 cms (14,400 cfs), the estimated flow velocities at mid-channel for three different flows were determined (by scaling proportional to discharge) for representative reaches beginning in the Menasha channel, just downstream of the region where the flow begins to move northward (beyond the extension of the point of land off the outlet of the Menasha channel, and at the mid-reach from there to the bridge (over E1). The flows chosen for examination were a typical freezeup flow of 4,000 cfs, a high winter flow of 11,100 cfs, and the 100 year return flow of 24,000 cfs. The results are presented in Table 3: (Note: the mapping of velocities available to the author was presented at a resolution of 0.2 m/sec for a discharge of 408 cms (14,408 cfs); nevertheless it is adequate for our purposes here since the resulting velocities are quite low relative to governing threshold velocities for ice behavior). We also note that these are flow velocities during open water conditions and hence are applicable to behavior at the time of onset of the ice cover formation. In a section below the effect of the thick ice cover that exists at the end of the winter season will be discussed.

Table 3
Summary of Maximum Velocities for Different Reaches

Reach	Typical Freezeup Flow	High Winter Flow	100 year Return Flow
	(4000 cfs)	(11,100 cfs)	(24,000 cfs)
In the Menasha Channel	0.27 fps	0.82 fps	1.6 fps
At mid-channel of lake reach where flow begins to move northward	0.36 fps	1.08 fps	2.2 fps
Mid-channel over E1	0.27 fps	0.82 fps	1.6 fps

We note that except for the "mid-reach of the lake opposite the Menasha channel outlet" the velocities are all less than 2 fps and for discharges up to 11,000 cfs are all less than or equal to 1.08 fps.

Formation of Frazil, Anchor Ice, and Surface Ice Cover

In very large lakes, and most rivers subject to very cold temperatures, frazil ice can form and be carried to great depths (Frazil is ice in very small crystals formed in supercooled flow (slightly below 0ºC)). In fast flowing rivers, frazil can be distributed through the depth of the flow and attach itself to the bottom sediments. In this form it is termed "anchor" ice. Upon warming slightly or when the buoyancy exceeds the adhesion at the bed, it can rise and sometimes bring a quantity of sediment to which it had adhered. There is considerable experience in assessing the nature and intensity of frazil formation based on mean water velocity and this is well represented by a diagram originated by Matousek (1984) and presented with some addition and simplification by Ashton (1988). From 0 to about 0.2 m/s (0.6 fps) the initial ice formation is in the form of thin sheets on the surface and little frazil formation. From about 0.2 m/s (0.6 fps) to about 0.7 m/s (2.3 fps) a "skim ice run" occurs, again, with little frazil formation. From about 0.7 m/s (2.3 fps) to about 0.95 m/s (3.1 fps) the frazil forms a "layered frazil and slush run" with the ice confined to the near surface of the water. Above about 0.95 m/s (3.1 fps) a "well mixed frazil run" occurs with frazil transported to some or the entire depth of flow. It is this last type of formation that can lead to anchor ice formation on the bed. There is some effect on these boundaries of types of ice formation due to the intensity of cooling with higher cooling rates tending to shift the types of ice formation somewhat towards the more severe types. At about 2 fps and below, the frazil formation is able to accumulate into an initial ice cover and, once stationary, will continue to thicken by thermal growth. Thus frazil produced in high velocity reaches is carried downstream until a lower velocity reach is present at which it forms a solid cover. Further arrival of frazil may be carried under the ice cover and either be further transported beneath the ice cover or deposit out (upwards) beneath the ice cover. In some cases such accumulations may form very thick "hanging dams". As the deposit thickens, the diminished cross section causes velocities to increase beneath the accumulation. The critical velocity beneath which frazil deposits out from the flow is about 2.0 fps based on observations of frazil deposits in rivers and is consistent with numerical models that use that value as the critical velocity, and with laboratory experiments. Once deposited, the frazil develops some cohesion between

particles and, as a consequence, the critical value for erosion is generally taken to be slightly higher and about 2.3 fps.

To summarize, it is expected that there will be frazil formation when the water surface does not have an intact ice cover. This corresponds to regions where the surface velocity is 2 fps or greater. There will be a possibility of anchor ice formation in regions where the flow velocity is greater than about 3 fps. However, as discussed above, the velocities in the Little Lake Butte des Morts are very much lower than the velocity associated with other than thin sheet formation and rapid ice cover formation such as occurs in lakes.

The Nature of the Ice Formation on Lake Butte des Mortes

With the above guidance, it is possible to describe the nature of ice formation at OU1 associated with the different flows shown in Table 3.

For typical freezeup flows of 4000 cfs, the average velocities in all reaches upstream of the narrow channel just above Appleton are less than 0.5 fps for flows typical of late December during the freeze-up period. We thus expect the ice cover to form rapidly over the entire lake upon the onset of cold air temperatures. The only exceptions to this are the reach further downstream where the river narrows above Appleton and just below the outlets from the Menasha and Neenah channels. The latter will be treated separately below.

The Neenah and Menasha channels derive their flow from Lake Winnebago. The writer does not have measurements of the water temperature in Lake Winnebago, but the typical behavior of water temperatures in similar lakes is as follows: The water first cools to the 4°C temperature associated with the maximum density of water. Further cooling results in cooling of the top surface with a weak density stratification occurring. Generally this temperature stratification is disturbed by wind mixing and the water further cools at depth to temperatures between 1°C and 4°C due to wind mixing until finally there is a more-or-less complete surface ice cover formed that halts further cooling. The result is a temperature beneath the ice that is typically between 0°C and 2°C and this is the water that enters the Menasha and Neenah channels. This water then takes some time (and distance) to further cool to 0°C after which further surface cooling results in ice formation. The result in the case of concern here is that the water entering Little Lake Butte des Morts is probably warmer than the freezing point and there will be a tongue of open water extending out into the lake downstream of the Menasha and Neenah channel outlets. With relatively warm air temperatures the extent of this open water may even extend to the far side of the lake and turn northward; however during very cold periods, the velocities just downstream of the outlet are such that a thin ice cover will form over this “tongue of warm water” and the warm water will be cooled as it passes beneath the ice. Approximate estimates were made of the aerial extents of open water that would result from a 1°C discharge of 4000 cfs from Lake Winnebago into Lake Butte des Morte. At a steady state average air temperature of -5°C (23°F) the corresponding open area would be about 2.25 km^2; at -10°C (14°F) 1.2 km^2; and at -15°C (- 5°F) 0.81 km^2. These are probably overestimates since at the very low velocities just downstream of the channel outlets, ice will form over slightly above freezing water temperatures. Thus any open water in the otherwise ice covered lake would likely be confined to the immediate areas just downstream of the Menasha and Neenah channel outlets, and during onset of

cold spells would become covered with a thin skim of ice that would stop frazil production there.

The production of frazil in a fast flowing open area through a winter period may be estimated from the cumulative degree-days of freezing. A simple heat balance between the production of frazil and the heat loss to the atmosphere results in

$$\rho \lambda h_f = H_{wa} (T_m - T_a) t$$

where ρ is the density of solid ice, λ is the heat of fusion of ice, h_f is the thickness of ice produced over time t when exposed to an air temperature T_a relative to the freezing point T_m. The value of ρ is accurately known at 916 kilograms per cubic meter, and λ is accurately known at 334,000 Joules per kilogram. Hwa is a heat transfer coefficient between the water surface and the air above. It varies with wind speed with higher wind speeds yielding higher heat transfer rates. Hwa typically varies from 10 Watts per square meter per °C under still air conditions and is about 30 Watts per square meter per °C for moderately windy conditions. Here we will use a more typical average value of 20 Watts per square meter per °C. The product $(T_m - T_a) t$ is the degree-days of freezing. At Green Bay the average cumulative degree-days of freezing December through March is 684 °C – days. Inserting these values into the above equation results in a potential thickness of solid ice production per unit area of 3.84 meters (about 12.5 feet) per unit area of open water surface exposed throughout the winter. The daily temperature records at Green Bay, WI from 1991 to 2005 were examined to find periods of extended consecutive very cold days, since such periods are more directly related to the production of frazil that may be of concern than are the total seasonal cumulative degree-days of freezing. The coldest period found was from 19 December 1998 to 15 January 1999. There were 677 freezing °F –days (376 °C –days) accumulated during this period, so use of the average seasonal accumulation of 684 °C -days is considered conservative in terms of estimating maximum ice production.

The area of open water that conceivably could produce frazil is the Menasha channel from the dam to the island at the mouth of the channel and has a surface area of about 167,000 square meters, although even there the typical velocities during winter are such that skim ice would form on the surface during cold periods (and assuming the withdrawal from Lake Winnebago is at 0°C). This yields a frazil production of 640,000 cubic meters of solid ice and a deposit (assuming a porosity of 0.5) volume of 1,280,000 cubic meters of bulk frazil. The volume available for the deposit is the area approximately 600 meters x 600 meters with a depth of 1 to 2 meters. Assuming the deposit occupies ½ the depth the volume that can be contained before the flow turns northward is about 360,000 cubic meters. Thus some frazil could be deposited downstream of that point. Frazil deposits out when the average flow velocity is about 0.6 m/sec and erodes at a slightly higher velocity of about 0.7 m/sec. Thus it would seem prudent to size the capping material in the region just downstream of the point where the flow turns northward (region D2N) to resist a velocity of 0.7 m/sec. The frazil deposit will not extend further downstream than the D2N region. It is also noted that this is a conservatively high calculation of frazil production since it relies on withdrawal water temperatures from Lake Winnebago of 0°C and that is probably colder than occurs in most, if not all, winters.

Thickness of the solid ice cover and effect on velocities

The maximum thickness of ice that might be expected at the site is given by a modified Stefan equation of the form $h_i = C\ S_f^{1/2}$ where, if h_i is given in inches and S_f is the degree days of freezing in °F – days, then C is typically about 0.5 to 0.7 for slow flowing rivers and protected still waters. For the average S_f of 684 °C days (= 1230 °F – days), this results in a thickness of 17.5 to 24.5 inches. For the extreme winters with an accumulated degree days of freezing of 2200 °F – days, this results in a thickness of 23.4 to 32.8 inches. We will use 26 inches as representative of the maximum ice thickness expected.

Thus it is expected that there will be an ice cover formed over most of Little Lake Butte des Morts with a thickness of a little over about 2 feet from mid-winter to just before breakup. The effect of this ice will alter the flow velocities somewhat and also alter the shear stresses exerted by those velocities on the bed materials.

In rivers where the slope of the river is determined by the roughness of the boundaries, the effect of adding an ice cover is to cause a rise in the depth to accommodate the increased flow resistance of the added second boundary. However in lakes, the depth does not increase due to the formation of the ice cover. Little Lake Butte des Morts is much closer to behaving like a lake, particularly in the region of concern (the upper end of the pool formed by the dam at Appleton), and we expect little change in depth to accommodate the throughflow in the reduced cross section caused by the ice cover cross section until the discharges significantly increase over the 4,000 cfs flows associated with the initial ice cover. The overall effect is a tendency to concentrate the flow in the deeper areas of the cross section with resulting somewhat higher velocities there as well as increase in average velocity overall due to the diminished cross section of flow. It is beyond the scope of this report to do a detailed analysis of the altered flow velocity distribution. However some simple considerations provide an estimate of the effects of this cross section blockage by ice on the shear stresses exerted on the bed materials.

When the flow is 4 feet deep and ice cover 2 feet thick the effective flow area is reduced by a factor of 2 and increases the flow velocity by a factor of 2. When 6 feet deep the flow area is decreased by 1/3 and the velocity increases by a factor of 1.5. These increased velocities, however exert a shear stress on both the underside of the ice cover and the bottom materials more or less equally so that $\tau_{bi} = \tau_i = \tau /2$, where τ_{bi} is the shear stress on the bed during period of thick ice cover, τ_i is the shear stress on the bottom materials during period of thick ice cover and τ is the total of the shear stresses exerted by the flow. Assuming the shear stress is more or less proportional to the square of the mean velocity, the shear stress on the bottom will increase relative to the open water value (for the same discharge) when the ratio of ice thickness to depth is greater than about 0.3 and the shear stress on the bottom will be less relative to the open water value when the ratio of ice thickness to depth is less than about 0.3. For an ice thickness near mid to end of winter of 2 feet this corresponds to a depth of 6.67 feet. Thus, all other things being equal, we may expect an increase in shear stresses on the bottom materials (relative to the open water case at the same discharge) when the open water depth is less than 6.67 feet and a decrease when the water depth is greater than 6.67 feet. This is somewhat offset by the shifting of the flow from shallower areas to deeper areas of the cross section and also by the rise in water level associated with accommodating the flow (Note: most of the water level rise relative to open water conditions is expected to occur in the narrower

reach just upstream of the dam at Appleton but that backwater effect will extend upstream through the wider pool considered here).

Cross sections at approximately the location of D2 and at E3S were plotted with an ice cover present assuming little elevation of the water surface due to the ice presence (see Figures 1 and 2) and approximate flow areas calculated for open water and ice-covered (2 feet thick) conditions and resulted in amplification of mean velocities at D2 by about a factor of 2 and amplification of mean velocities at E3S by about a factor of 1.5. Following the same logic as presented above, at D2 we would expect shear stresses on the bottom to increase by about a factor of 2 (approximately $2^2/2 = 2$) and at E3S shear stresses to increase slightly by about a factor of 1.125 (approximately $1.5^2/2 = 1.125$), both relative to open water flows at the same discharge. However while this blockage effect increases the shear stresses on the bottom over those for open water conditions at the same discharge, they are still lower than the shear stresses associated with higher open water discharges about 2 or 3 times the winter discharge of about 4 to 5000 cfs.

As the discharge increases, the flow transitions from a lake-with-slow-through-flow to a river-like behavior. In rivers the depth increases to accommodate the flow. An approximate calculation was made of the increase in depth to accommodate a flow of 12,000 cfs with a resulting increase in depth of about 0.5 feet. For this case the amplification of mean velocities at D2 changes somewhat to $1.84^2/2 = 1.69$ and at E3S shear stresses to decrease by about a factor of $1.09^2/2 = 0.59$. Finally at even higher flows the shear stress is more or less equally distributed to the underside of the ice cover and the bottom and the bottom thus experiences ½ the shear stress associated with the equivalent open surface discharge.

The capping materials are selected to resist the shear stresses associated with a 100 year return period flow of about 24,000 cfs. These shear stresses in OU1 are above those that are amplified by the blockage effect at low discharges and hence the net effect of the blockage on the selection of capping materials is moot.

References

Ashton, G. D. 1988. Intake design for ice conditions, Chapter 2 In: P. Novak (editor) Advances in Hydraulic Engineering, Vol. 5, p. 107-138, Elsevier Applied Science, London, 1988.)

Foth & Van Dyke, Figure 6-1 OU1 FINAL OPTIMIZED REMEDY, dated October 2006.

Foth & Van Dyke, Figure 6-2 POST REMEDY WATER DEPTH, dated October 2006.

Matousek, V. 1984. Types of ice run and conditions for their formation. Proceedings IAHR Ice Symposium 1984, Hamburg, Vol. I, pp. 315-28.

RETEC Figure 2-5: Maximum velocity rate estimated for flow condition of 408 cms at Rapid Croche Dam: Little Lake Butte des Morts, dated 01/03/03.

U.S. Army Corps of Engineers Detroit District. 1994. Lake Winnebago Fox-Wolf River Basin (pamphlet), 16 p.

U.S. Army Corps of Engineers, Table 3-12: Lower Fox River Stream Velocity Estimates, date unknown.

Figure 1

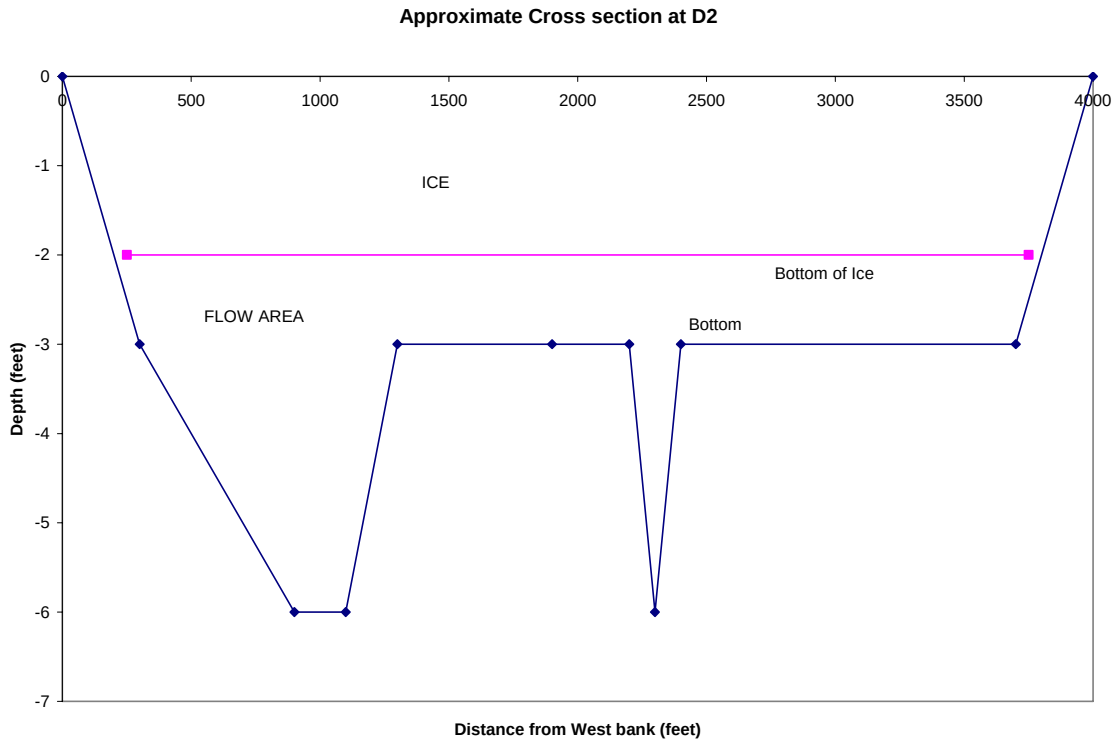

Figure 2

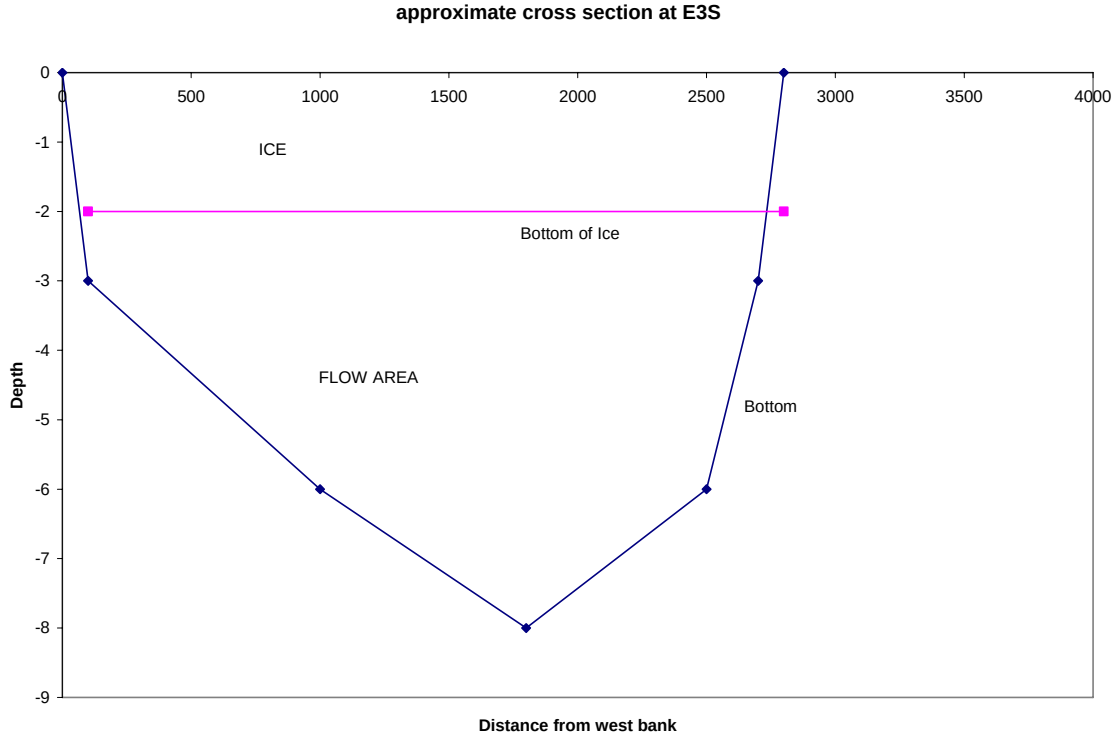

Follow-up Agency Questions and Responses to November 8, 2006 Ice Scour Report

This is in response to questions on ice scour.

Question No. 1: Is ice jamming at the old railroad trestle and at the 441 bridge possible. Include the appropriate discussion of this in the plan.

Response to Question No. 1: *Ice jamming at the old railroad trestle is highly unlikely. The maximum likely velocity there for a very high winter flow of 11,100 cfs is only about 0.82 fps (See Table 3 of original report). It is generally considered that the threshold velocity at which ice pieces are swept under an ice cover and begin forming a jam is about 2 fps. Thus ice pieces may lodge against the trestle but will remain at the surface and no jam would form. At the 441 bridge the velocities are even lower and estimated at less than 0.5 fps for the same conditions. Again, large floating ice sheets may lodge against the piers but would not submerge to form a jam.*

Question No. 2: During cold years where thick ice can accumulate, shear velocities can more than double for areas 6.67 feet and shallower. Address this possibility.

Response to Question No. 2: *The observation that "shear velocities can more than double for areas 6.67 feet and shallower" was stated in the original report. It was meant to refer to "areas" where the overall cross section is of average depth of 6.67 feet and shallower. To elaborate on cases where the average depth is shallower than 6.67 feet a more detailed analysis was made of Section D2 where the average depth under open water conditions is about 3.3 feet. As part of that analysis the effect of shifting of the flow from shallower areas to deeper areas (due to higher resistance to flow of shallower areas of the cross section) is also addressed.*

A detailed analysis of the redistribution of the flow due to creating locally shallower flow passages was not carried out in the original report since the resulting shear stresses from the analysis presented in the report were considerably less than those experienced by the bed at the 100 year open water flow discharge of about 24,000 cfs.

However, to address the Comment 2 above in more detail, an analysis of the redistribution of the flow for section D2 was carried out by dividing the cross section into four portions labeled Sections A, B, C and D in the Figure 1 below (adapted from Figure 1 of the original report). The results are also presented in Table I below. This cross section was selected since it well illustrates the redistribution of the flow from shallower to deeper areas and represents a cross section with extensive relatively shallow depths. In Table I the open water velocities are denoted by Vow and the ice covered velocities by Vic.

Table 1

Calculations Based on a Total Discharge of 5000 cfs
and 26 inch Thick Ice Cover
(submerged depth of 24 inches)

	Section A	**Section B**	**Section C**	**Section D**	**Total X Section**
Average velocity Open water case	0.41 fps	0.36 fps	0.44 fps	0.34 fps	0.38 fps
Average velocity Ice covered case	1.1 fps	0.78 fps	1.23 fps	0.66 fps	0.96 fps
V_{ic} / V_{ow}	2.68	2.17	2.80	1.94	2.53
Ratio of shear stresses on bottom V_{ic} / $V_{ow}^2/2$	3.59	2.35	3.92	1.88	3.2

From the Table, it is seen that the amplification of velocities and shear stresses are greater in the deeper parts of the flow than the shallower portions due to the flow redistribution effects.

Note also that the shear stresses on the bottom for the open water 100 year case of 24,000 cfs would be greater than the reference value of shear stress for a 5000 cfs open water flow by approximately $(24000/5000)^2$ ~= 23 based on the simple concept that shear stresses are more or less proportional to the square of the average velocity. A similar ratio of $(24000/11000)^2$ ~= 4.8 results for the very extreme winter discharge of 11,000 cfs, although historically such high winter discharges were always associated with warm weather and there would undoubtedly be a great deal of melting of the ice cover as this flow occurred. Additionally such high flows would also result in the reach changing from a lake-with-through-flow to a more river-like flow situation and result in elevation of water levels to accommodate the flow and a consequent reduction in the amplification effect calculated in Table I where no such elevation was allowed.

Figure 1

(adapted from Figure 1 of original report)

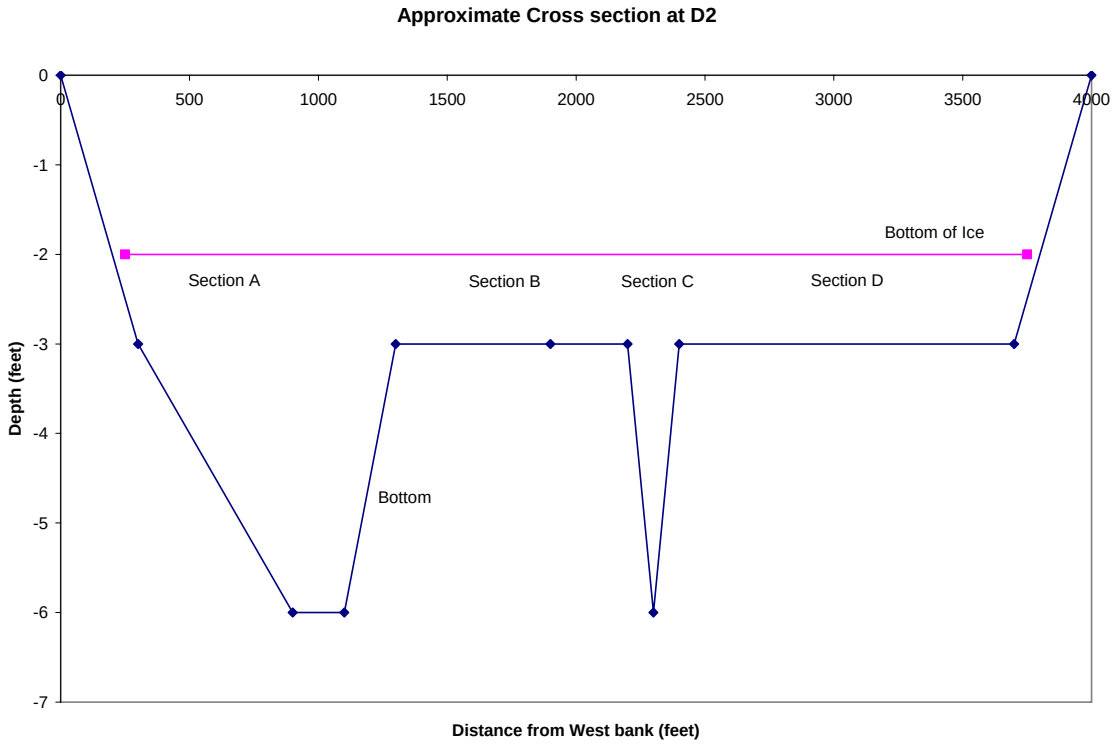

Appendix F

Lower Fox River Feasibility Study Cost Analysis

TABLE X

Alternative C2: Dredge Sediment With Off-site Disposal (Mechanical Dewatering)

Capital Items	Quantity	Units	Cost
Site Preparation	2	Each	$200,000
Mobilization - Equipment and Silt Curtain	1	LS	$170,000
Debris Sweep	526	acre	$8,416,000
Dredging - 12 hour shifts	747	Day	$4,257,900
Dredge Monitoring (Water Quality)	747	Day	$2,241,000
Sediment Removal QA	747	Day	$896,400
Site Remediation	2	Each	$1,200,000
Direct Capital:			$17,381,300
Engineering, Procurement & Construction Management:			$2,085,756
Contractor Overhead/Profit:			$2,607,195
Total Capital:			**$22,100,000**

SEDIMENT DEWATERING (MECHANICAL)

Capital Items	Quantity	Units	Cost
Mobilization/Site Prep	1	LS	$100,000
Dewatering	187,106	bdt	$14,968,480
Direct Capital:			$15,068,480
Engineering, Procurement & Construction Management:			$1,808,218
Total Capital:			**$16,900,000**

WATER TREATMENT

Capital Items	Quantity	Units	Cost
Unit Purchase	484	gpm	$781,094
Water Treatment (Includes Operator)	729,148,320	gal	$291,659
Water Treatment QA	1,046	day	$209,200
Direct Capital:			$1,281,953
Engineering, Procurement & Construction Management:			$153,834
Total Capital:			**$1,400,000**

TABLE X

SEDIMENT DISPOSAL (Existing NR 500 Commercial Disposal Facility)

Capital Items	**Quantity**	**Units**	**Cost**
Soil Loading	374,212	ton	$1,047,794
Soil Hauling	374,212	ton	$1,754,119
Tipping Fees (non-TSCA)	366,498	ton	$15,759,412
Tipping Fees (TSCA)	7,714	ton	$424,272
Direct Capital:			$18,985,597
Engineering, Procurement & Construction Management:			$2,278,272
Total Capital:			**$21,300,000**

INSTITUTIONAL CONTROLS

Capital Items	**Quantity**	**Units**	**Cost**
Deed Restrictions	1	LS	$5,000
Direct Capital:			$5,000
Engineering, Procurement & Construction Management:			$600
Total Capital:			**$5,600**

Present Worth of Longer Term Operating Costs	**Years**	**Annual Cost**	
Long-term Monitoring (no action)	40	$300,000	$4,513,889
Total Present Worth, Long Term O&M Costs			$4,513,889
Total Project Capital and O&M Cost			**$4,500,000**
TOTAL COST			**$66,200,000**